

© 2012

DEBORA ARAUJO ESPOSITO

ALL RIGHTS RESERVED

**PHARMACOLOGICAL CHARACTERIZATION OF BRASSINOSTEROIDS
FOR ANABOLIC AND COSMETIC APPLICATIONS**

by

DEBORA ARAUJO ESPOSITO

A Dissertation submitted to the
Graduate School-New Brunswick
Rutgers, The State University of New Jersey
in partial fulfillment of the requirements

for the degree of

Doctor of Philosophy

Graduate Program in Plant Biology

written under the direction of

Professor Ilya Raskin

and approved by

New Brunswick, New Jersey

January, 2012

ABSTRACT OF THE DISSERTATION

Pharmacological Characterization of Brassinosteroids

For Anabolic and Cosmetic Applications

By **DEBORA ARAUJO ESPOSITO**

Dissertation Director:

Professor Ilya Raskin

Brassinosteroids (BR) are plant-specific polyhydroxylated derivatives of 5 α -cholestane, structurally similar to cholesterol-derived animal steroid hormones and insect ecdysteroids, with unknown function in mammals. This research project was designed to conduct a pharmacological characterization of brassinosteroids in cell culture and small animal models in order to: (1) Elucidate the putative anabolic effect of BR in mammals (2) Establish a structure-activity relationship between BR and their effects on protein synthesis and (3) Measure the effects of BR on glucose metabolism and wound healing.

28-Homobrassinolide (HB) stimulated protein synthesis and inhibited protein degradation in L6 rat skeletal muscle cells ($EC_{50} = 4 \mu\text{M}$) mediated in part by PI3K/Akt. Oral administration of HB to healthy rats increased food intake, body weight gain, lean body mass, and gastrocnemius muscle mass. Both oral (up to 60 mg/kg) and subcutaneous (up to 4 mg/kg) administration of HB showed low androgenic activity. Moreover, HB showed no direct binding to the androgen receptor *in vitro*. These findings

suggest that oral application of HB triggers selective anabolic response with minimal or no androgenic side effects. Next, we synthesized a set of HB analogues and studied their anabolic efficacy in the L6 rat skeletal muscle cells. All anabolic brassinosteroids tested in this study selectively activated the PI3K/Akt signaling pathway as seen by increased Akt phosphorylation *in vitro*.

In C57BL/6J high fat diet-induced obese mice, acute oral administration of 50-300 mg/kg HB to obese mice resulted in a dose-dependent decrease in fasting blood glucose. Daily chronic administration of HB (50 mg/kg for 8 weeks) ameliorated hyperglycemia and improved oral glucose tolerance associated with obesity without significantly affecting body weight or body composition.

Akt is also a key signaling integrator suppressed in slow healing wounds. When C57BL/6J mice were given a dermal wound, topical application of brassinosteroids significantly reduced wound size after 10 days of treatment. Our data suggest that topical brassinosteroids accelerate the wound-healing process in part by shortening the early inflammatory phase and enhancing migration and wound repair by stimulating the PI3K/Akt pathway. Targeting this specific signaling pathway with brassinosteroids may represent a promising approach to the therapy of physical performance, glucose metabolism, and delayed wound healing.

DEDICATION

I dedicate this work to my family

ACKNOWLEDGEMENTS

These five years that I carried out this research were an arduous journey of challenge, construction and maturation. During this period, I learned that research is an extension of the scientist's life. For something of value to be produced, one must first create something of value in itself. For this reason, I sincerely thank all the people who really encouraged me to produce something of value in my life.

I would first like to express my deepest appreciation to my advisor, Professor Ilya Raskin, for his encouragement and advice throughout my graduate work. I would like to thank my committee members, Professor Thomas Gianfagna, Professor Bingru Huang, Professor Sue Shapses, and Professor Wendie Cohick for their support and helpful insight.

I would like to acknowledge my collaborators, colleagues, and friends: Professor Slavko Komarnytsky, Professor Gregory Henderson, Professor Malcolm Watford, Dr. Thirumurugan Rathinasabapathy, Dr. Alexander Poulev, Dr. Pablo Kizelsztejn, Dr. Dimitry Govorko, Dr. Sithes Logendra, Dr. Yanxin Wang, Dr. David Ribnicky, Dr. Peter Kuhn, Dr. John Munafo, Dr. Luis Mejia, Dr. Aniça Amini, Dr. Thomas Widiez, Dr. Daniela Linder-Basso, Dr. Leonel Rojo, Dr. Barbara Schmidt, Ruth Dorn, Reneta Pouleva, Ivan Jenkins, Barbara Halpern, Tolo Fridlender, Brittany Graf, Rocky Graziose, Patricio Rojas, Anna Zdepski, Carmen Golazzo, Alison L. Burnett, Ari Novy, Csanad Gurdon, Emily Merewitz, Jennifer Huang, Teresa Lucibello, Kimberly Palatini, Manoel Freitas, Ludmila Freitas, Daniela Carraro, and Reshma Nayyar, and all other faculty and staff members of Rutgers University and the Federal University of Viçosa.

Finally, special thanks to my family, Orestes, Rosangela, Mariana, Rafael, Laura and Barbara; to my relatives, aunt Ana, aunt Ormi, aunt Deuslira, uncle Otavio and their families for their love and support. I want to thank my cat, Tato, to remind me to go home after a long day of work. I would also like to give a special thanks to my husband, Slavko, for his constant care and support.

“Aqueles que passam por nós, não vão sós, não nos deixam sós. Deixam um pouco de si, levam um pouco de nós.” Antoine de Saint-Exupéry

TABLE OF CONTENTS

Abstract of the dissertation	ii
Dedication	iv
Acknowledgements	v
Table of contents	vii
List of tables	viii
List of figures	x
Chapter I: General introduction	1
Chapter II: Anabolic effect of plant brassinosteroid	12
Chapter III: Akt-dependent anabolic activity of natural and synthetic brassinosteroids in rat skeletal muscle cells	46
Chapter IV: Brassinosteroid treatment improves glucose homeostasis in obese mice	82
Chapter V: Cutaneous wound healing is accelerated by topical brassinosteroids	104
Chapter VI: Summary and conclusion	126
Appendix: Steroidal glycosides from the bulbs of Easter lily promote wound healing	130
Literature cited	158
Curriculum vita	170

LIST OF TABLES

Chapter I

Table 1	Brassica species with highest levels of brassinosteroids	8
Table 2	Distribution of brassinosteroids in the plant kingdom	9
Table 3	Quantification of brassinosteroids in selected plant organs	11

Chapter II

Table 1	Body composition and blood biochemistry of rats treated with HB	37
Table 2	Weights of androgen-sensitive tissues from sham and ORX rats treated with HB	38

Chapter III

Table 1	Effect of HB and its analogues on protein accumulation in the L6 rat skeletal muscle cells	72
---------	--	----

Chapter IV

Table 1	Body composition and blood biochemistry of mice treated with HB	97
---------	---	----

Chapter V

Table 1	Effect of HB and its analogues on cell viability, proliferation, and scratch wound closure in 3T3 mouse fibroblasts	120
---------	---	-----

Chapter VI

Appendix

Table 1	Cytotoxicity of compounds 1 through 5 to 3T3 Swiss albino	151
---------	---	-----

mouse fibroblast cells

LIST OF FIGURES

Chapter I

Chapter II

- Figure 1 Chemical structure of 28-homobrassinolide, HB in comparison 39
with testosterone and 20-hydroxyecdysone
- Figure 2 Concentration- and time-dependent effects of HB on protein 40
synthesis and degradation in L6 rat myotubes
- Figure 3 HB increases Akt (Ser473) phosphorylation in L6 myotubes 41
- Figure 4 Stimulation of protein synthesis by HB depends on PI3K/Akt 42
and PKC, but not on MAPK signaling
- Figure 5 Effect of HB on body weight gain and food intake in rats fed 43
normal and high protein diet
- Figure 6 HB has low androgenic activity 44
- Figure 7 HB increases physical fitness of untrained ORX rats 45

Chapter III

- Figure 1 Chemical structure of homobrassinolide and its analogues 73
investigated in this study
- Figure 2 Dose dependent effect of 1 and 2 on protein synthesis and 74
protein degradation in L6 rat myotubes.
- Figure 3 Cell survival curves as measured by MTT assay for 1-9 against 75
the murine fibroblast cell line NIH-3T3
- Figure 4 Effect of HB and its analogues on Akt (Ser473) phosphory- 76

	lation in L6 myotubes ⁷⁷	
Figure 5	Pharmacogenomic effect of HB <i>in vivo</i>	77
Supp Figure 1	Synthesis of (22S, 23S, 24S)-2 α , 3 α , 22, 23-tetrahydroxy-24-ethyl-5 α -cholestan-6-one (2) from stigmasterol	78
Supp Figure 2	Synthesis of (22S, 23S, 24S)-3 α -fluoro- 22, 23-dihydroxy-24-ethyl-5 α -cholestan-6-one and (22S, 23S, 24S)-3 α -fluoro- 22, 23-dihydroxy-7-oxo-24-ethyl-5 α -cholestan-6-one	79
Supp Figure 3	Synthesis of (22S, 23S, 24S)-2 α ,3 α ,22, 23-tetraacetoxy-24-ethyl-B-homo-6-aza-5 α -cholestan-6-one	80
Supp Figure 4	Synthesis of (22S, 23S, 24S)-2 α ,3 α ,22,23-tetrahydroxy-24-ethyl-B-homo-7-aza-5 α -cholestan-6-one	81
Chapter IV		
Figure 1	Chemical structure of 28-homobrassinolide, HB in comparison with other synthetic and natural brassinosteroid analogues	98
Figure 2	Acute lowering effect of HB on plasma glucose in C57BL/6J mice 3 h after administration of 50, 100, or 300 mg/kg HB	99
Figure 3	Chronic insulin sensitizing effect of HB on body weight gain, fasting blood glucose, and oral glucose tolerance test (OGTT) in the C57BL/6J mice	100
Figure 4	Hepatic expression of gluconeogenic enzymes PEPCK and G6Pase and activation of liver AMPK phosphorylation in C57BL/6J mice treated with 50 mg/kg HB	101
Figure 5	Production of glucose in the H4IIE rat hepatoma cell culture in	102

	response to HB treatment following induction with dexamethasone/cAMP mixture	
Figure 6	Production of glucose in the H4IIE rat hepatoma cell culture in response to treatment of HB, homocastasterone, and other synthetic and natural brassinosteroid analogues	103
Chapter V		
Figure 1	Chemical structure of 28-homobrassinolide, HB in comparison with other synthetic and natural brassinosteroid analogues	121
Figure 2	Effect of HB treatment on body weight change associated with wounding	122
Figure 3	Time course of wound healing in mouse cutaneous injury model	123
Figure 4	Effect of HB on cytokine and chemokine mRNA expression in wounds of C57Bl/6J mice	124
Figure 5	Dose dependent effect of brassinosteroid treatment on scratch wound closure <i>in vitro</i>	125
Chapter VI		
Appendix		
Figure 1	Schematic diagram of fractionation strategy	152
Figure 2	Bioactivity guided fractionation of <i>Lilium longiflorum</i> extract	153
Figure 3	Structures of bioactive steroidal glycoalkaloids 1 and 2	154
Figure 4	Structures of bioactive furostanol saponins 3, 4, and 5	155
Figure 5	Effect of bioactive steroidal glycoalkaloids 1 and 2 and	156

furastanol saponin 3 on scratch wound closure

Figure 6

Bioactive steroidal glycoalkaloids 1 and 2 induce nitric oxide
production and TGF- β signaling

157

CHAPTER I

GENERAL INTRODUCTION

This chapter has the purpose of a general introduction on the subject of plant brassinosteroids, a class of plant hormones with high-growth promoting activity with little known effects in animals; on the phenomenon of muscle loss/atrophy that contributes substantially to many disease states and has no satisfactory therapies; and on the complexity of anabolic/androgenic responses associated with animal steroids. In the following chapters, subject-specific introductions provide additional information on the involvement of the PI3K/Akt and AMPK signaling pathway in regulation of cell proliferation, differentiation, and migration as relevant to the area of musculoskeletal, metabolic, and wound healing disorders.

1.1 Brassinosteroids

Brassinosteroids are steroid plant hormones that play essential regulatory roles in various physiological processes, including growth, differentiation, root and stem elongation, stress tolerance and senescence. Immediately after the discovery of brassinosteroids in plant systems, studies were initiated to explore the possibilities of using these new substances for improving the yield of economically useful plants. The use of brassinolide demonstrated improvement in the yield of lettuce, radish, bush bean and pepper, as well as many other crops (1).

Brassinosteroids are polyhydroxylated derivatives of common plant membrane sterols such as campesterol. They occur throughout 40 families and have been shown by genetic and biochemical analyses to be essential for normal plant growth and development (2). The first biologically active plant brassinosteroid was isolated from the pollen of rapeseed *Brassica napus* (Table 1) in 1979 (3). The natural occurrence of more

than 50 compounds of this group (Table 2) has been reported following the initial discovery (4). It is clear that like their animal steroid counterparts, brassinosteroids have a defined receptor, can regulate the expression of specific genes, and can orchestrate complex physiological responses involved in growth. The brassinosteroid signaling pathway has become a paradigm for both receptor kinase signaling in plants and steroid signaling by cell surface receptors in general (5). Detailed studies of brassinosteroid biosynthesis and metabolism, coupled with the recent identification of BR-insensitive and BR-deficient mutants, have greatly expanded our view of steroids as signals controlling plant growth and development (6).

However, brassinosteroids are present at very low levels in plant tissues (Table 3) and it is very difficult to synthesize them chemically. For example, 28-homobrassinolide (HB) is almost as active as 24-epibrassinolide in inducing plant growth in various bioassay systems. HB is a steroidal lactone initially isolated from the pollen of Chinese cabbage *Brassica campestris var pekinensis* and the anthers of Japanese cedar *Cryptomeria japonica*. It is readily available through chemical synthesis, as its concentration in plants is low (7). In addition, HB activated total protein synthesis, induced de novo polypeptide synthesis, and increased thermotolerance of total protein synthesis in plants subjected to heat shock (8).

Very little is known about the effects of brassinosteroids in animals. A natural brassinosteroid and its synthetic derivatives were found to inhibit herpes simplex virus type 1 (HSV-1) and arenavirus, measles, Junin, and vesicular stomatitis virus replication in cell culture (9). A synthetic brassinosteroid analogue prevented HSV-1 multiplication and viral spreading in a human conjunctival cell line with no cytotoxicity and reduced the

incidence of herpetic stromal keratitis in mice when administered topically, possibly by the modulation of the response of epithelial and immune cells to HSV-1 infection (10). Natural brassinosteroids also inhibited the growth of several human cancer cell lines without affecting the growth of normal cells (11). 24-Epibrassinolide, the most widely used brassinosteroid in agriculture, has a favorable safety profile. The median lethal dose (LD₅₀) of this compound is higher than 1000 mg/kg in mice and higher than 2000 mg/kg in rats when applied orally or subcutaneously (12). HB was administered by oral gavage at doses of 0, 100, and 1000 mg/kg body weight in water during the gestation days (GD) of six through fifteen in groups of 20 mated females. Maternal and embryo-fetal toxicities were analyzed by studying the effects such as clinical signs, mortality/morbidity, abortions, body weight, feed consumption, and pregnancy data, gravid uterine weights, implantation losses, litter size, external, visceral, and skeletal malformations. No treatment-related effect was observed on any of the maternal/fetal end points in any dose group. From the results, it can be concluded that HB is nonteratogenic at doses as high as up to 1000 mg/kg body weight in Wistar rats (13). While some potential pharmacological applications of brassinosteroids have been suggested, in order to determine their potential uses additional mode of action studies are needed to explain how they interact with animal regulatory pathways.

1.2 Skeletal muscle atrophy

The combination of osteoporosis and sarcopenia results in the significant frailty often seen in the elderly population. The two most critical issues facing current aging therapy are the lack of adequate treatment and the insufficient recognition of the disease.

Loss of muscle mass is a normal consequence of aging. The decline in muscle mass is estimated to be 0.2-0.5% per year from 60 years old onwards in healthy subjects with the decline worsened by chronic illness, poor appetite and diet, and reduced physical activity in the elderly (14). Increased morbidity is demonstrable with as little as a 5% loss of muscle mass - therefore, treatments that can prevent or slow the progression of muscle loss with aging are much desired. As men age, testosterone (T) levels decline during the so-called andropause. Men lose bone density as they age, although men do not suffer the equivalent of the dramatic bone loss that occurs after female menopause. This is due to deterioration in both bone density and muscle strength: in other words, frailty. Because of its stimulation of the prostate, T has not been explored as an option for osteoporosis treatment or prevention.

A major cause for the loss of muscle mass with advanced age is the inability of aging muscle to increase the rate of muscle protein synthesis in response to nutritional stimuli. The blunted anabolic response to nutritional stimuli is at least in part due to defects in the anabolic-signaling cascade in muscle (i.e., decreased activation of the mTOR-p70s6K signaling pathway). The PI3K/Akt/mTOR pathway is a crucial intercellular regulator of muscle hypertrophy (15). Activation of PI3K by upstream ligands such as IGF-1 or IGF-2 phosphorylates the membrane phospholipids and creates a lipid binding site for Akt, which in turn increases protein synthesis and suppresses proteolytic activity and gene expression of the proteolytic genes (16). Interventions that can overcome this anabolic resistance are therefore likely to prevent or slow the progression of muscle loss with aging or disease.

1.3 Anabolic response

Anabolic steroids, officially known as anabolic-androgen steroids (AAS) or colloquially simply as "steroids", are drugs which mimic the effects of the male sex hormones testosterone and dihydrotestosterone. They increase protein synthesis within cells, which results in the buildup of cellular tissue (anabolism), especially in muscles (17). Almost half a century before the discovery of androgens, Brown-Sequard had recognized that the contents of testicular extracts could improve libido, energy, and muscle strength (18). Androgens are male sex hormone and include several steroids, such as testosterone, dehydroepiandrosterone, androstenedione, androstenediol, androsterone, and dihydrotestosterone (19). Androgens are required for the maintenance of normal sexual activity in adulthood and for enhancing muscle growth and lean body mass in adolescents and adults. Androgens have anabolic activity in prostate, bone, muscle, and hair follicles of the scalp and skin (20). In short, anabolism results in growth and differentiation of cells and tissues in the body, which result in an increase in muscle mass in the resulting increase in lean body mass. However, there are health risks associated with long-term use or excessive doses of anabolic steroids (21). These effects include harmful changes in cholesterol levels (increased low-density lipoprotein and decreased high-density lipoprotein), acne, high blood pressure, liver damage (mainly with oral steroids), and dangerous changes in the structure of the left ventricle of the heart.

Androgenic-anabolic steroids (AAS) are synthetic derivatives of the male hormone testosterone. Although AAS have been used in sports for ergogenic purposes for decades, many believed that the improved performance seen with AAS was due to their influence on motivation and aggression. It took landmark studies from Bhasin et al. (22)

to prove that testosterone dose-dependently increases muscle mass, maximal voluntary strength, and power and that these improvements are correlated with circulating testosterone concentrations. There are multiple mechanisms that lead to this anabolic response. Androgens are known to increase fractional muscle protein synthesis and increase the size of both type I and type II muscle fibers. Studies have also shown that testosterone directs the pluripotent mesenchymal stem cell toward myogenic lineage rather than adipogenic lineage (15).

1.4 Objectives of this study

The overall goal of this study was to characterize pharmacological effects of brassinosteroids in animals, concentrating on anabolic activity and possible modes of action. Specifically, we aimed at identification and characterization of brassinosteroids with applications in human health and disease in relationship to brassinosteroid-induced changes in body composition, muscle mass and strength, glucose metabolism, and wound healing. Measures of protein synthesis and degradation in muscle, glucose production in liver, and determination of the status of the PI3K/Akt and AMPK signaling pathways in the affected tissues were undertaken to establish selective anabolic action of plant brassinolides in animals and provide novel early pre-clinical leads and pharmacological tools to investigate the biological functions of muscle growth and regeneration pathways.

Table 1. Brassica species with highest levels of brassinosteroids after (2).

Scientific name	Common name
<i>Brassica chinensis</i> Linn.	Chinese Cabbage
<i>Brassica rapa</i> Linn.	Raps
<i>Brassica oleracea</i> Linn.	Cabbage
<i>Brassica oleracea</i> Linn. acephala DC.	Cole and kale
<i>Brassica oleracea</i> Linn. botrytis cymosa DC.	Broccoli
<i>Brassica oleracea</i> Linn. bullata gemmifera DC.	Brussels sprouts
<i>Brassica oleracea</i> Linn. bullata major DC.	Savoy cabbage
<i>Brassica oleracea</i> Linn. capitata DC.	Cabbage and cauliflower
<i>Brassica oleracea</i> Linn. caulorapa communis DC.	Kohlrabi
<i>Brassica campestris</i> Linn.	Turnip
<i>Brassica alba</i> Boiss.	White Mustard
<i>Brassica juncea</i> Coss.	Indian Mustard
<i>Brassica nigra</i> Koch.	Black Mustard

Table 2. Distribution of brassinosteroids in the plant kingdom after (2).

Monocotyledons		
Family	Number of species	Plant parts
Arecaceae	1	Pollen
Gramineae	6	Pollen, shoot, seeds
Liliaceae	4	Pollen
Typhaceae	1	Pollen
Dicotyledons - the Apetalae		
Family	Number of species	Plant parts
Betulaceae	1	Pollen
Cannabaceae	1	Seeds
Caryophyllaceae	4	Seeds
Fagaceae	1	Galls, shoot, leaves
Polygonaceae	2	Pollen, panicles
Dicotyledons - the Chloripetalae		
Family	Number of species	Plant parts
Apiaceae	2	Seeds
Brassicaceae	4	Pollen, shoot, seeds
Fabaceae	8	Pollen, shoot, seeds
Myrtaceae	2	Pollen
Rosaceae	1	Flower buds
Rutaceae	2	Pollen
Theaceae	1	Leaves
Dicotyledons - the Sympetalae		
Family	Number of species	Plant parts
Apocynaceae	1	Cultured cells

Asteraceae	3	Cultured cells, pollen, shoot
Boraginaceae	1	Pollen
Convolvulaceae	1	Seeds
Cucurbitaceae	1	Seeds
Lamiaceae	1	Seeds
Solanaceae	2	Cultured cells, root, shoot

Gymnosperms

Family	Number of species	Plant parts
Cupressaceae	1	Seeds
Ginkgoaceae	1	Pollen, shoot, seeds
Pinaceae	3	Pollen, shoot, seeds
Taxodiaceae	1	Pollen

Lower plants

Family	Number of species	Plant parts
Equisetaceae	1	Whole plant
Hydrodictyaceae	1	Whole plant
Marchantiaceae	1	Cultured cells

Table 3. Quantification of brassinosteroids in selected plant organs after (2).

Species	Tissues	Levels (ng g⁻¹ f.w.)
<i>Arabidopsis thaliana</i>	shoot, seed	0.11 - 5,4
<i>Brassica napus</i>	pollen	> 100
<i>Helianthus annuus</i>	pollen	25 - 106
<i>Pinus thumbergii</i>	pollen	89
<i>Cupressus arizonica</i>	pollen	1.0 - 6,400
<i>Zea mays</i>	pollen, shoot	2.0 - 120
<i>Typha latifolia</i>	pollen	68

CHAPTER II

ANABOLIC EFFECT OF PLANT BRASSINOSTEROID

Published in: FASEB J (2011) 25: 3708-3719

2.1 Abstract

Brassinosteroids are plant-derived polyhydroxylated derivatives of 5 α -cholestane, structurally similar to cholesterol-derived animal steroid hormones and insect ecdysteroids, with no known function in mammals. 28-Homobrassinolide (HB) stimulated protein synthesis and inhibited protein degradation in L6 rat skeletal muscle cells ($EC_{50} = 4\mu\text{M}$) mediated in part by the PI3K/Akt signaling pathway. Oral administration of HB (20 or 60 mg/kg per d for 24 days) to healthy rats fed a normal diet (protein content 23.9%) increased food intake, body weight gain, lean body mass, and gastrocnemius muscle mass. The effect of HB administration increased slightly in animals fed a high protein diet (protein content 39.4%). Both oral (up to 60 mg/kg) and subcutaneous (up to 4 mg/kg) administration of HB showed low androgenic activity when tested in the Hershberger assay. Moreover, HB showed no direct binding to the androgen receptor *in vitro*. HB treatment was also associated with an improved physical fitness of untrained healthy rats as seen by the 6.7% increase in lower extremity strength measured by the grip test. In the gastrocnemius muscle of castrated animals, HB treatment significantly increased the number of type IIa and IIb fibers and the cross-sectional area of type I and type IIa fibers. These findings suggest that oral application of HB triggers selective anabolic responses with minimal or no androgenic side effects and begins to elucidate the putative cellular targets for plant brassinosteroids in mammals.

2.2 Introduction

Brassinosteroids are plant-specific polyhydroxylated derivatives of 5 α -cholestane, structurally similar to cholesterol-derived animal steroid hormones and ecdysteroids from

insects. They are found at low levels in pollen, seeds, leaves, and young vegetative tissues throughout the plant kingdom (2). The first biologically active plant brassinosteroid was isolated from the pollen of rapeseed *Brassica napus* in 1979 (3). The natural occurrence of more than 50 compounds of this group has been reported following initial discovery (4). The brassinosteroids function in cell elongation and cell division, and have been particularly studied in relation to processes such as germination and plant photomorphogenesis (23).

Similar to animal steroid hormones (24), brassinosteroids regulate the expression of specific plant genes and complex physiological responses involved in growth (25), partly via interactions with other hormones setting the frame for brassinosteroid responses (26). While animal steroid hormones are perceived by the nuclear receptor family of transcription factors, brassinosteroids signal through a cell surface receptor kinase-mediated signal transduction pathway (27, 28) that includes inactivation of GSK3-like kinase BIN2 by dephosphorylation at a conserved phospho-tyrosine residue pTyr 200, therefore allowing for the accumulation of transcriptional factors BZR1 and BES1 in the nucleus (6). This signal transduction pathway shares a striking parallel with animal Wnt signaling. In mammals, Wnt binds to its receptor, Frizzled, causing inhibition of GSK-3 β kinase activity and subsequent accumulation of β -catenin in the nucleus, where it directly affects the transcription of target genes (29). Although BIN2 is homologous to GSK-3 β , the transcriptional factors BZR1 and BES1 are unique plant proteins that do not share sequence similarity with β -catenin (30).

Akt is a serine/threonine kinase that signals downstream of the growth factor receptors and phosphoinositide-3 kinase PI3K. Therefore, growth factor receptors,

nutrients, and even muscle contraction increase Akt activity (31). Akt stimulates glucose uptake, glycogen synthesis, and protein synthesis via Akt/mTOR and Akt/GSK-3 β signaling networks (32), and inhibits apoptosis and protein degradation in skeletal muscle by inactivating FoxO transcription factors (33). Akt is therefore situated at a critical juncture in muscle signaling where it responds to diverse anabolic and catabolic stimuli.

Very little is known about effects of brassinosteroids in animals. A natural brassinosteroid and its synthetic derivatives were found to inhibit herpes simplex virus type 1 (HSV-1) and arenavirus (34), measles (35), Junin (9), and vesicular stomatitis virus (36) replication in cell culture. A synthetic brassinosteroid analogue prevented HSV-1 multiplication and viral spreading in a human conjunctival cell line with no cytotoxicity and reduced the incidence of herpetic stromal keratitis in mice when administered topically (37), possibly by the modulation of the response of epithelial and immune cells to HSV-1 infection (38). Natural brassinosteroids also inhibited growth of several human cancer cell lines without affecting the growth of normal cells (11). 24-Epibrassinolide, the most widely used brassinosteroid in agriculture, has a favorable safety profile. The median lethal dose (LD₅₀) of this compound is higher than 1000 mg/kg in mice and higher than 2000 mg/kg in rats when applied orally or subcutaneously (12).

28-Homobrassinolide (HB, Fig. 1A) is almost as active as 24-epibrassinolide in inducing plant growth in various bioassay systems (39). HB is a steroidal lactone initially isolated from the pollen of Chinese cabbage *Brassica campestris var pekinensis* (40) and the anthers of Japanese cedar *Cryptomeria japonica* (41). It is readily available through chemical synthesis, as its concentration in plants is very low (42). The plant growth

promoting effect of HB is associated with the increased synthesis of nucleic acids and proteins (7, 43). In addition, HB activated total protein synthesis, induced *de novo* polypeptide synthesis, and increased thermotolerance of total protein synthesis in plants subjected to heat shock (8).

Almost no data exist on the *in vivo* effects of brassinosteroids in animals. Given the importance of identifying novel agents that influence muscle growth, development, and/or regeneration with possible therapeutic application for the age or disease-related skeletal muscle atrophy (sarcopenia), we sought to explore the effects of HB on protein synthesis and degradation in animals, and to study the signal transduction pathways with which it interacts. Furthermore, we compared the activity of HB to that of insulin-like growth factor-1 (IGF-1) *in vitro* and showed that the PI3K/Akt pathway is upregulated in skeletal muscle cells treated with HB. We also found that HB treatment produced anabolic effects and improved physical fitness in healthy animals without detrimental androgenic effects. These data establish selective anabolic action of plant brassinolides in animals and provide important insight into the role of Akt signaling in mediating this activity.

2.3 Materials and methods

2.3.1 Chemicals

HB [(22S, 23S, 24S)-2 α , 3 α , 22,23-tetrahydroxy-24-ethyl- β -homo-7-oxo-5 α -cholestane-6-one] (Fig. 1A) was purchased from Waterstone Technology (Carmel, IN) and its structure was confirmed by ESI-LCMS and NMR. L-[2,3,4,5,6-³H]-phenylalanine

was obtained from GE Healthcare (Piscataway, NJ). Reagents and enzymes used for qPCR were obtained from Stratagene (La Jolla, CA) and Applied Biosystems (Foster City, CA). SB203580 and PD98059 were from EMD Chemicals (Gibbstown, NJ). All other chemicals and cell culture media were obtained from Invitrogen (Carlsbad, CA) and Sigma (Saint Louis, MO) unless otherwise specified.

2.3.2 Cell culture

The rat L6 skeletal muscle cell line CRL-1458 was obtained from ATCC (Manassas, VA). Myoblasts were routinely maintained in Dulbecco's modified Eagle's medium (DMEM) containing 10% FBS and 0.1% penicillin-streptomycin at 37°C and 5% CO₂. Cells were subcultured into 24 well plates for protein synthesis, degradation, and cell viability studies and 6 well plates for Western blot analysis (Greiner Bio One, Monroe, NC). Once cells reached 90% confluence, differentiation was induced by lowering the serum concentration to 2%, and the medium was changed every two days. After seven to nine days of culture the myoblasts had fused into multinucleated myotubes (44).

2.3.3 Cell viability assay and dose range determination

Cell viability was measured by the MTT (3-(4,5-Dimethylthiazol-2-yl)-2,5-diphenyltetrazolium bromide) assay in triplicate essentially as described (45) and quantified spectrophotometrically at 550 nm using a microplate reader (Molecular Devices, Sunnyvale, CA). The concentrations of test reagents that showed no changes in

cell viability compared with that of the vehicle (0.1% ethanol) were selected for further studies.

2.3.4 Measurement of protein synthesis

For the HB dose response, fully differentiated myotubes were washed with serum-free DMEM and treated in triplicate with vehicle (0.1% ethanol), increasing concentrations of HB, or 6.5 nM of insulin-like growth factor-1 (IGF-1) as positive control. Compounds were added to serum-free medium containing 0.5 $\mu\text{Ci/mL}$ [^3H]-phenylalanine and incubated for 4 h. For the HB time course study, fully differentiated myotubes were treated with 3 μM HB for 1-24 h using the same culture conditions. The incubation was stopped by placing the cells on ice, discarding the medium, and washing the cells extensively with ice cold PBS to remove the non-incorporated trace. Proteins were precipitated with 5% trichloroacetic acid and dissolved in 0.5N NaOH (46). Specific radioactivity of protein-bound phenylalanine was quantified using the liquid scintillation counter LS 6500 (Beckman Coulter, Fullerton CA) and normalized to mg of the total protein determined by the BCA protein assay (Pierce Biotechnology, Rockford, IL).

2.3.5 Measurement of protein degradation

The effect of HB on protein degradation was investigated in fully differentiated myotubes as described (47) with slight modifications. For the HB dose response, fully differentiated myotubes were incubated for 16 h to allow labeling of cellular proteins with 1.5 $\mu\text{Ci/mL}$ [^3H]-phenylalanine. Cells were washed twice with PBS to remove the non-incorporated trace and treated for 4 h with vehicle (0.1% ethanol), increasing

concentrations of HB, or 10 nM of insulin in serum-free medium. The incubation was stopped by placing the cells on ice, and protein in the medium was precipitated with 5% trichloroacetic acid. Specific radioactivity of protein-free phenylalanine was quantified using the liquid scintillation counter LS 6500 (Beckman Coulter, Fullerton, CA) and normalized to mg of the total cell protein determined by the BCA protein assay (Pierce Biotechnology, Rockford, IL).

2.3.6 Western blot analysis

Fully differentiated L6 myotubes were cultured as described above, and whole cell extracts were prepared in ice-cold RIPA buffer supplemented with 10 mM sodium fluoride, 2 mM sodium orthovanadate, 1 mM PMSF, and protease inhibitor cocktail (Sigma) and centrifuged at 12,000 g for 20 min at 4°C. Equal amounts of protein (50 µg) from the supernatants were separated on 10% SDS polyacrylamide gels and blotted onto the nitrocellulose membrane. Western blot detection was performed with monoclonal phospho-Akt (Ser473) antibodies according to the manufacturer's instructions (Cell Signaling Technology, Danvers, MA). After being washed, the blots were incubated with an anti-rabbit peroxidase-labeled secondary antibody and visualized using ECL Western Blotting Detection Reagent (GE Healthcare, Piscataway, NJ). After being stripped, the same blots were probed with total Akt antibodies to serve as loading controls.

2.3.7 Androgen receptor binding

Rat androgen receptor binding assays were performed by MDS Pharma Services, Taiwan (study no 1019130 and 1096057) as described elsewhere (48). Vehicle (1%

DMSO), increasing concentrations of HB or methandrostenolone were incubated in the presence of the specific binding ligand [³H]-mibolerone for 4 h at 4 °C and DPMs of the incubation buffer were measured to quantify displacement of the ligand. Each treatment was repeated two to three times, and the results were averaged.

2.3.8 Animal studies

All animal experiments were performed according to procedures approved by the Rutgers Institutional Animal Care and Use Committee in an AAALAC accredited animal care facility. Six weeks old male Wistar rats (180-220 g, Charles River Laboratories, MA) were housed in individual chambers, in a room maintained at a constant temperature with a 12 h light-dark cycle and had free access to food and water. Animals were allowed to adapt to their new conditions for seven days and handling the animals was performed daily during this time to reduce the stress of physical manipulation. Animals were randomized into groups according to bodyweight one day prior to dosing.

Protocol 1: Three groups of Wistar rats (n=6) fed a normal diet containing 23.9% protein, 10.7% fat, 5.1% fiber, and 58.7% carbohydrates, resulting in a 4.61 kcal/g energy value (#5001 Rodent Chow diet, Purina, St. Louis, MO) were gavaged daily for 24 d with 1 ml of vehicle (5% DMSO in corn oil), 20 or 60 mg/kg body weight of HB. The body weight of each animal and the total amount of food consumed (accounting for spillage) were recorded every two days for the duration of the experiment. At the end of experiment, blood was collected by heart puncture after CO₂ inhalation and animal body composition was assessed prior to necropsy. At necropsy, tissue weights were recorded,

then tissue samples were collected by snap-freezing in the liquid nitrogen and stored at -80°C for further studies.

Protocol 2: Three groups of Wistar rats (n=8) fed a high protein diet containing 39.4% protein, 10.0% fat, 4.3% fiber, and 37.0% carbohydrates, resulting in a 3.93 kcal/g energy value (#5779 diet, Testdiet/Purina, Richmond, IN) were gavaged daily for 24 d with one ml of vehicle (5% DMSO in corn oil), 20 or 60 mg/kg HB. All procedures and measurements followed the protocol 1 setup.

Protocol 3: Four weeks old sham-operated (sham, n=6) or orchietomized (ORX, n=24) Wistar rats (Charles River Laboratories, MA) were subject to 10 d Hershberger assay (surgically castrated peri-pubertal adult model) under the following experimental conditions: sham, ORX (vehicle), ORX (20 mg/kg HB orally), ORX (60 mg/kg HB orally), and ORX (0.4 mg/kg testosterone propionate subcutaneously, serving as a positive control for the assay). All procedures and measurement followed the protocol 1 setup except no body composition measurements were taken. Limb grip strength was measured for control animals and animals receiving 60 mg/kg HB using digital force gauge (Wagner Instruments model FDV5) by Product Safety Laboratories (Dayton, NJ). After the rats were allowed to grip the screen with their paws, the animals were quickly pulled until their paws released from the screen, and the required release force was recorded. Three trials on each animal were performed in triplicate, and significance was determined using the Student's t test ($p < 0.05$). In addition to gastrocnemius muscle, androgen-sensitive tissues (ventral prostate, seminal vesicles, bulbocavernosus/levator ani muscle complex, glans penis, Cowper's gland) were dissected and weighed.

Protocol 4: Four weeks old sham-operated (sham, n=6) or orchiectomized (ORX, n=24) Wistar rats (Charles River Laboratories, MA) were subject to 10 d Hershberger assay (surgically castrated peri-pubertal adult model) under the following experimental conditions: sham, ORX (vehicle), ORX (0.4 mg/kg HB subcutaneously), ORX (4 mg/kg HB subcutaneously), and ORX (0.4 mg/kg testosterone propionate subcutaneously, serving as a positive control for the assay). All procedures and measurements followed the protocol 4 setup.

2.3.9 Body composition

Body composition was assessed by dual-energy x-ray absorptiometry using the Lunar Prodigy total body scanner with a total body scanner (Prodigy Advanced, GE-Lunar Corp., Milwaukee, WI) that uses Encore small animal body software. Quality control was performed daily. The coefficient of variation for total body fat and lean mass, and bone mineral content were 1.93%, 3.43%, and 2.10%, respectively as measured in five rats scanned three times each.

2.3.10 Muscle histology

The muscle samples for histochemical analysis were taken from the middle section of the mixed-fiber gastrocnemius muscle of the castrated animals according to the protocol 4 setup to allow us to observe differences in fiber type distribution and the cross section area associated with ORX and HB treatments. Serial transverse cryosections (10 μ m) were prepared from each muscle and were analyzed for myofibrillar adenosine triphosphatase (mATPase) histochemistry after alkaline (pH=9.5) preincubation. The

fiber cross section area and enzyme activity levels were determined from digitized images of the muscle cross-sections that were stored as gray-level pictures using ImageJ software (National Institutes of Health, Bethesda, MD).

2.3.11 Assays of plasma samples

Blood samples were taken from overnight fasted animals by heart puncture, collected in EDTA-coated tubes, centrifuged at 1,500 g for 20 min, and separated plasma was stored at -80°C until analysis. Glucose was measured in blood samples using a Lifescan glucometer (Johnson and Johnson, New Brunswick, NJ). Plasma concentrations of insulin were determined by a rat/mouse insulin ELISA kit (Millipore, Billerica, MA): assay sensitivity (0.2 ng/ml), intra-assay (0.9-8.4%) and inter-assay (6.0-17.9%) coefficients of variation, accuracy (83-102%). Plasma triglycerides and total cholesterol were measured by enzymatic colorimetric assays (Wako Diagnostics, Richmond, VA): intra- and inter-assay coefficients of variation (9-10%). Total testosterone in plasma samples was quantified by ELISA assay (DRG Diagnostics, Marburg, Germany): assay sensitivity (0.066 ng/ml), intra-assay (6.5-11.1%) and inter-assay (9.3-11.3%) coefficients of variation, accuracy (84-123%).

2.3.12 Statistics

Statistical analyses were performed using Prism 4.0 (GraphPad Software, San Diego, CA). Unless otherwise noted, data were analyzed by one-way ANOVA with treatment as a factor. Post hoc analyses of differences between experimental groups were made using the Dunnett's multiple comparison test. Body weight gain was analyzed by

two-factor repeated-measures ANOVA, with time and treatment as independent variables. Significance was set at $p < 0.05$. Values are reported as means \pm SEM.

2.4 Results

2.4.1 Effect of HB on protein synthesis

HB showed no toxicity to fully differentiated L6 rat skeletal myotubes up to 25 μM as established by the MTT assay and cytological observations (data not shown). To determine whether or not HB induces protein synthesis, the incorporation of radiolabelled [^3H]-phenylalanine was assessed. Cells were treated with several concentrations of HB (0.3-20 μM) for 4 h. At the lower concentration, 1 μM HB increased protein synthesis by $12.4 \pm 2.3\%$ above control levels ($p < 0.05$). A response approached saturation between 10 and 20 μM of HB ($\text{EC}_{50} = 4\mu\text{M}$), with increases of $34.9 \pm 3.1\%$ and $36.9 \pm 2.9\%$, respectively (Fig. 2A). IGF-1 at 6.5 nM served as a positive control in this assay; it increased protein synthesis by $42.5 \pm 4.5\%$. Higher concentration of HB were less effective (not shown). To investigate the kinetic of HB effect on protein synthesis, a 1-24 h study was performed with 3 μM HB, selected as a 50% effective dose to treat myotubes. A time-dependent increase in protein synthesis in response to HB was observed (Fig. 2B). HB-stimulated protein synthesis peaked at 3 h and started to decrease after 4 h. We observed a similar kinetic of protein synthesis increase in response to IGF-1 treatment, although of a greater magnitude.

2.4.2 Effect of HB on protein degradation

IGF-1 has both anabolic effect on protein synthesis and anti-catabolic effect on protein degradation in skeletal muscle similar to insulin (49). Protein synthesis is more sensitive to IGF-1 infusion than to insulin infusion, and is not mediated by insulin receptors (50). On the contrary, insulin affects protein turnover by inhibiting protein degradation (51). In order to assess whether or not HB affects protein degradation, we monitored the degradation of proteins labeled with [³H]-phenylalanine by the release of acid-soluble radioactivity into the medium. HB at concentrations of 0.3-20 μM inhibited protein degradation dose-dependently and its activity reached a plateau between 3 and 10 μM (Fig. 2c). At the lower concentration, 1 μM HB decreased protein degradation by $8.2 \pm 0.6\%$ above control levels ($p < 0.05$). At the higher concentration, 10 μM HB decreased protein degradation by $9.5 \pm 0.9\%$ above control levels ($p < 0.05$). Insulin at 10 nM served as positive control in this assay; it reduced protein degradation by $13.0 \pm 1.6\%$. To investigate the kinetic of protein degradation in response to HB, a 1-4 h study was performed with 3 μM HB. Suppression of protein degradation occurred time-dependently and reached plateau at 3 h for both HB and insulin (Fig. 2D).

2.4.3 HB stimulates phosphorylation of Akt

IGF-1 inhibits protein degradation in myotubes through PI3K/Akt/GSK-3β and PI3K/Akt/mTOR-dependent mechanisms (52). Therefore, Akt is the key intermediate in the IGF-1 signaling pathway that modulates downstream targets known to regulate protein synthesis and degradation (53). To characterize the transduction pathway more closely through which HB signals to induce positive net protein balance, next we investigated the phosphorylation level of Akt in L6 myotubes. Consistent with the results

obtained with the [³H]-phenylalanine incorporation assay, HB stimulated phosphorylation of Akt in a dose- and time-dependent manner (Fig. 3). Increasing concentrations of HB stimulated Ser473 phosphorylation of Akt up to 3 fold with 3 μM after 1 h of treatment (Fig. 3A). Akt stimulation was detected at 30 min after the addition of HB and phosphorylation was maintained up to 1 h, whereas total Akt protein levels were also increased at some time points. The ratio of phospho-Akt to total Akt normalized to control values increased up to 3 fold following the treatment (Fig. 3B). Although the effect of HB on Akt phosphorylation is not as robust as that described for IGF-1 (32), these data support a role for the PI3K/Akt pathways in HB stimulation of anabolic signaling in L6 myotubes.

Next, we wanted to investigate the molecular mechanism responsible for the anabolic effect of HB in mammalian cells. To test whether or not PI3K signaling is responsible for HB-mediated protein synthesis, we used the specific Akt inhibitor triciribin and PI3K inhibitor LY294002. The anabolic response of L6 cells to HB treatment was abolished by the addition of both inhibitors from 50% over control to only 4%. A similar effect was observed with the PKC inhibitor GO6976, while the MEK1 inhibitor PD98059 and the p38 MAPK inhibitor SB203580 had no effect (Fig. 4).

2.4.4 Anabolic effects of HB on body composition

Anabolic is defined as any state in which nitrogen is differentially retained in lean body mass, either through stimulation of protein synthesis and/or decreased breakdown of protein anywhere in the body (21). To evaluate the potential anabolic effects of plant brassinosteroids in animals, we orally administered 20 and 60 mg/kg body weight of HB

(HB20 and HB60, respectively) daily to healthy rats fed a normal diet for 24 d. By the end of the treatment, the total body weight gain relative to initial body weight in rats treated with HB20 or HB60 was 18.3% and 26.8% more compared with vehicle-treated controls (Fig. 5A). A slight but statistically significant increase in total daily food intake (20.8 ± 0.4 g for controls; 22.2 ± 0.8 g for HB20; and 23.6 ± 0.5 g for HB60 group) was associated with HB administration, but when adjusted for body weight, food intake did not differ among all groups (Fig. 5B). Therefore, an increase in body weight gain in the HB-treated groups could not be attributed to changes in the animal feeding habits. Body composition determined by DEXA analysis showed that increase in lean body mass was significantly higher in HB20 (7.0%) and HB60 animals (14.2%). Fat mass was slightly lower in HB20 (-3.9%) and HB60 groups (-4.9%) versus their control counterparts. Thus, the greater body weight gain in the HB-treated rats was predominantly due to increased lean mass (Table 1). Administration of HB increased gastrocnemius muscle mass by 15.6% and 19.0% in HB20 and HB60 animals, respectively. Total body BMC was slightly higher in HB-treated animals but the difference did not reach any significance. Supplementation with HB had no effect on basal plasma cholesterol or triglycerides. A higher dose of HB was associated with slightly lower plasma glucose levels (4.5 ± 0.3 mM) versus controls (5.0 ± 0.3 mM), but the difference did not reach statistical significance. Insulin levels were slightly elevated (Table 1).

2.4.5 Anabolic effects of HB in rats fed a high protein diet

It has been shown that a short-term increase in dietary protein can favor lean body mass and reduce body fat in rats, possibly due to an initial decrease in food intake that

gradually returns to normal with time (54). In order to investigate whether or not a high protein diet can further enhance HB-associated effect on lean mass and muscle mass, rats fed a high protein diet (39.4% protein) were orally administered with 20 and 60 mg/kg body weight HB daily for 24 d. Indeed, control animals fed a high protein diet consumed less food and gained less weight than the control animals on a normal diet (Table 1). Stimulatory effects of HB on body weight and food consumption were apparent on the background of both normal and high protein diet. The high protein diet possibly enhanced the stimulatory effect of the lower dose of HB (20 mg/kg) on the body weight gain (Fig. 5C). No HB-associated increase in food intake was observed in these animals (Fig. 5D). There were no additional differences in body composition or blood biochemistry that could be attributed to the high protein diet (Table 1).

2.4.6 Androgen receptor binding

Since administration of classical mammalian steroids often causes both anabolic and androgenic effects, we performed a study to rule out the possibility that HB activates the androgen receptor. Competitive binding assay to the rat nuclear androgen receptor in the presence of the labeled [³H]-mibolerone was used to compare HB with methandrostenolone, an androgen analogue used therapeutically as an anabolic agent (55). Methandrostenolone produced specific binding to the androgen receptor with an IC₅₀ of 24 nM, and a binding curve similar to the endogenous ligand, testosterone. However, HB showed no significant binding from concentrations of 0.01 μM up to 10 μM (Fig. 6A).

2.4.7 Selective effects of HB in ORX rats

All steroids that are anabolic are derivatives of testosterone and are androgenic as well as anabolic, as they stimulate growth and function of the male reproductive system. Individual drugs vary in their balance of anabolic/androgenic activity but none of the currently available drugs are purely anabolic (21). Therefore, we examined the ability of HB versus injected testosterone propionate (positive control) to restore androgen-dependent tissues after androgen deprivation in surgically castrated peri-pubertal rat model (56). Oral and subcutaneous treatments at appropriate dose ranges were initiated two weeks after ORX and continued for 10 d. As expected, androgen deprivation caused significant decrease in the size of the prostate, seminal vesicles, bulbocavernosus/levator ani muscle complex, glans penis, and Cowper's gland with these organs shrinking to 8.6%, 6.5%, 23.9%, 54.6%, 40.5%, respectively, of those observed in sham-operated animals (Table 2). Injection of testosterone propionate at 0.4 mg/kg increased the weight of androgen sensitive organs 3- to 8-fold, however it failed to restore ventral prostate, seminal vesicles, and bulbocavernosus/levator ani muscle complex to their original size as compared with sham controls. After 10 d of treatment, oral administration of HB at 20 and 60 mg/kg failed to prevent the loss of androgen sensitive tissue weight associated with ORX, although a slight but significant dose-dependent increase in glans penis was associated with HB treatment (55.3 ± 1.7 mg for H20 and 59.6 ± 1.6 mg for H60 versus 45.7 ± 1.5 mg for control animals). In contrast, HB increased the weight of bulbocavernosus/levator ani muscle complex (the skeletal muscle biomarker of anabolic activity), although the change was not statistically significant. When HB was injected subcutaneously at one- and ten-fold doses relative to positive control in the Hershberger

assay (testosterone propionate at 0.4 mg/kg), androgen sensitive tissue weights did not differ from those of ORX controls with the exception of glans penis and bulbocavernosus/levator ani muscle complex, for which a significant increase was observed at 4 mg/kg HB (Table 2).

In sham animals, oral administration of 20 or 60 mg/kg HB did not modify plasma testosterone levels. As expected, no plasma testosterone was detected following an oral or subcutaneous administration of HB to ORX animals that have virtually no detectable levels of testosterone due to orchiectomy, while a 0.4 mg/kg injection of testosterone propionate partially restored plasma testosterone levels in ORX rats to 20.5% of their original level (Fig. 6B).

2.4.8 Physical performance and muscle fiber distribution in ORX rats

Change in grip strength of lower extremities was significantly larger in ORX animals receiving an oral administration of 60 mg/kg HB for 10 days (0.0851 ± 0.0197 kg versus -0.0143 ± 0.0392 kg for controls). The change in grip strength for the front limbs was also greater in HB-treated animals (Fig. 7A) but did not reach significance (0.2711 ± 0.0660 kg versus 0.1631 ± 0.0405 kg for controls).

As expected, androgen deprivation caused a significant decrease in the gastrocnemius muscle mass to 85.8% of that observed in sham-operated animals (Fig. 7B). Oral administration of HB to ORX rats increased the gastrocnemius muscle mass by 13.8% and 10.3% in HB20 and HB60 animals, respectively, therefore almost restoring the muscle to its original size. At the same time, subcutaneous administration of HB at

doses of one- and ten-fold of the positive control increased gastrocnemius muscle mass by 2.8% and 9.1%, respectively.

To determine the structural events underlying the alterations in muscle mass and function, we analyzed changes in fiber distribution (Fig. 7C) and cross section area (Fig. 7D) using ATPase stain that differentiates between muscle fiber types based upon their oxidative and glycolytic activity. Under these conditions, type I fibers stain black, while type IIb fibers stain dark grey, and type IIa fibers remain pale grey. HB treatment in castrated mice prevented gastrocnemius fiber atrophy and increased median fiber area of type I and type IIa fibers above castrated control levels ($P < 0.001$). Compared with the control animals, fiber type distribution was significantly affected in HB-treated animals (20 or 60 mg/kg per d for 10 d). While the total number of type IIa and type IIb fibers increased by approximately 60% independent of HB dose, the significant increase in number of type I fibers was observed only with a higher dose of HB.

2.5 Discussion

Brassinosteroids are present in small quantities in foods and plants (2). They are similar in many respects to animal steroids, but appear to function very differently at the cellular level. While animal steroid hormones act through a nuclear receptor family of transcription factors, plant brassinosteroids signal through a cell surface receptor kinase-mediated signal transduction pathway (27, 28). In plants, brassinosteroids play an essential role in plant growth and development (23-26), as well as thermotolerance (8). For example, 24-epibrassinolide limited loss and increased the expression level of some of the components of the translational apparatus during heat stress, which was correlated

with a more rapid resumption of cellular protein synthesis (57). Plant growth promoting effects of 28-homobrassinolide, the brassinosteroid used in this study (Fig. 1A), are associated with increased synthesis of nucleic acids and proteins (7, 43). At the same time, brassinosteroids share some similarities with ecdysteroids (Fig. 1C) that have a wide array of physiological and pharmacological effects in animals and insects (58), including modulation of protein synthesis (59) and carbohydrate metabolism (60).

The present study demonstrates a selective anabolic effect of plant brassinosteroid in animals. Our findings suggest that HB dose- and time-dependently stimulated protein synthesis and inhibited protein degradation in L6 rat skeletal muscle cells ($EC_{50} = 4 \mu\text{M}$), in part by inducing Akt phosphorylation (Fig. 2 and 3). The effective HB concentrations that produced Akt activation were comparable with the concentration required to modulate protein synthesis, suggesting that HB involves Akt activation in the stimulation of protein synthesis and suppression of protein degradation. Akt is a serine/threonine kinase that signals downstream of growth factor receptors and phosphoinositide-3 kinase PI3K. Therefore growth factor receptors, nutrients, and even muscle contraction all increase Akt activity (31). Akt stimulates glucose uptake, glycogen synthesis, and protein synthesis via Akt/mTOR and Akt/GSK-3 β signaling networks (32) and inhibits apoptosis and protein degradation in skeletal muscle by inactivating FoxO transcription factors (33). Akt is therefore situated at a critical juncture in muscle signaling where it responds to diverse anabolic and catabolic stimuli. Moreover, both FOXO3a and GSK-3 β modulate transcription of androgen receptor (AR); while the former promotes transcriptional activity of AR (61), the latter acts as its inhibitor (62). At the same time, GSK-3 β also controls cell survival through regulation of β -catenin, one of the key

molecules in Wnt signaling (29), and inhibition of Akt suppresses the Wnt pathway by activation of GSK-3 β and degradation of β -catenin (63). Curiously, brassinosteroid signaling in plants resembles the Wnt pathway and is mediated by GSK3-like kinase (6).

Since our initial data suggested that brassinosteroid might modulate cell survival and growth via Akt activation similar to plant ecdysteroids (64), we performed a set of experiments with known antagonists to further elucidate the signal transduction pathways involved in mediating brassinosteroid effects in mammalian cells. Specifically, we analyzed the effects of triciribine (selective direct inhibitor of the cellular phosphorylation/activation of Akt1/2/3) and LY294002 (competitive inhibitor of the PI3K kinase upstream of Akt). Both treatments abolished the anabolic effects of the brassinosteroid treatment on protein synthesis in muscle cells. Interestingly, when the same experiment was repeated with GO6976 (specific inhibitor of another serine/threonine kinase family, the calcium-dependent protein kinase C isoforms), effect of brassinosteroid treatment on protein synthesis was also reduced to a great extent, suggesting that PKC isozymes may also act as a link between an unknown receptor and Akt activation induced by brassinosteroids. However, neither PD98059 (specific inhibitor of MEK1 kinase that functions in a mitogen activated protein kinase cascade) nor SB203580 (specific inhibitor of p38 MAP kinase homologues) had any measurable effect on brassinosteroid-driven modulation of protein synthesis in muscle cells (Fig. 4). Taken together, we demonstrated that brassinosteroid-mediated protein synthesis in muscle cells is positively influenced by the PI3K/Akt and PKC, but not by MAPK pathways.

This raises an interesting possibility of direct activation of an unidentified mammalian steroid hormone receptor by the brassinosteroid. In addition to classical

nuclear receptor responses, mammalian steroid hormones have been shown to elicit rapid non-genomic signaling events that mediate cell proliferation and survival. For example, cell membrane-localized estrogen receptor has been demonstrated to interact with the regulatory subunit of PI3K and thereby to increase Akt activity (65). Additionally, the putative progesterone G-protein coupled receptor has been cloned, and a putative membrane-bound AR has been suggested (66). A similar receptor may be responsible for the rapid effects of HB in mammalian cells.

Oral 24 d administration of HB to healthy rats selectively increased body weight gain, lean body mass, and gastrocnemius muscle mass as compared to vehicle treated controls (Fig. 5 and Table 1). *In vivo* action of HB on body composition and bone could not be attributed to endogenous testosterone (Fig. 1B) action, as plasma testosterone levels did not differ in response to HB treatment (Fig. 6B). Supplementation of HB-treated animals with a high protein diet enhanced the effect of the lower dose of HB (Table 1). As expected (54), control animals fed a high protein diet (Fig. 5C and D) exhibited decreased body weight gain, food intake, and other body composition parameters compared to control animals fed a normal diet (Fig. 5A and B). Their plasma tryglicerides were also decreased (Table 1). Experiments comparing diets with different protein contents demonstrated favorable changes in body composition for high-protein diets, with part of these alterations being attributed to an increased intake of leucine (67). Since leucine and other branched amino acid do not affect the phosphorylation status of Akt but rather stimulate anabolic signaling in skeletal muscle cells through modulation of mTOR and 4EBP1 phosphorylation (68), we proposed that a high protein diet may potentiate the anabolic effects of HB. Treatment with HB did not modify blood

biochemistry in animals fed either a normal or a high protein diet, with the exception of fasting glucose that was slightly lower in cohorts receiving a higher dose of HB.

HB showed very low androgenic activity when tested in the Hershberger assay (Table 2) and improved physical fitness of untrained ORX rats (Fig. 7). Although HB produced anabolic effects in animals similar to androgens, they seemed to be pharmacologically different, as HB administration (oral or subcutaneous) produced only minimal androgenic side effects, in sharp contrast to powerful androgenic effects of anabolic steroids. The additional observation that HB has low or no significant binding to the androgen receptor and did not modulate plasma testosterone levels (Fig. 6A) suggests that HB may exert its anabolic effect through an androgen-independent mechanism. Even though both HB and androgens contain a similar steroid backbone, there are major structural differences that distinguish the two classes of compounds, including the lactone function at C6/C7, the two hydroxyls at C2 and C3, and the methyl substitution at C24. These chemical differences may restrict HB from activating the nuclear androgen receptor and explain the difference in pharmacological responses. It cannot be ruled out that HB administration could change the abundance or phosphorylation status of the androgen receptor by modulating FOXO3a and GSK-3 β signaling networks downstream of Akt (61, 62). However, the differential effect of HB on physical fitness of front and hind limbs of untrained rats (Fig. 7) seems to indicate that a stronger pharmacological response was observed in the hind limb area where the abundance of the androgenic receptor is typically lower in males (69).

Skeletal muscle shows plasticity and can undergo conversion between different fiber types in response to exercise training, modulation of motoneuron activity, or

castration (55). In this study we show that a 10 d oral administration of HB to castrated animals led to substantial increases in the total number of myofibers and the cross-sectional area of oxidative type I and type IIa muscle fibers important for increased physical performance and endurance.

HB was safe in rats when tested at doses up to 1000 mg/kg (13). At the same time, brassinosteroids caused cell cycle arrest and apoptosis of human breast cancer cells when tested at doses above 30 μ M, without affecting the normal non-tumor cell growth of BJ fibroblasts (11). This effect is similar to classical mammalian steroid hormones that either inhibit or induce apoptosis in the concentration- or tissue-specific manner (70).

In conclusion, we hypothesize that HB may exert its anabolic effect by stimulating protein synthesis and inhibited protein degradation in muscle cells, in part by inducing PI3K/Akt signaling. Stimulatory effects of HB on protein synthesis in muscle cells subsequently translates into whole body anabolic effects, such as increases in lean body mass, muscle mass and physical performance. Moreover, our data demonstrate that oral application of HB triggers an anabolic response with minimal or no androgenic side effects. This property may pharmacologically differentiate HB from anabolic steroids.

2.6 Acknowledgments

The authors thank Dr. David Lagunoff (NJMS-UMDNJ, Newark, NJ) for muscle histology and microscopic imaging. This work was supported in part by the NIH Center for Dietary Supplements Research on Botanicals and Metabolic Syndrome, grant 1-P50 AT002776-01; and the Fogarty International Center of the NIH grant U01 TW006674 for the International Cooperative Biodiversity Groups and Rutgers University.

Table 1. Body composition and blood biochemistry of rats treated with HB.

	Normal diet			High protein diet		
	Control	HB20	HB60	Control	HB20	HB60
Body weight, g	308.8 ± 4.2	324.3 ± 11.5	342.3 ± 4.9*	316.9 ± 6.5	337.6 ± 6.4	335.8 ± 5.1
Body weight gain, g	107.0 ± 2.9	126.6 ± 7.1	135.7 ± 9.4*	76.2 ± 5.7	98.3 ± 5.2*	91.1 ± 3.2*
Lean mass, g	250.8 ± 9.1	268.3 ± 9.0	286.5 ± 4.3*	232.8 ± 6.9	246.8 ± 7.4	258.6 ± 2.7*
Fat mass, g	51.0 ± 5.9	49.0 ± 4.3	48.5 ± 3.8	62.7 ± 1.6	68.6 ± 3.1	61.2 ± 3.8
Bone mineral content, g	7.1 ± 0.2	7.0 ± 0.3	7.4 ± 0.1	7.0 ± 0.1	7.5 ± 0.2	7.4 ± 0.1
Gastrocnemius muscle, g	1.79 ± 0.06	2.07 ± 0.06	2.13 ± 0.12*	1.90 ± 0.04	1.98 ± 0.01	2.17 ± 0.03***
Glucose, mM	5.0 ± 0.2	5.1 ± 0.5	4.5 ± 0.3	5.2 ± 0.1	5.1 ± 0.2	4.8 ± 0.2
Insulin, ng/ml	1.92 ± 0.16	2.39 ± 0.58	2.65 ± 0.45	1.80 ± 0.27	2.39 ± 0.34	2.38 ± 0.41
Cholesterol, mg/dl	69.0 ± 3.2	69.9 ± 6.0	84.2 ± 5.3	89.2 ± 4.2	97.5 ± 6.0	87.4 ± 2.9
Triglycerides, mM	1.9 ± 0.2	1.8 ± 0.2	1.8 ± 0.5	1.4 ± 0.1	1.2 ± 0.1	1.3 ± 0.1

Rats were fed either normal (23.9% protein content) or high protein (39.4% protein content) diet, and gavaged daily with 20 or 60 mg/kg body weight HB for 24 d. Body composition was measured by DEXA. Results are expressed as the mean ± SEM (* P<0.05, ** P<0.01, *** P<0.001 when compared with the appropriate control by one-way ANOVA and Dunnett's post-test).

Table 2. Weights of androgen-sensitive tissues from sham and ORX rats treated with HB.

Admini- stration	Treatment group	Ventral prostate, mg	Seminal vesicles, mg	Bulbocavernosu s/levator ani, mg	Glans penis, mg	Cowper's gland, mg
Oral	Sham	222.5 ± 15.2***	515.0 ± 12.9***	517.0 ± 10.5***	83.7 ± 0.8***	26.7 ± 1.8***
	ORX	19.2 ± 2.5	33.3 ± 3.0	123.7 ± 6.8	45.7 ± 1.5	10.8 ± 1.3
	ORX + HB20	26.0 ± 2.5	37.3 ± 3.5	109.2 ± 8.6	55.3 ± 1.7*	11.2 ± 0.7
	ORX + HB60	23.0 ± 2.4	34.7 ± 3.3	137.7 ± 9.9	59.6 ± 1.6**	12.5 ± 1.1
	ORX + TP0.4 ¹	110.50 ± 9.5***	262.5 ± 12.5***	382.0 ± 22.0***	93.8 ± 4.2***	34.5 ± 4.7***
Subcu- taneous	ORX	22.2 ± 3.1	27.8 ± 1.3	109.2 ± 6.4	41.3 ± 2.6	11.3 ± 0.7
	ORX + HB0.4	18.3 ± 1.2	29.0 ± 3.1	131.3 ± 7.1	50.7 ± 1.9	11.3 ± 0.5
	ORX + HB4	23.2 ± 1.2	30.2 ± 1.2	147.5 ± 6.9*	56.3 ± 3.3*	10.5 ± 0.3
	ORX + TP0.4	92.8 ± 6.3***	228.7 ± 35.3	293.8 ± 19.0***	72.3 ± 4.5***	34.3 ± 1.9***

Rats were fed normal diet (23.9% protein content) and gavaged daily with 20 or 60 mg/kg body weight HB or subcutaneously injected with 0.4 and 4 mg/kg body weight HB for 10 d. Results are expressed as the mean ± SEM (* P<0.05, ** P<0.01, *** P<0.001 when compared with ORX by one-way ANOVA and Dunnett's post-test). ¹Testosterone propionate (TP) was given as subcutaneous injection at 0.4 mg/kg and served as a positive control.

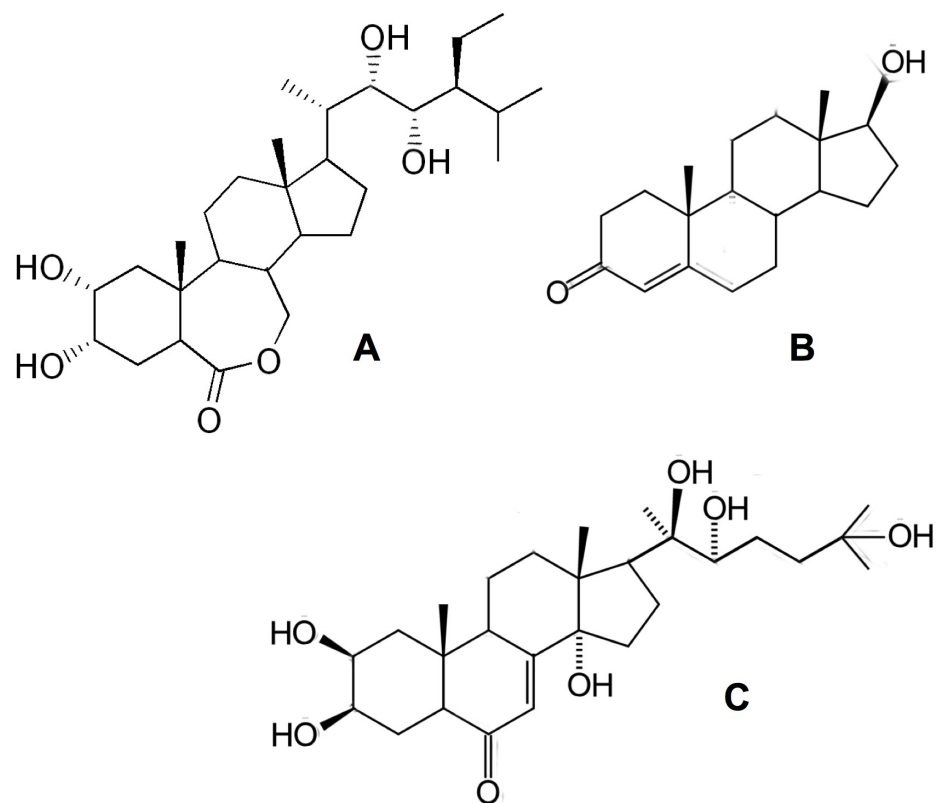


Figure 1. Chemical structure of (A) 28-homobrassinolide, HB in comparison with (B) testosterone and (C) 20-hydroxyecdysone.

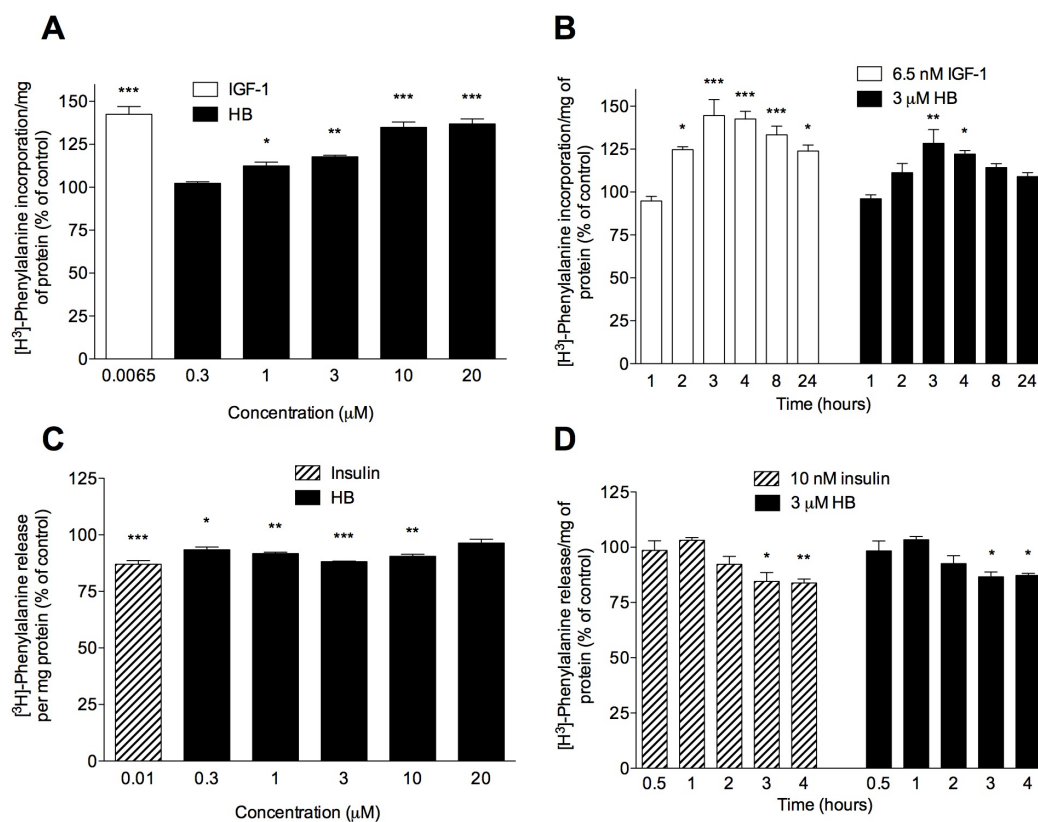


Figure 2. Concentration- and time-dependent effects of HB on protein synthesis and degradation in L6 rat myotubes. (A) Cells were incubated for 4 h with [^3H]-phenylalanine and treated in triplicate with vehicle (0.1% ethanol), increasing concentrations of HB, or 6.5 nM of IGF-1 as a positive control and protein synthesis was measured as the incorporation of [^3H]-phenylalanine into protein normalized by total protein (B) To measure the time-dependent effect of HB treatment on protein synthesis, cells were treated with 3 μM HB or 6.5 nM IGF-1 for 1-24 h. (C) Dose-dependent effect of HB on protein degradation was observed in cells labeled overnight with [^3H]-phenylalanine and subsequently treated for 4 h with increasing concentrations of HB or 10 nM of insulin as a positive control, and then protein degradation was measured as the release of acid-soluble [^3H]-phenylalanine into media. (D) For the HB time course study of protein degradation, fully differentiated myotubes were treated with 3 μM HB or for 1-4 h. Results are expressed as the mean \pm SEM of determinations performed in triplicate (* $P < 0.05$, ** $P < 0.01$, *** $P < 0.001$ when compared with the control by one-way ANOVA and Dunnett's post-test).

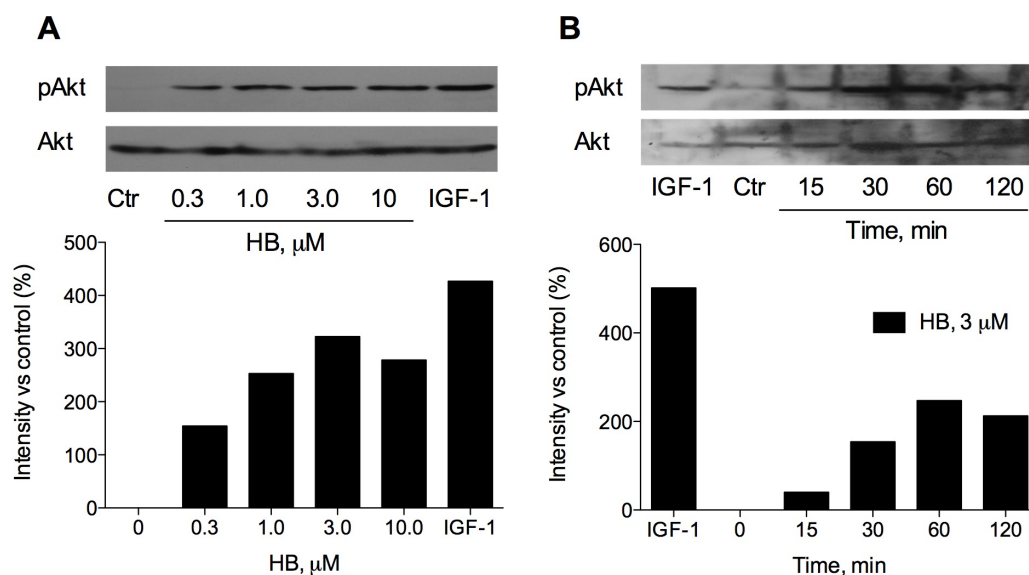


Figure 3. HB increases Akt (Ser473) phosphorylation in L6 myotubes. (A) Representative immunoblot of Akt phosphorylation stimulated with increasing doses of HB or 6.5 nM IGF-1 as a positive control. (B) Representative immunoblot of time-dependent Akt phosphorylation in response to 3 μ M HB or 15 min exposure to 6.5 nM IGF-1 as a positive control. Cells were treated with indicated doses of HB and cell lysates were then analyzed by immunoblotting with phospho- and nonphospho-specific antibodies. Phospho-Akt (pAkt) bands were quantified by ImageJ software, normalized to unphosphorylated protein and depicted as a relative increase in band intensity compared to control lysate.

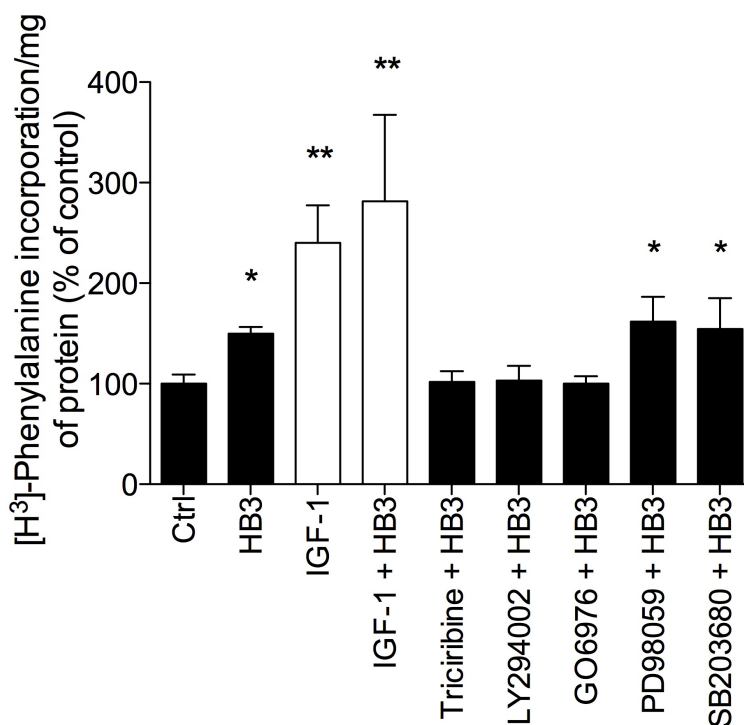


Figure 4. Stimulation of protein synthesis by HB depends on PI3K/Akt and PKC, but not on MAPK signaling. Pretreatment with Akt inhibitor triciribine (20 mM), PI3K inhibitor LY294002 (25 mM), and PKC inhibitor GO6976 (10 nM) inhibited HB-mediated (3 mM) protein synthesis in L6 rat skeletal muscle cells, while MEK1 inhibitor PD98059 (2 mM) and p38 MAPK inhibitor SB203580 (50 nM) had no effect. IGF-1 (6.5 nM) served as a positive control. The figure represents an average of 3 independent experiments \pm SEM (* $P < 0.05$, ** $P < 0.01$ when compared to vehicle-treated animals by one-way ANOVA and Dunnett's post-test).

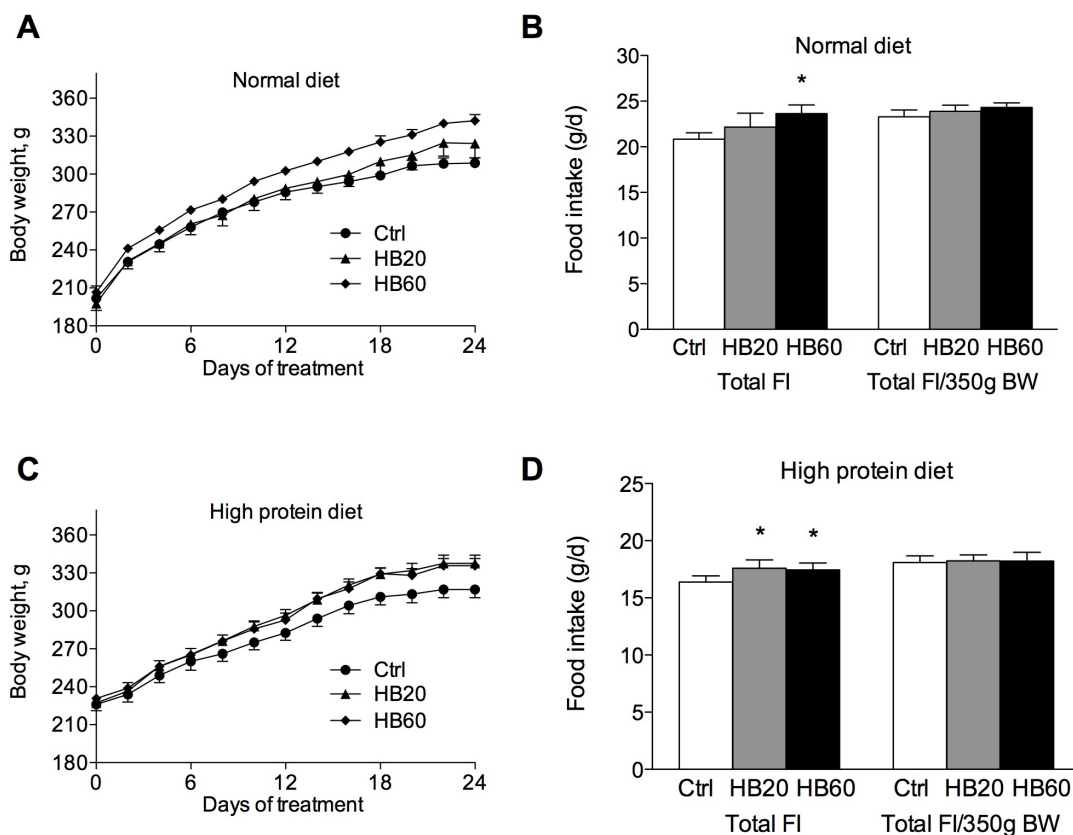


Figure 5. Effect of HB on body weight gain and food intake in rats fed normal (A-B) and high protein diet (C-D). Animals received 20 (HB20) or 60 (HB60) mg/kg body weight HB daily for 24 d. Food intake (FI) was recorded daily and cumulative food intake was normalized for 350 g body weight. Results are expressed as the mean \pm SEM (* $P < 0.05$ when compared to vehicle-treated animals by one-way ANOVA and Dunnett's post-test). Body weight gain was analyzed by two-factor repeated-measures ANOVA, with time and treatment as independent variables.

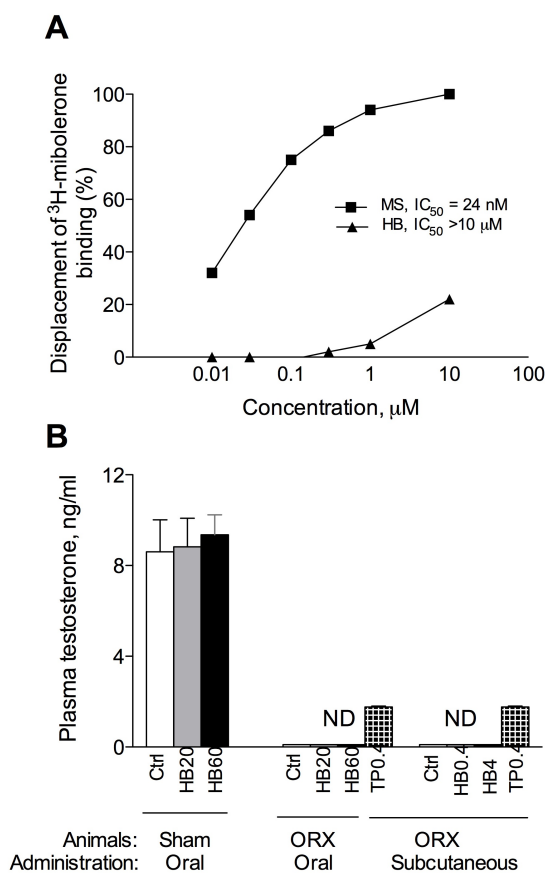


Figure 6. HB has low androgenic activity. (A) Increasing concentrations of HB or methandrostenolone (positive control, $IC_{50} = 24$ nM) were incubated in the presence of the specific androgen receptor binding ligand [³H]-mibolerone for 4 h at 4 °C and DPMs of the incubation buffer were measured to quantify displacement of the ligand. (B) Oral or subcutaneous administration of HB to intact or ORX rats did not affect plasma testosterone levels in animals. Sham-operated or ORX animals received either 20 or 60 mg/kg HB daily for 10 d orally, or 0.4 and 4 mg/kg HB daily for 10 d via subcutaneous injection. No plasma testosterone was detected (ND) in ORX animals and ORX animals treated with HB as compared to a positive control, a subcutaneous injection of 0.4 mg/kg testosterone propionate daily for 10 d. Results are expressed as the mean \pm SEM (* $P < 0.05$ when compared to vehicle-treated animals by one-way ANOVA and Dunnett's post-test).

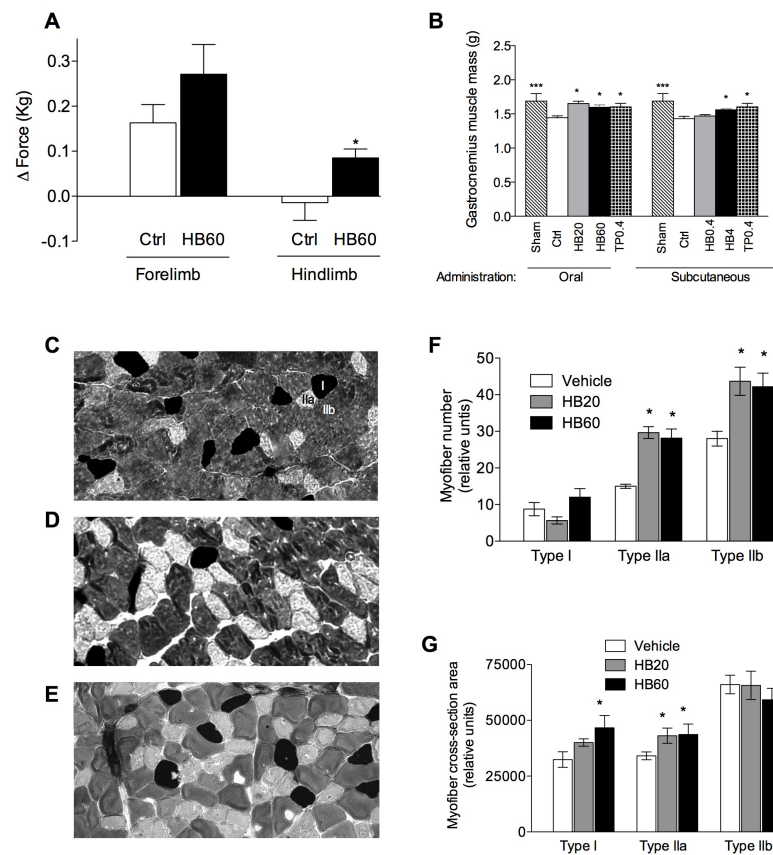


Figure 7. HB increases physical fitness of untrained ORX rats (A), increases mass of mixed-fiber gastrocnemius muscle (B), and induces favorable changes in myofiber type distribution and cross-section area (C-G). ORX rats received vehicle, 20 or 60 mg/kg HB daily for 10 d orally. At the end of the study, the grip strength of hind- and forelimbs of the castrated animal was measured using a digital force gauge. The gastrocnemius muscle was excised, weighed, and the serial transverse cryosections of the middle section of the muscle of vehicle-treated animals (C), or animals receiving 20 (D) or 60 (E) mg/kg HB were stained for mATPase activity to analyze myofiber type distribution (F) and cross-section area (G). Results are expressed as the mean \pm SEM (* $P < 0.05$ when compared to vehicle-treated animals by one-way ANOVA and Dunnett's post-test).

CHAPTER III**AKT-DEPENDENT ANABOLIC ACTIVITY OF NATURAL AND SYNTHETIC
BRASSINOSTEROIDS IN RAT SKELETAL MUSCLE CELLS**

Published in: J Med Chem (2011) 54: 4057-4066

3.1 Abstract

Brassinosteroids are plant-derived polyhydroxylated derivatives of 5α -cholestane, structurally similar to cholesterol-derived animal steroid hormones and insect ecdysteroids. In this study, we synthesized a set of brassinosteroid analogues of a natural brassinosteroid (22S,23S)-homobrassinolide (HB, **1**) including (22S,23S)-homocastasterone (**2**), (22S,23S)- 3α -fluoro-homobrasinolide (**3**), (22S,23S)- 3α -fluoro-homocastasterone (**4**), (22S,23S)-7-aza-homobrassinolide (**5**), (22S,23S)-6-aza-homobrassinolide (**6**), and studied their anabolic efficacy in L6 rat skeletal muscle cells in comparison to other synthetic and naturally occurring brassinosteroids (22R,23R)-homobrassinolide (**7**), (22S,23S)-epibrassinolide (**8**), and (22R,23R)-epibrassinolide (**9**). Presence of the 6-keto group in the B ring and stereochemistry of $22\alpha,23\alpha$ -vicinal hydroxyl groups in the side chain were critical for anabolic activity, possibly due to higher cytotoxicity of the $22\beta, 23\beta$ -hydroxylated brassinosteroids. All anabolic brassinosteroids tested in this study selectively activated the PI3K/Akt signaling pathway as evident by increased Akt phosphorylation *in vitro*. Plant brassinosteroids and their synthetic derivatives may offer a novel therapeutic strategy for promoting growth, repair, and maintenance of skeletal muscles.

3.2 Introduction

Brassinosteroids are plant-specific polyhydroxylated derivatives of 5α -cholestane, structurally similar to cholesterol-derived animal steroid hormones and ecdysteroids from insects. They are found at low levels in pollen, seeds, leaves, and young vegetative tissues throughout the plant kingdom (2). Similar to animal steroid hormones (24),

brassinosteroids regulate the expression of specific plant genes and complex physiological responses involved in growth (25), partly via interactions with other hormones setting the frame for brassinosteroid responses (26). While animal steroid hormones are perceived by the nuclear receptor family of transcription factors, brassinosteroids signal through a cell surface receptor kinase-mediated signal transduction pathway (27, 28).

The (22S,23S)-28-homobrassinolide (HB, Fig. 1) is one of the most active brassinosteroids in inducing plant growth in various plant bioassay systems (39). The growth promoting effect of HB in plants is associated with the increased synthesis of nucleic acids and proteins (7, 43), and activation of total protein synthesis in plants subjected to heat shock (8). Due to the practical use of HB for increasing yield production, efforts are being made towards its synthesis (71, 72). Brassinosteroids have a favorable safety profile, since no treatment-related effect was observed at doses up to 4000 mg/kg when applied orally for epibrassinolide (12) or HB (13). Natural brassinosteroids also inhibited growth of several human cancer cell lines without affecting the growth of normal cells (11).

The natural brassinosteroid and their synthetic analogues that have been identified so far have a common 5- α -cholestane skeleton and their structural variations come from the type and position of functional groups on the skeleton and the stereochemistry present in the A and B rings and the side chain (73). Recent structure-activity studies of brassinosteroids in the rice leaf lamina inclination bioassay have revealed that the 5- α -configuration is required for optimum activity, but the B-ring tolerates considerable variation, providing that the presence of a polar functional group is maintained (74).

Structure-activity studies have also demonstrated that the (2 α , 3 α)- and (22R, 23R)-vicinal diol moieties are required for optimum bioactivity in plants (75). Although the structural requirements for biological activity in plants have been clearly recognized, a number of compounds bearing minor to major structural modifications retained potent plant growth promoter activity (76).

In the previous study we found that orally applied HB produced significant anabolic effects and improved physical fitness in healthy animals with minimal androgenic effects (77). The importance of identifying novel agents that influence muscle growth, development, or regeneration with possible therapeutic application for the age or disease-related skeletal muscle atrophy prompted us in this study to explore, for the first time, the structure-activity relationship between HB and its natural and synthetic analogues and their effects on protein synthesis and degradation in rat skeletal muscle cells.

3.3 Materials and methods

3.3.1 Chemicals and analytical methods

Structures of HB and its analogues used in this study are shown in Figure 1. HB [(22R, 23R, 24S)-2 α , 3 α , 22,23-tetrahydroxy-24 ethyl- β -homo-7-oxo-5 α -cholestane-6-one] (**1**) was purchased from Waterstone Technology (Carmel, IN). (22R,23R,24S)-2 α ,3 α ,22,23-tetrahydroxy-B-homo-7-oxa-5 α -cholestan-6-one (**7**), (22S,23S,24R)-2 α ,3 α ,22,23-tetrahydroxy-24-methyl-B-homo-7-oxa-5 α -cholestan-6-one (**8**), and (22R,23R,24R)-2 α ,3 α ,22,23-tetrahydroxy-24-methyl-B-homo-7-oxa-5 α -cholestan-6-one

(9) were purchased from SciTech (Praha, Czech Republic). Structures and purity (>95%) of all compounds were confirmed by Varian 1200 L (Varian, Palo Alto, CA) triple quadrupole mass detector with electrospray ionization (ESI) interface using a Dionex Acclaim RSLC 120 C18 reverse phase column (150 mm × 2.1 mm, 2.2 μm), ¹H NMR, and ¹³C NMR spectra recorded on Varian 400, 500 MHz & Bruker Avance 950 MHz spectrophotometer.

L-[2,3,4,5,6-³H]-phenylalanine was obtained from GE Healthcare (Piscataway, NJ). Phospho-Akt and Akt mAbs were purchased from Cell Signaling Technology (Danvers, MA). All other chemicals and cell culture media were obtained from Invitrogen (Carlsbad, CA) and Sigma (Saint Louis, MO) unless otherwise specified.

3.3.2 Synthesis of brassinosteroid analogues

Steroidal-3 α ,5-cyclo-6-one and steroidal-2-en-6-one were synthesized from stigmasterol using a previously reported procedure with modifications as shown on Supporting Fig. 1. Stigmasterol (4.85 mmol, 2.0 g) was dissolved in methyl ethyl ketone (140 ml) and triethylamine (14.5 mmol, 1.47 g, 2.4 ml, 3 eq) was added and stirred for 10 min at room temperature; then the reaction mixture was cooled to 5°C. Methanesulfonylchloride (1.112 g, 1.0 ml, 2 eq) was added dropwise to the mixture at 5°C. After stirring for 1.5 h, a 15% sodium chloride solution (20 ml) was added to the mixture, the organic layer was separated and washed with a saturated sodium bicarbonate, brine solution and dried over anhydrous sodium sulphate and concentrated to dryness (2.80 g). This crude product **1a** was dissolved in methyl ethyl ketone (50 ml) and stirred with water (16 ml); then potassium bicarbonate (9.7 mmol, 0.972 g, 2 eq) was

added and refluxed at 120 °C for 5 h. The organic layer was separated and washed with brine, dried over anhydrous sodium sulphate, and concentrated (2.01 g). This crude product **1b** was dissolved in methyl ethyl ketone (35 ml) and cooled to 0°C. Jones reagent (1.05 ml) was added dropwise to the reaction mixture and stirred for 3 h at the same temperature. After adding a 15% sodium chloride solution (17 ml), the organic layer was separated and washed with a saturated aqueous sodium bicarbonate solution, and a brine solution, dried over anhydrous sodium sulphate, and concentrated in vacuo. The crude 3α , 5-cyclo-6-one (compound **1c**) was chromatographed over silica gel with hexane/ethyl acetate (97:3) as eluent, yielding 54% from stigmasterol. The purity of the compound was confirmed by TLC using Hexane: EtOAc (80:20) as the developing solvent ($R_f = 0.7$).

Compound **1c** (5.6 mmol, 2.315 g) was dissolved in dimethyl formamide (23 ml) and stirred. P-toluenesulfonic acid (1.13 mmol, 0.214 g, 0.2 eq) and sodium bromide (2.82 mmol, 0.29 g, 0.5 eq) were added and heated under reflux for 3 h. The cooled reaction mixture was concentrated to dryness in vacuo and ethyl acetate (150 ml) was added to the reaction mixture, washed with water (100 ml), a saturated sodium bicarbonate solution, and brine solution, dried over anhydrous sodium sulphate, and concentrated. The crude compound **1d** was chromatographed over silica gel with hexane/ethyl acetate (98:2) as an eluent, yielding 81.6%. The purity of the compound was confirmed by TLC [Hexane: EtOAc (90:10); $R_f = 0.68$] and ESI-MS (m/z): 411.39 (M+1).

3.3.3 Synthesis of (22S, 23S, 24S)- 2α , 3α , 22, 23-tetrahydroxy-24-ethyl- 5α -cholestan-6-one

(22S, 23S)-homocastasterone (**2**) was synthesized according to the reported procedure with following modifications. The solution of ruthenium tetroxide was prepared by adding a solution of sodium m-periodate (782 mg, 3.6 mmol) in water (2.9 ml) to ruthenium trichloride trihydrate (45 mg, 0.17 mmol). Half of the ruthenium tetroxide solution was added at once to a stirred solution of diene (0.5 g, 1.22 mmol) in ethyl acetate (17 ml), acetone (7.3 ml), and acetonitrile (7.3 ml) at 4 °C. After 5 min, the remaining half of the ruthenium tetroxide solution was added, and the reaction mixture was stirred at 5-6 °C for a further period of 5 min. Then, a 20% sodium metabisulphite solution (12 ml) was added to the reaction mixture and stirred for 5 min. Solvents were evaporated and the residue was extracted with ethyl acetate (3 X 100 ml). The combined ethyl acetate layer was washed with water, and a brine solution and dried over anhydrous sodium sulphate and concentrated. The crude product was purified by column chromatography on a silica gel using chloroform/methanol (95:5) as the eluent, yielding 54.0%. The purity of the compound was confirmed by TLC using CHCl₃: CH₃OH (90:10); (R_f = 0.45), ESI-MS: (m/z) 479.35 (M+1) and ¹H NMR (400MHz, CDCl₃): δ = 0.70 (s, 3H), 0.76 (s, 3H), 0.88 (d, 3H, J = 6.9 Hz), 0.96 (m, 6H), 1.04 (d, 3H, J = 6.9 Hz), 2.30 (dd, 2H, J = 13.1, 4.5 Hz), 2.68 (dd, 1H, J = 12.1, 3.0 Hz), 3.60 (d, 2H, J = 7.3 Hz), 3.77 (dd, 1H, J = 6.9, 3.3 Hz), 4.05 (br, s, 1H). ¹³C NMR (100 MHz, CDCl₃): δ = 11.9, 13.5, 13.9, 14.1, 14.5, 17.7, 18.5, 21.2, 21.7, 24.2, 26.3, 26.9, 27.8, 37.6, 39.3, 39.9, 42.3, 42.5, 43.4, 49.6, 50.7, 52.6, 53.7, 56.3, 68.3, 68.4, 70.6, 72.1, 211.9.

3.3.4 Synthesis of (22S, 23S, 24S)-3 α -fluoro-22, 23-dihydroxy-24-ethyl-5 α -cholestan-6-one and (22S, 23S, 24S)-3 α -fluoro-22, 23-dihydroxy-7-oxo-24-ethyl-5 α -cholestan-6-one

Two brassinosteroid analogues containing a fluorine atom in the 3 α position were prepared using standard operations with the following modifications (Supporting Fig. 2). The compound **1c** (2.0 g, 4.88 mmol) was dissolved in 1,4-dioxane (42 ml). To this solution, 7.5 ml of 1M sulphuric acid was added and refluxed at 110 °C for 12 h. After cooling to room temperature, potassium carbonate (0.70 gm, 1.05 eq) was added and stirred for 30 min and most of the solvents was evaporated in vacuum. After dilution with brine solution (40 ml), the product formed a white precipitate that was filtered off, washed with water and dried. The crude product **2a** was purified by flash column chromatography using silica gel as an adsorbent and eluted with hexane/ethyl acetate (75:25), yielding 59%. The purity of the compound was confirmed by TLC using Hexane: EtOAc (90:10) solvent (R_f = 0.28) and ESI-MS: (m/z) 429.32 (M+1).

Next, DAST (1.38 g, 1.12 ml, 8.55 mmol) was dissolved in dichloromethane (8.4 ml) and stirred at -78 °C. The solution of **2a** (1.2 g, 2.8 mmol) in dichloromethane (50 ml) was added to DAST solution slowly. After 10 min, the reaction mixture was warmed to room temperature and maintained for 5 min. The reaction mixture was poured into water and extracted with dichloromethane (2 X 100 ml). The combined dichloromethane layer was washed with a saturated sodium bicarbonate solution, and a brine solution, dried over anhydrous sodium sulphate, and concentrated. Purification of the crude product by flash column chromatography using silica gel and eluting with hexane/ethyl

acetate (98.5:1.5) yielded 26.14% of **2b**. The purity of the compound was confirmed by TLC using Hexane: EtOAc (80:20) solvent ($R_f = 0.7$) and ESI-MS (m/z): 431.56 ($M+1$).

Then, the solution of ruthenium tetroxide was prepared by adding a solution of sodium m-periodate (558 mg, 2.6 mmol) in water (2.1 ml) to ruthenium trichloride trihydrate (31 mg, 0.12 mmol). To a stirred solution of **2b** (0.375 g, 0.87 mmol) in ethyl acetate (12.75 ml), acetone (5.5 ml), and acetonitrile (5.5 ml) at 4°C were added to half of the ruthenium tetroxide solution at once. After 5 minutes the remaining half of the ruthenium tetroxide solution was added and the reaction mixture was stirred at 5-6°C for a further period of 5 min. 20% sodium metabisulphite solution (9 ml) was then added to the reaction mixture and continued the stirring for 5 min. All the solvents were evaporated and the residue was extracted with ethyl acetate (3 X 100 ml). The combined ethyl acetate layer was washed with water, brine solution and dried over anhydrous sodium sulphate and concentrated. The crude product was purified by column chromatography on a silica gel using hexane/ethyl acetate (85:15) as the eluent, yielding 45.0% of **4**. The purity of the compound was confirmed by TLC using Hexane: EtOAc (2:1) solvent ($R_f = 0.58$) and ESI-MS (m/z): 465.34 ($M+1$) and ^1H NMR (500 MHz, CDCl_3): $\delta = 0.71$ (s, 3H), 0.74 (s, 3H), 0.88 (d, 3H, $J = \text{Hz}$), 0.96 (m, 6H), 1.04 (d, 3H, $J = 6.9$ Hz), 2.32 (dd, 1H, $J = 13.1, 4.5$ Hz), 2.63 (dd, 1H, $J = 12.6, 3.0$ Hz), 3.61 (d, 2H, $J = 5.0$ Hz), 4.91 (d, 1H, $J = 48.3$). ^{13}C NMR (125 MHz, CDCl_3): $\delta = 11.9, 12.2, 12.3, 14.1, 14.5, 17.7, 18.5, 21.1, 21.7, 24.2, 26.9, 27.8, 31.9, 37.9, 39.4, 41.2, 42.3, 42.5, 43.4, 46.7, 49.6, 51.9, 52.6, 53.6, 56.3, 70.6, 72.1, 87.8, 211.7$.

The solution of **4** (100 mg, 0.22 mmol) in dichloromethane (4 ml) was added dropwise to a stirred solution of trifluoroacetic acid (2.2 mmol, 10 eq, prepared from

30% aqueous hydrogen peroxide (0.25 ml) and trifluoroacetic anhydride (1.5 ml) in dichloromethane (4 ml) at 0°C. After 1 h, the reaction mixture was warmed to room temperature and maintained for 1 h. The reaction mixture was diluted with dichloromethane (10 ml) and the resulting solution was washed with saturated sodium bicarbonate solution, saturated sodium bisulphite, and a brine solution, dried over anhydrous sodium sulphate, and concentrated. The crude product was purified by column chromatography on silica gel using hexane/ethyl acetate (80:20) as the eluent, yielding 19.0% of **3**. The purity of the compound was confirmed by TLC using Hexane: EtOAc (2:1) solvent ($R_f = 0.26$) and ESI-MS (m/z): 481.30 ($M+1$).

3.3.5 Synthesis of (22S,23S,24S)-2 α ,3 α ,22,23-tetraacetoxy-24-ethyl-B-homo-6-aza-5 α -cholestan-6-one

Two brassinosteroid analogues containing 6-aza and 7-aza substitutions in the B ring were prepared using previously published methods with the following modifications (Supporting Fig. 3-4). Acetic anhydride (2 ml) and DMAP (15 mg, 0.125 mmol) were added to the solution of **2** (600 mg, 1.25 mmol) in dry pyridine (4 ml). The reaction mixture was stirred at room temperature for 16 h, poured into ice water and extracted with ethyl acetate (50 ml X 2). The organic layer was washed with dilute HCl, saturated NaHCO₃ solution, brine solution, and dried over anhydrous sodium sulphate. The crude **3a** was purified by flash column chromatography using silica gel and hexane/ethyl acetate (90:10) to yield 700 mg. The purity of the compound was confirmed by TLC using Hexane: EtOAc (2:1) solvent ($R_f = 0.3$) and ESI-MS (m/z): 647.58 ($M+1$).

Compound **3a** (200 mg, 0.31 mmol) was dissolved in glacial acetic acid (5 ml) and methanesulphonic acid (298 mg, 0.24 ml, 3.1 mmol) and sodium azide (40 mg, 0.512 mmol) were added and stirred at room temperature. After 4 h, the reaction mixture was poured into a saturated sodium bicarbonate solution and extracted with ethyl acetate (50 ml X 3). The combined ethyl acetate extracts were washed with brine solution and dried over anhydrous sodium sulphate. This crude compound was chromatographed over silica gel and eluted with dichloromethane/methanol (98:2) yielding 73% of **3b**. The purity of the compound was confirmed by TLC using CHCl₃: CH₃OH (90:10) solvent ($R_f = 0.57$) and ESI-MS (m/z): 662.68 (M+1).

Next, the solution of **3b** (150 mg, 0.23 mmol) and a 40% sodium hydroxide solution (3 ml) in methanol (8 ml) was refluxed for 1 h and cooled to room temperature. The reaction mixture was neutralized with 6M HCl in aqueous methanol, followed by removal of methanol in vacuo. The aqueous extract was extracted with ethyl acetate (50 ml X 3), and the combined ethyl acetate extracts were washed with water, and a brine solution, and dried over anhydrous sodium sulphate. The crude compound **5** was purified by flash column chromatography using silica gel with dichloromethane/methanol (98:2) as the eluent, yielding 70%. The purity of the compound was confirmed by TLC using CHCl₃: CH₃OH (90:10) solvent ($R_f = 0.2$) and ESI-MS (m/z): 494.32 and ¹H NMR (500MHz, CD₃OD): $\delta = 0.76$ (s, 3H), 0.86 (s, 3H), 0.96 (m, 6H), 1.03 (d, 3H, $J = 6.9$ Hz), 2.05 (m, 1H), 2.13 (dtd, 1H, $J = 9.4, 6.9, 2.4$ Hz), 2.21 (d, 1H, $J = 13.3$ Hz), 2.44 (m, 1H), 3.55 (dd, 2H, $J = 8.5, 5.6$ Hz), 3.60 (ddd, 1H, $J = 7.0, 6.0, 3.3$ Hz), 3.73 (dd, 1H, $J = 12.2, 4.8$ Hz), 3.92 (m, 1H). ¹³C NMR (125 MHz, CD₃OD): $\delta = 10.8, 12.1, 13.3, 13.6, 14.4,$

16.6, 17.3, 18.4, 21.1, 22.4, 25.6, 26.7, 27.4, 34.3, 34.4, 39.7, 39.9, 42.5, 42.9, 49.6, 52.5, 53.1, 55.2, 58.6, 67.8, 68.2, 70.0, 71.7, 178.2.

3.3.6 Synthesis of (22S,23S,24S)-2 α ,3 α ,22,23-tetrahydroxy-24-ethyl-B-homo-7-aza-5 α -cholestan-6-one

NBS (207 mg, 1.16 mmol) and NaHSO₄.SiO₂ (100 mg, activated at 120 °C for 48 h) were added to a solution of **3a** (500 mg, 0.77 mmol) in diethyl ether (15 ml), and stirred at room temperature. After 2.5 h, the reaction mixture was filtered to remove silica and diluted with diethyl ether (100 ml). The crude **4a** was washed with a saturated sodium bicarbonate solution, and a brine solution, and dried over anhydrous sodium sulphate.

Compound **4a** (450 mg, 0.565 mmol) was dissolved in 75% pyridine (16 ml) and 1M NaOH (0.88 ml, 1.5 eq) was added slowly at room temperature. After 4 h, the reaction mixture was poured into an ice cooled 1M HCl solution (200 ml) and extracted with ethyl acetate (100 ml X 2). The combined ethyl acetate extracts were washed with a saturated sodium bicarbonate solution, and a brine solution and dried over anhydrous sodium sulphate. The crude **4b** was chromatographed over silica gel and eluted with hexane/ethyl acetate (85:15) yielding 32%.

NaIO₄ (100 mg, 0.453 mmol) was added to a solution of **4b** (100 mg, 0.151 mmol) in acetic acid (4.5 ml) and stirred well at room temperature. After 18 h, the reaction mixture was diluted with diethyl ether (100 ml), washed with a brine solution and dried over anhydrous sodium sulphate. The crude product was dissolved in methanol (4 ml), followed by addition of ammonium acetate (235 mg) and sodium

cyanoborohydride (8 mg). The reaction mixture was stirred for 110 h at room temperature. Next, the mixture was diluted with water (25 ml), extracted with ethyl acetate (50 ml X 3), and the combined ethyl acetate extracts were washed with water, and a brine solution and dried over anhydrous sodium sulphate. This crude **4c** was chromatographed on a silica gel and eluted with dichloromethane/methanol (85:15) yielding 20%. The purity of the compound was confirmed by TLC using CHCl₃: EtOAc (2:1) solvent ($R_f = 0.45$) and ESI-MS (m/z): 662.68 (M+1).

Next, a 40% NaOH solution (0.5 ml) was added to the solution of **4c** (20 mg, 0.03 mmol) in methanol (5 ml) and refluxed for 30 min. After cooling, the mixture was neutralized by addition of an ice-cold solution of 6M HCl in aqueous methanol and concentrated to remove methanol in vacuo. The remaining aqueous layer was diluted with water (10 ml), extracted with ethyl acetate (40 ml X 2), and the combined ethyl acetate extracts were washed with water, and a brine solution and dried over anhydrous sodium sulphate. The resulting **6** was chromatographed on silica gel and eluted with dichloromethane/methanol (97:3) yielding 53%. The purity of the compound was confirmed by TLC using CHCl₃: CH₃OH (90:10) solvent ($R_f = 0.22$); ESI-MS (m/z): 494.30 (M+1) and ¹H NMR (500MHz, CD₃OD): $\delta = 0.76$ (s, 3H), 0.86 (d, 3H, $J = 6.9$ Hz), 0.90 (s, 3H), 0.95 (dd, 3H, $J = 14.8, 7.2$ Hz), 1.03 (d, 3H, $J = 6.9$ Hz), 2.05 (m, 1H), 2.13 (dtd, 1H, $J = 9.3, 6.8, 2.4$ Hz), 3.01 (m, 1H), 3.08 (m, 2H), 3.56 (m, 1H), 3.92 (s, 1H). ¹³C NMR (125 MHz, CD₃OD): $\delta = 10.8, 13.3, 13.6, 14.4, 16.6, 17.3, 18.4, 21.1, 22.4, 25.0, 26.7, 30.6, 37.3, 40.1, 41.2, 41.4, 42.5, 42.9, 48.6, 48.3, 49.6, 52.7, 52.9, 59.5, 68.1, 68.2, 70.0, 71.7, 178.8$.

3.3.7 Cell culture

The rat L6 skeletal muscle cell line CRL-1458 was obtained from ATCC (Manassas, VA). Myoblasts were routinely maintained in Dulbecco's modified Eagle's medium (DMEM) containing 10% FBS and 0.1% penicillin-streptomycin at 37°C and 5% CO₂. Cells were subcultured into 24 well plates for protein synthesis, degradation, and cell viability studies and six well plates for Western blot analysis (Greiner Bio One, Monroe, NC). Once cells reached 90% confluence, differentiation was induced by lowering the serum concentration to 2%, and the medium was changed every two days. After seven to nine days of culture the myoblasts had fused into multinucleated myotubes (44). The NIH 3T3 murine embryonic fibroblast cell line (ATCC #CCL-92) was maintained in DMEM and 10% FBS at 37°C in 5% CO₂, and passaged every three to four days.

3.3.8 Cell viability assay and dose range determination

Cell viability was measured by the MTT (3-(4,5-Dimethylthiazol-2-yl)-2,5-diphenyltetrazolium bromide) assay in triplicate essentially as described (45) and quantified spectrophotometrically at 550 nm using a microplate reader (Molecular Devices, Sunnyvale, CA). The concentrations of test reagents that showed no changes in cell viability compared with that of the vehicle (0.1% ethanol) were selected for further studies.

3.3.9 Measurement of protein synthesis

Fully differentiated myotubes were washed with serum-free DMEM and treated in triplicate with vehicle (0.1% ethanol), increasing concentrations of HB, or 6.5 nM of insulin-like growth factor-1 (IGF-1) as a positive control. Compounds were added to serum-free medium containing 0.5 $\mu\text{Ci/mL}$ [^3H]-phenylalanine and incubated for 4 h. The incubation was stopped by placing the cells on ice, discarding the medium, and washing the cells extensively with ice cold PBS to remove the non-incorporated trace. Proteins were precipitated with 5% trichloroacetic acid and dissolved in 0.5N NaOH (46). Specific radioactivity of protein-bound phenylalanine was quantified using the liquid scintillation counter LS 6500 (Beckman Coulter, Fullerton, CA) and normalized to mg of total protein determined by the BCA protein assay (Pierce Biotechnology, Rockford, IL).

3.3.10 Measurement of protein degradation

The effect of brassinosteroids on protein degradation was investigated in fully differentiated myotubes as described (47) with slight modifications. Fully differentiated myotubes were incubated for 16 h to allow labeling of cellular proteins with 1.5 $\mu\text{Ci/mL}$ [^3H]-phenylalanine. Cells were washed twice with PBS to remove the non-incorporated trace and treated for 4 h with vehicle (0.1% ethanol), increasing concentrations of brassinosteroids, or 10 nM of insulin in serum-free medium. The incubation was stopped by placing the cells on ice, and protein in the medium was precipitated with 5% trichloroacetic acid. Specific radioactivity of protein-free phenylalanine was quantified using the liquid scintillation counter LS 6500 (Beckman Coulter, Fullerton, CA) and normalized to mg of total cell protein determined by the BCA protein assay (Pierce Biotechnology, Rockford, IL).

3.3.11 Western blot analysis

Fully differentiated L6 myotubes were cultured as described above, and whole cell extracts were prepared in ice-cold RIPA buffer supplemented with 10 mM sodium fluoride, 2 mM sodium orthovanadate, 1 mM PMSF, and protease inhibitor cocktail (Sigma) and centrifuged at 12,000 g for 20 min at 4°C. Equal amounts of protein (50 µg) from the supernatants were separated on 10% SDS polyacrylamide gels and blotted onto the nitrocellulose membrane. Western blot detection was performed with monoclonal phospho-Akt (Ser473) antibodies according to the manufacturer's instructions (Cell Signaling Technology, Danvers, MA). After being washed, the blots were incubated with an anti-rabbit peroxidase-labeled secondary antibody and visualized using ECL Western Blotting Detection Reagent (GE Healthcare, Piscataway, NJ). After being stripped, the same blots were probed with total Akt antibodies to serve as loading controls.

3.3.12 Animal study and gene expression studies

Animal experiment was performed according to procedures approved by the Rutgers Institutional Animal Care and Use Committee in the AAALAC accredited animal care facility as described previously (77). Briefly, six weeks old male Wistar rats (Charles River Laboratories, MA) fed a normal diet (#5001 Rodent Chow diet, Purina, St. Louis, MO), were randomized into two groups (n=6) and gavaged daily for 24 d with either 1 ml of vehicle (5% DMSO in corn oil) or 60 mg/kg body weight of HB. At necropsy, tissue weights were recorded, then tissue samples were collected by snap-freezing in the liquid nitrogen and stored at -80°C for further studies. Total RNA was

isolated using Trizol, its quantity and purity were determined using a NanoDrop (Nanodrop Technologies, Wilmington, DE). Pooled RNA samples were used for the rat insulin signaling PCR array (Qiagen, Valencia, CA) and analyzed according to the manufacturer's protocol. cDNA synthesis and quantitative PCR analysis were performed essentially as described (78) with the following primers selected using the Primer Express version 2.0 software (Applied Biosystems, Foster City, CA) as follows: cyclophilin, forward primer 5'-AAT GCT GGA CCA AAC ACA AAT G-3', reverse primer 5'-GCC ATC CAG CCA CTC AGT CT-3'; MyoD1, forward primer 5'-CAG AAC TGG GAC ATG GAG CTA CT-3', reverse primer 5'-TGT CGC AAA GGA GCA GAG AGA-3'; Myf5, forward primer 5'-CTC GCC TTC CGA GTA CTT CTA TG-3', reverse primer 5'-CAA ACT GGT CCC CAA ACT CAT C-3'; Myf6, forward primer 5'-GAG AAG TGC CAT CAA CTA CAT TGA G-3', reverse primer 5'-CCC CAG CTC CTG CAT TTT C-3'; myogenin, forward primer 5'-GGT ACC CAG TGA ATG CAA CTC-3', reverse primer 5'-CAA TGC ACT GGA GTT TGG TCC-3'; IGF-2, forward primer 5'-TGT CTA CCT CTC AGG CCG TAC TT-3', reverse primer 5'-TCC AGG TGT CGA ATT TGA AGA A-3'; and actin, forward primer 5'-GGG AAA TCG TGC GTG ACA TT-3', reverse primer 5'-GCG GCA GTG GCC ATC TC-3'.

3.3.13 Statistics

Statistical analyses were performed using Prism 4.0 (GraphPad Software, San Diego, CA). Unless otherwise noted, data were analyzed by one-way ANOVA with treatment as a factor. Post hoc analyses of differences between individual experimental groups were made using the Dunnett's multiple comparison test. Significance was set at p

< 0.05. Values are reported as means \pm SEM. The 50% inhibitory concentration (IC₅₀) was calculated by a nonlinear regression curve analysis.

3.4 Results

3.4.1 Synthesis of brassinosteroid analogues

To investigate the structure-activity relationship between position or stereochemistry of functional groups of HB and its anabolic activity, we synthesized a series of HB analogues **2-6** and compared them to other synthetic and naturally occurring brassinosteroids **7-9** in their ability to stimulate protein synthesis or inhibit protein degradation in the L6 rat skeletal muscle cells. (22S,23S)-Homocastasterone (**2**) was synthesized to evaluate the influence of the C-6 lactone group on the anabolic activity of brassinosteroids. By synthesizing **3-4** that lack the hydroxyl functional group at C-2 and are fluorinated at C-3, we tested the requirement for (2 α , 3 α)-vicinal diol moieties in the ability of brassinosteroids to promote protein accumulation in muscle cells. Finally, **5-6** were synthesized to contain 7-aza and 6-aza substitutions in the B ring of the brassinosteroid molecule, therefore evaluating the requirement for the 6-keto group for their biological activity. Additionally, we compared the anabolic activity of HB to other naturally occurring brassinosteroids that differ in the stereochemistry of the (22R, 23R)-vicinal diol moieties (**7**) or bearing a methyl group at C-24 in the side chain of its 5 α -ergostane structure (**8-9**). Structures of HB and its analogues used in this study are shown in Fig. 1, while detailed synthetic routes for each compound are summarized in Supporting Fig. 1-4.

3.4.2 Protein synthesis

The bioactivity of HB and its analogues was evaluated by measuring the increase in protein synthesis in L6 rat skeletal muscle cells *in vitro*. Cells were incubated for 4 h with [³H]-phenylalanine and treated in triplicate with vehicle (0.1% ethanol) or test compound (10 μM), and protein synthesis was measured as the incorporation of [³H]-phenylalanine into protein normalized by total protein (Table 1). Under these conditions, both HB and (22S,23S)-homocastasterone increased protein synthesis by $37.2 \pm 5.9\%$ ($p < 0.001$) and $41.0 \pm 2.7\%$ ($p < 0.001$), respectively. This compared favorably to the biological activity of IGF-1 at 6.5 nM ($42.5 \pm 4.5\%$, $p < 0.001$) that served as a positive control in this assay. Removal of the 2 α -hydroxyl group and fluorination at C-3 in the A ring (**3-4**) led to a 50% decrease in bioactivity ($24.6 \pm 5.3\%$, $p < 0.01$ and $22.5 \pm 2.7\%$, $p < 0.01$, respectively). Replacement of the 7-oxalactone group with amine in the B ring of **6** reduced biological activity by half, while a similar replacement of the 6-carbonyl group with amine in **5** resulted in a complete loss of activation of protein synthesis. Modifications in the side chain (**7-9**) also abolished the activity.

To investigate a dose dependence effect of the most active brassinosteroids on protein synthesis, a study was performed with 0.3-30 μM of **1-2**. Both responses approached saturation between 10 and 20 μM, with maximum increases of $36.9 \pm 2.9\%$ and $40.7 \pm 4.9\%$ ($p < 0.01$), respectively (Fig. 2A).

3.4.3 Protein degradation

The bioactivity of HB and its analogues was also evaluated by measuring the decrease in protein degradation in the L6 rat skeletal muscle cells *in vitro*. Cells were labeled overnight with [3H]-phenylalanine and subsequently treated for 4 h in triplicate with vehicle (0.1% ethanol) or test compound (10 μ M), and protein degradation was assessed as the release of acid-soluble [³H]-phenylalanine into the media normalized by total protein (Table 1). HB, homocastasterone (**2**), as well as brassinosteroid analogs **3-5** and **7** reduced protein degradation *in vitro*, but the potency of their activities differed according to their structure. **1-3** showed the strongest prevention of protein degradation, by more than 20%, compared favorably with 10 nM insulin treatment that served as a positive control in this assay ($20.2 \pm 1.6\%$, $p < 0.05$). Prevention of degradation was dependent on the presence of the ethyl group at the C-24 in the side chain (compare **1** and **7** versus **8-9**) and was partially dependent on the stereochemistry of the (22R, 23R)-vicinal diol moieties (compare **1** and **7**). Interestingly, replacement of 7-oxalactone group with amine in the B ring of compound **6** completely abolished its effect on protein degradation, while a similar replacement of the 6-carbonyl group with an amine in **5** had only a minor effect on its biological activity.

Among the most active compounds in this assay, HB at concentrations of 0.3-20 μ M, inhibited protein degradation dose-dependently and its activity reached plateau between 3 and 10 μ M (Fig. 2B). At a lower concentration, 1 μ M HB decreased protein degradation by $8.2 \pm 0.6\%$ above control levels ($p < 0.05$). **2** at concentrations of 0.3-30 μ M inhibited protein degradation dose-dependently and its activity reached plateau at 10 μ M. At the lower concentration, **2** at 1 μ M suppressed protein degradation by $8.7 \pm 1.7\%$ above control levels ($p < 0.05$).

3.4.4 Cytotoxicity in L6 muscle and 3T3 fibroblast cells

All brassinosteroids and their analogues showed no toxicity in fully differentiated L6 rat skeletal myotubes up to 30 μM as established by the MTT assay and cytological observations (data not shown). We therefore tested all compounds in the standard test for basal cytotoxicity using a 3T3/NIH murine fibroblast cell culture. **5** was the only brassinosteroid analogue that inhibited cell proliferation in a dose-dependent manner with IC_{50} of 12.5 μM . Fluorination at C-3 in the A ring (**3-4**) led to increased cytotoxicity as compared to the original brassinosteroids **1-2** (Fig. 3).

3.4.5 Akt phosphorylation

Akt is the key intermediate in the IGF-1 signaling pathway that modulates downstream targets known to regulate protein synthesis and degradation (53). Consistent with the results obtained with the [^3H]-phenylalanine incorporation assay, bioactive brassinosteroids stimulated phosphorylation of Akt in rat skeletal muscle cell culture (Fig. 4).

3.4.6 Pharmacogenomic effect of HB *in vivo*

Earlier we studied the anabolic effects of the biologically active brassinosteroid HB in animals. HB treatment (60 mg/kg body weight daily to healthy rats fed a normal diet for 24 d) was associated with a 14.2% increase in the lean body mass and the improved physical fitness of untrained rats (limb grip strength was measured using a digital force gauge) (77). Pooled RNA samples obtained from frozen gastrocnemius

muscle biopsies of vehicle- (Ctr) and HB-treated animals were used for the rat insulin signaling PCR array. Of the 84 genes responsible for insulin signaling, PI3K and MAPK pathways, carbohydrate metabolism, and cell cycle regulation, two subsets of genes were higher expressed in HB-treated group than in the Ctr group, but the magnitude of the difference varied (Figure 5A). The first subset included a set of target genes upregulated through the PI3K/Akt signaling pathway: *Adra1d* (6.5 fold), *Igfbp1* (2.5 fold), and *Srebfl* (2.5 fold). The second subset contained genes that regulate muscle cell growth and carbohydrate metabolism: *Fbp2* (4.5 fold) and *Igf2* (1.4 fold). We further verified these results for the *Igf2* gene by RT-PCR on individual muscle samples from Ctr and HB-treated animals (Figure 5B). No changes in expression of *Eif2b1* were noted. Additionally, we analyzed expression levels of a series of the myogenic transcriptional factors that modulate muscle growth and differentiation, including positive regulators *Myod1* (2.1 fold), *Myf5* (1.3 fold), *Myf6* (1.3 fold), *Myog* (1.7 fold) (Figure 5C).

3.5 Discussion

Brassinosteroids are a class of plant hormones with a polyoxygenated steroid structure showing pronounced plant growth regulatory activity (79). They also exhibit striking structural similarities with arthropod hormones of the ecdysteroid type such as 20-hydroxyecdysone (80) that have been reported to produce anabolic effects in mammals (58). Previously we reported that orally applied HB produced significant anabolic effects and improved physical fitness in healthy animals with minimal androgenic effects (77). In this study, a series of brassinosteroid analogues **2-6** related to HB were synthesized (Fig. 1), and the structure activity relationships of these compounds

were explored by carrying out protein synthesis and degradation assays in the L6 rat skeletal muscle cells. The results showed that (22S,23S)-homocastasterone could significantly increase protein accumulation in muscle cells similar to HB (Fig. 2). Since the only difference between these compounds is an additional 7-oxalactone group in the B ring of HB, these results indicated that the 7-oxalactone moiety is not necessary for their anabolic properties. On the contrary, moving from lactone to 6-ketone in plants, it was observed that the brassinolide activity decreased by 50% between brassinolide and castasterone (39). Transformation of this moiety to either 6-oxo-7-aza (**5**) or 6-aza-7-oxalactone (**6**) groups dramatically reduced their ability to stimulate protein synthesis (Table 1). This is similar to plant brassinolide activity that was significantly reduced in 7-aza-homobrassinolide (81), while 6-aza-7-oxo-homobrassinolide was inactive (82).

The effect of ring A substituents on anabolic activity of brassinosteroids was less evident. Replacement of the two 2α , 3α -vicinal hydroxyl groups by α -fluoro group decreased but did not abolish bioactivity. However the cytotoxicity of these compounds against 3T3-NIH murine fibroblast cells was increased (Fig. 3). Similarly, replacement of 3-hydroxy function by a 3-fluoro group yielded compounds active at the rice lamina inclination assay, but not as active as their parent compounds (83). Many papers have dealt with the relationship between the side chain structure and brassinolide activity in plants, suggesting that epibrassinolide is more active than homobrassinolide (79). On the contrary, our data indicated that the side chain at C-24 (methyl versus ethyl) is critically important for bioactivity in the mammalian system; therefore epibrassinolides **8-9** possess very low anabolic activity in skeletal muscle cells as compared to homobrassinolides **1** and **7**. The reason for this is not clear, and may be a result of the interaction of plant

brassinosteroid with yet an unknown nuclear or membrane receptor site through three structural motives: the B ring lactone and 22 α ,23 α -hydroxyls, which are critical for anabolic activity, while 2 α ,3 α -hydroxyls on the A ring have lesser receptor affinity. Several binding components on erythrocyte plasma membrane specific for ecdysteroids may indicate the existence of such receptor (84).

The PI3K/Akt/mTOR pathway is a crucial intercellular regulator of muscle hypertrophy (32). Activation of PI3K by upstream ligands such as IGF-1 or IGF-2 phosphorylates the membrane phospholipids and creates a lipid binding site for Akt, which in turn increases protein synthesis and suppresses proteolytic activity and gene expression of the proteolytic genes. Consistent with the results obtained with the [³H]-phenylalanine incorporation assays, bioactive brassinosteroids stimulated phosphorylation of Akt in rat skeletal muscle cell culture (Fig. 4). Both HB and (22S,23S)-homocasterone treatments resulted in significant activation of Akt after 1 h, a much slower response than that produced by IGF-1, which phosphorylates Akt within 10 min. A similar delayed Akt response has been reported for ecdysteroids (59).

The pharmacogenomic properties of HB were further characterized in healthy rats administered with 60 mg/kg HB orally for 24 d. The results indicated that HB potently stimulated two sets of genes involved in muscle cell growth and carbohydrate metabolism. Among those, adrenergic receptor alpha 1d (*Adra1d*) showed the most notable 6.5-fold induction (Fig. 5A). The α 1 adrenergic receptors mediate endogenous functions of catecholamines, which involve coupling to G proteins followed by activation of phospholipase C β and protein kinase C (85). Recently, it has also been suggested that *Adra1d* may potentially regulate muscle survival and differentiation (86). mRNA levels

of the insulin-like growth factor 2 (*Igf2*) and the insulin-like growth factor binding protein 1 (*Igfbp1*) were also upregulated in skeletal muscle of rats administered with HB. IGF-2 expression during skeletal muscle differentiation is regulated at the transcriptional level (87), and signaling through the IGF-1 receptor by locally produced IGF-2 defines a pathway that is critical for normal muscle growth and regeneration (88). *Igfbp1* has been proposed as an acute regulator of IGF-1 bioactivity (89) and its elevation in association with HB treatment is unclear. The physiological role of the observed fructose-1,6-bisphosphatase (*Fbp2*) upregulation is also unknown. A contribution of this enzyme to a de novo production of glucose from lactate within the muscle is unlikely due to the lack of glucose-6-phosphatase in this tissue. However it is possible that the substrate cycle formed by this enzyme and phosphofructokinase may provide the basis for amplification of flux regulation of glycolysis versus glyconeogenesis (90).

Activation of Akt in skeletal muscle leads to rapid muscle hypertrophy (91) accompanied by improved metabolism (92). Even though inducible activation of Akt is sufficient to increase skeletal muscle mass and force without satellite cell activation (16), we also evaluated the effect of HB supplementation on the expression of genetically-determined transcriptional programs regulated by myogenic transcription factors *Myod1*, *Myf5*, *Myf6*, and *Myog*. The myogenic regulatory protein MyoD was the only transcriptional factor associated with greater than two fold upregulation following HB treatment (Fig. 5C). This factor induces cell differentiation by activating muscle specific genes and is important in the switch from cellular proliferation to differentiation (15).

In conclusion, this study provides evidence that the 6-keto group and 22 α ,23 α -hydroxyls are critical for the anabolic activity of brassinosteroids in rat skeletal muscle

cells. This may be useful for the design of novel therapeutic molecules possessing high anabolic selectivity. In addition, (22S,23S)-homobrassinolide and (22S,23S)-homocastasterone, which were confirmed to possess the greatest anabolic activity among the molecules analyzed, may be employed as pharmacological tools to investigate the biological functions of muscle growth and regeneration pathways.

3.6 Acknowledgements

The authors wish to acknowledge Rocky Graziose for NMR measurements, and Reneta Pouleva and Ruth Dorn for excellent technical assistance. This work was supported, in part, by Rutgers University, by the 5P50AT002776-05 grant from the National Center for Complementary and Alternative Medicine (NCCAM), and by Phytomedics Inc.

Table 1. Effect of HB (1) and its analogues (2-9) on protein accumulation in the L6 rat skeletal muscle cells. Compounds were tested at 10 μ M and results are expressed as the mean \pm SEM of determinations performed in triplicate (* P<0.05, ** P<0.01, *** P<0.001 when compared with control by one-way ANOVA and Dunnett's post-test).

ID	Common name	Formula	MW	Protein synthesis, % increase over control	Protein degradation, % decrease over control
1	(22S,23S)-homobrassinolide	C29H50O6	494.70	37 \pm 6***	-24 \pm 6*
2	(22S,23S)-homocastasterone	C29H50O5	478.70	41 \pm 3***	-23 \pm 4*
3	(22S,23S)-3 α -fluoro-homobrasinolide	C29H49FO4	480.70	25 \pm 5**	-21 \pm 1*
4	(22S,23S)-3 α -fluoro-homocastasterone	C29H49FO3	464.70	23 \pm 3**	-16 \pm 4
5	(22S,23S)-7 ν -aza-homobrassinolide	C29H51NO5	493.72	21 \pm 2**	-1 \pm 3
6	(22S,23S)-6-aza-homobrassinolide	C29H51NO5	493.72	3 \pm 12	-14 \pm 4
7	(22R,23R)-homobrassinolide	C29H50O6	494.70	13 \pm 2	-15 \pm 4
8	(22S,23S)-epibrassinolide	C28H48O6	480.68	4 \pm 2	-6 \pm 8
9	(22R,23R)-epibrassinolide	C28H48O6	480.68	12 \pm 4	-7 \pm 8
Ref	IGF-1, 6.5 nM			43 \pm 5***	--
Ref	Insulin, 10 nM			--	-20 \pm 2*

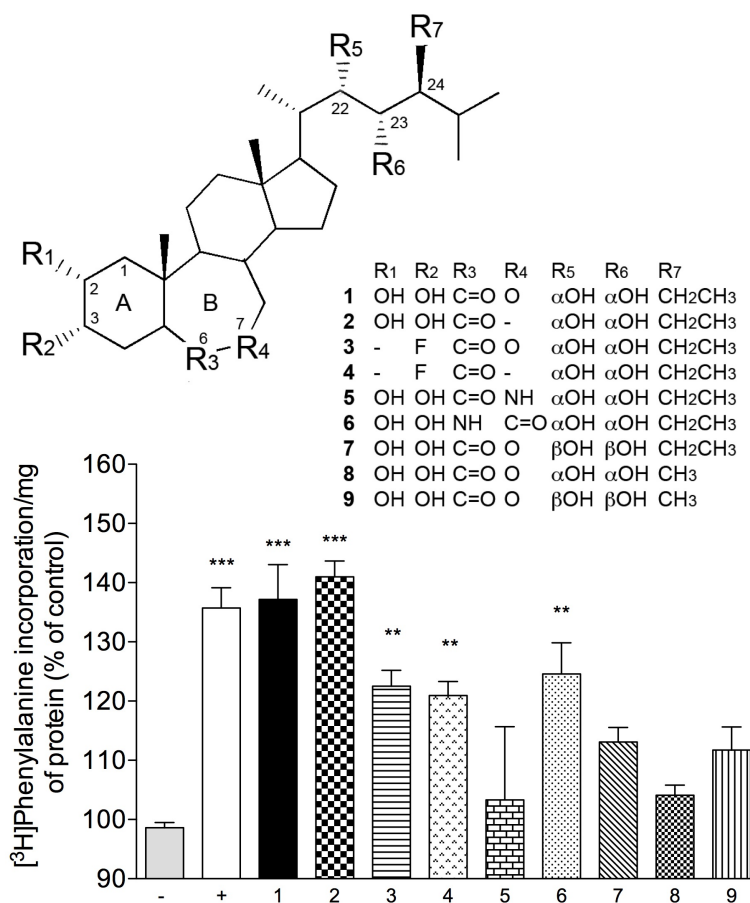


Figure 1. Chemical structure of homobrassinolide (1) and its analogues (2-9) investigated in this study.

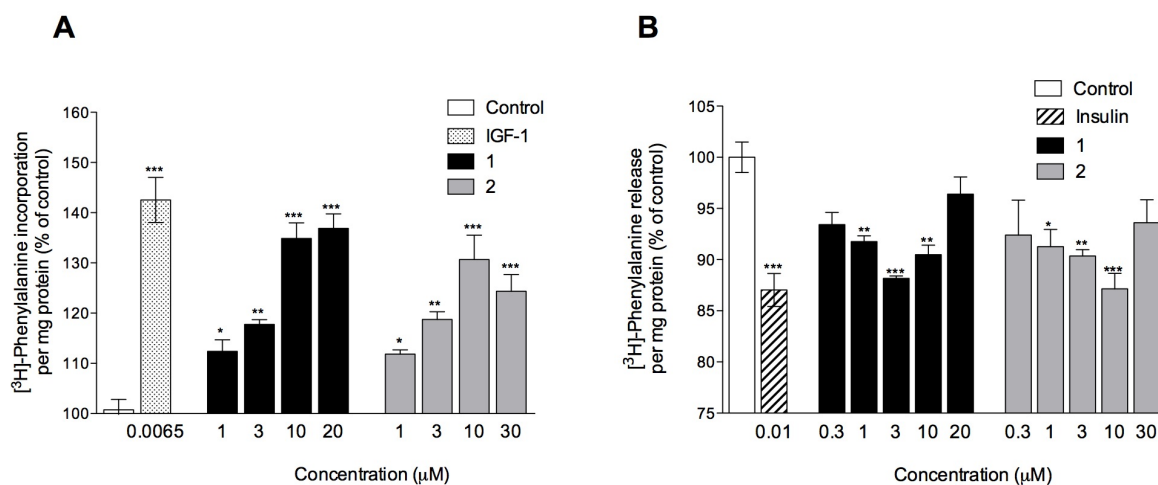


Figure 2. Dose dependent effect of 1 and 2 on protein synthesis (A) and protein degradation (B) in L6 rat myotubes. (A) Cells were incubated for 4 h with [³H]-phenylalanine and treated in triplicate with vehicle (0.1% ethanol), 6.5 nM of IGF-1 as a positive control, or test compound (0.3-30 µM), and protein synthesis was measured as the incorporation of [³H]-phenylalanine into protein normalized by total protein. (B) Dose-dependent effect of HB on protein degradation were observed in cells labeled overnight with [³H]-phenylalanine and subsequently treated for 4 h with vehicle (0.1% ethanol), 10 nM of insulin as a positive control, or brassinosteroid analogues (0.3-30 µM); then protein degradation was measured as the release of acid-soluble [³H]-phenylalanine into the media. Results are expressed as the mean ± SEM of determinations performed in triplicate (* P<0.05, ** P<0.01, *** P<0.001 when compared with control by one-way ANOVA and Dunnett's post-test).

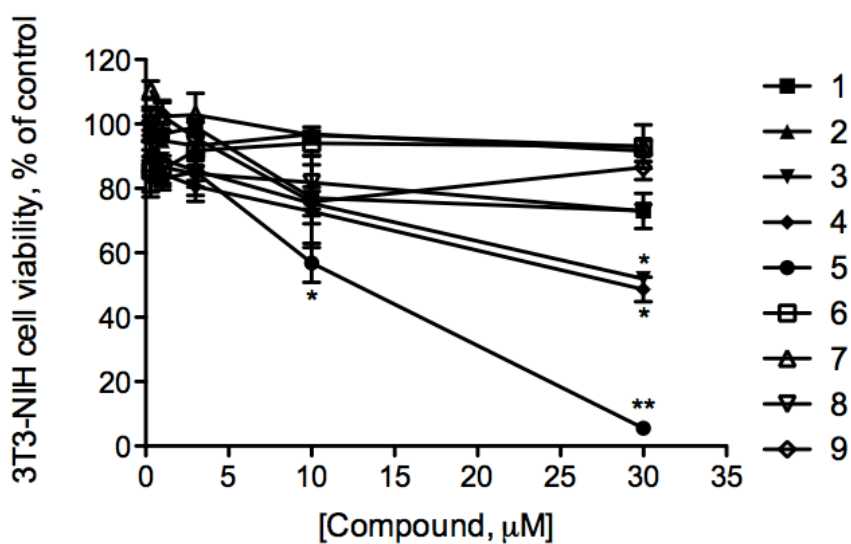


Figure 3. Cell survival curves as measured by MTT assay for 1-9 against the murine fibroblast cell line NIH-3T3. Cells were incubated with various concentrations of brassinosteroids (0.3-30 μM) for 24 h at 37 $^{\circ}\text{C}$. The mean absorbance of the control cells represented 100% cell proliferation, and the mean absorbance of treated cells was related to control values to determine sensitivity. Error bars represent standard error (n=6) from mean cell proliferation as determined by repeated experiments.

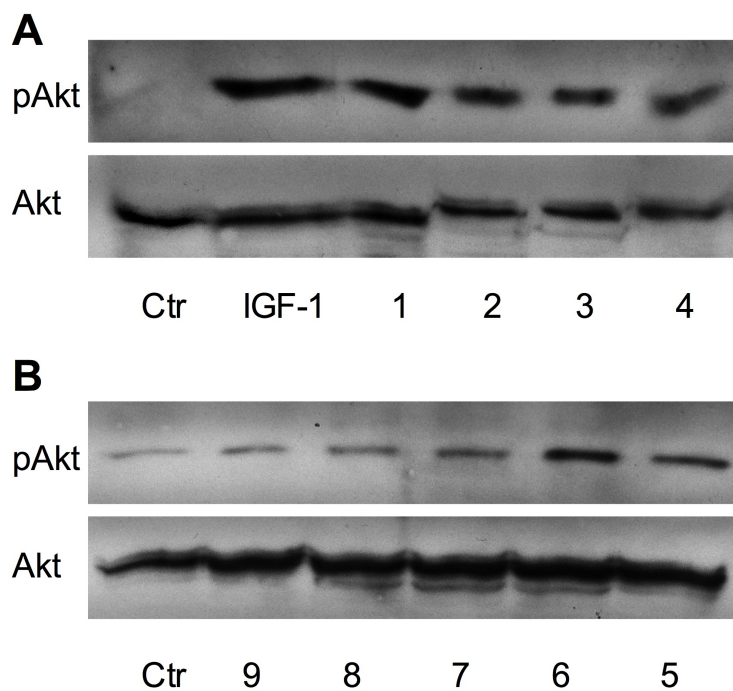


Figure 4. Effect of HB and its analogues on Akt (Ser473) phosphorylation in L6 myotubes. Representative immunoblots of Akt phosphorylation stimulated with 10 μ M 1-9 for 1 h or 6.5 nM IGF-1 for 10 min (positive control). Cells lysates normalized to contain 50 μ g of total soluble protein were analyzed by immunoblotting with phospho- and nonphospho-specific antibodies.

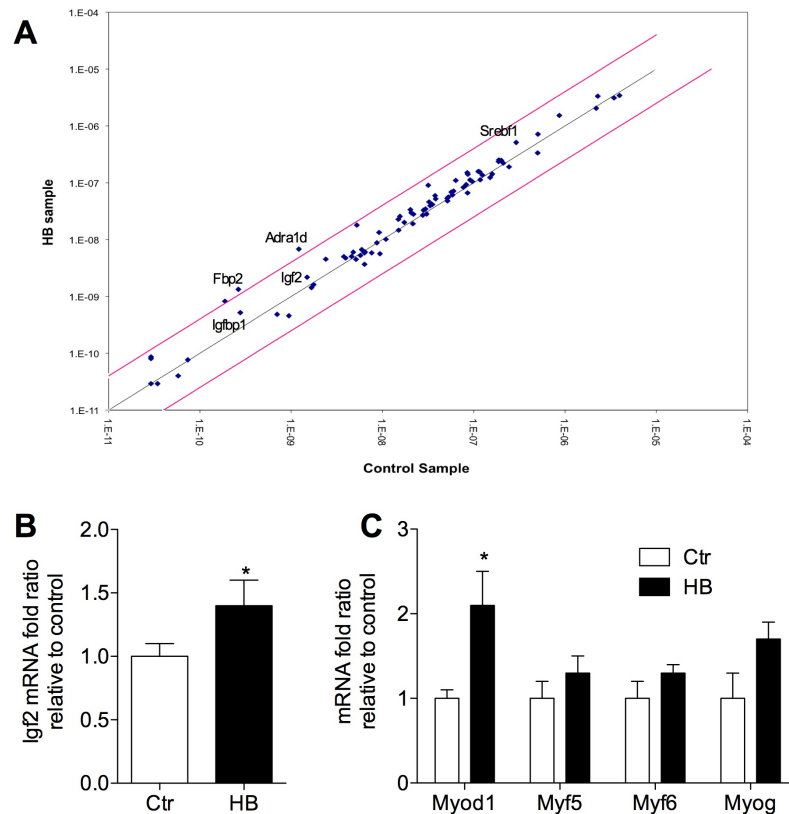
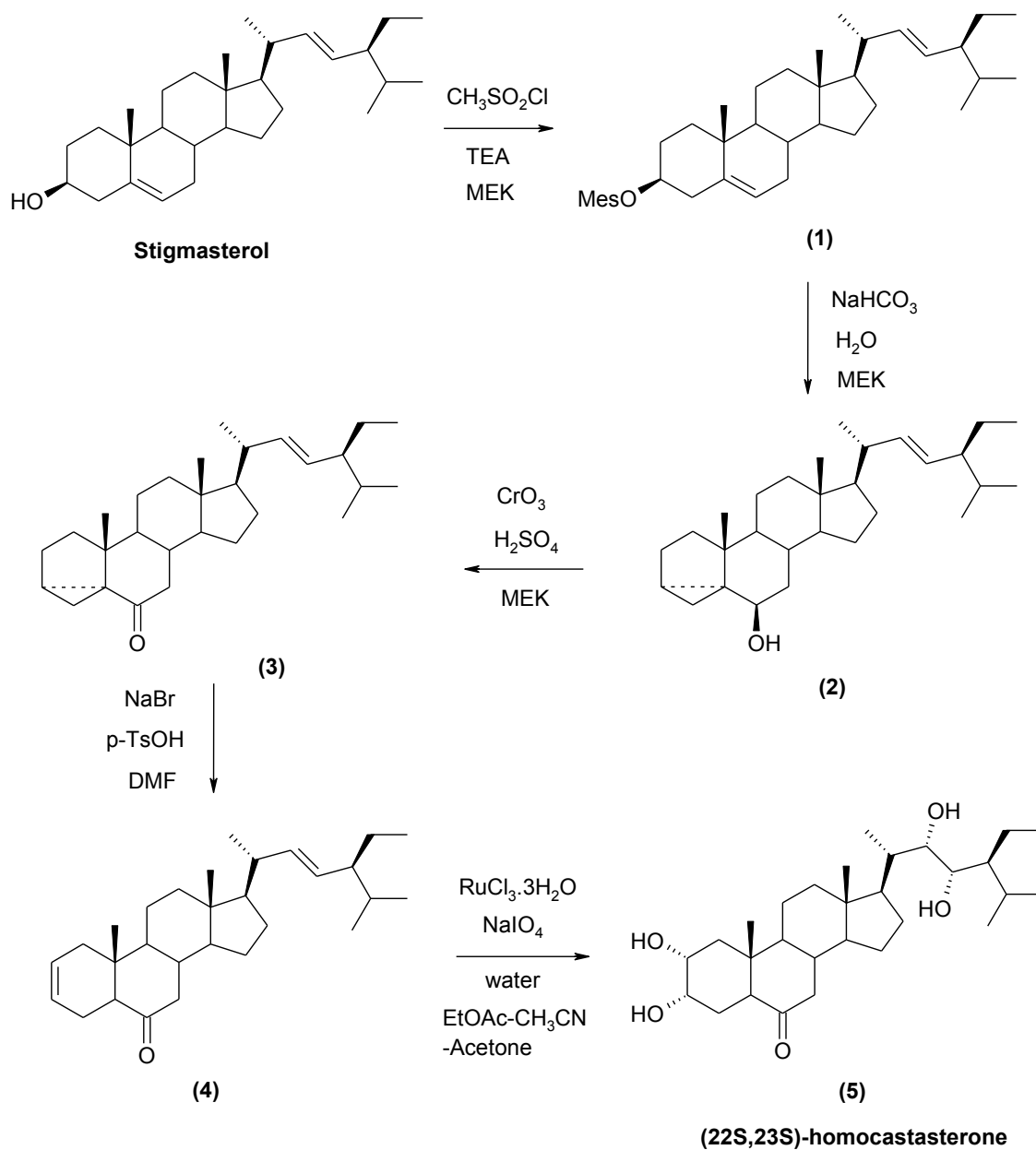
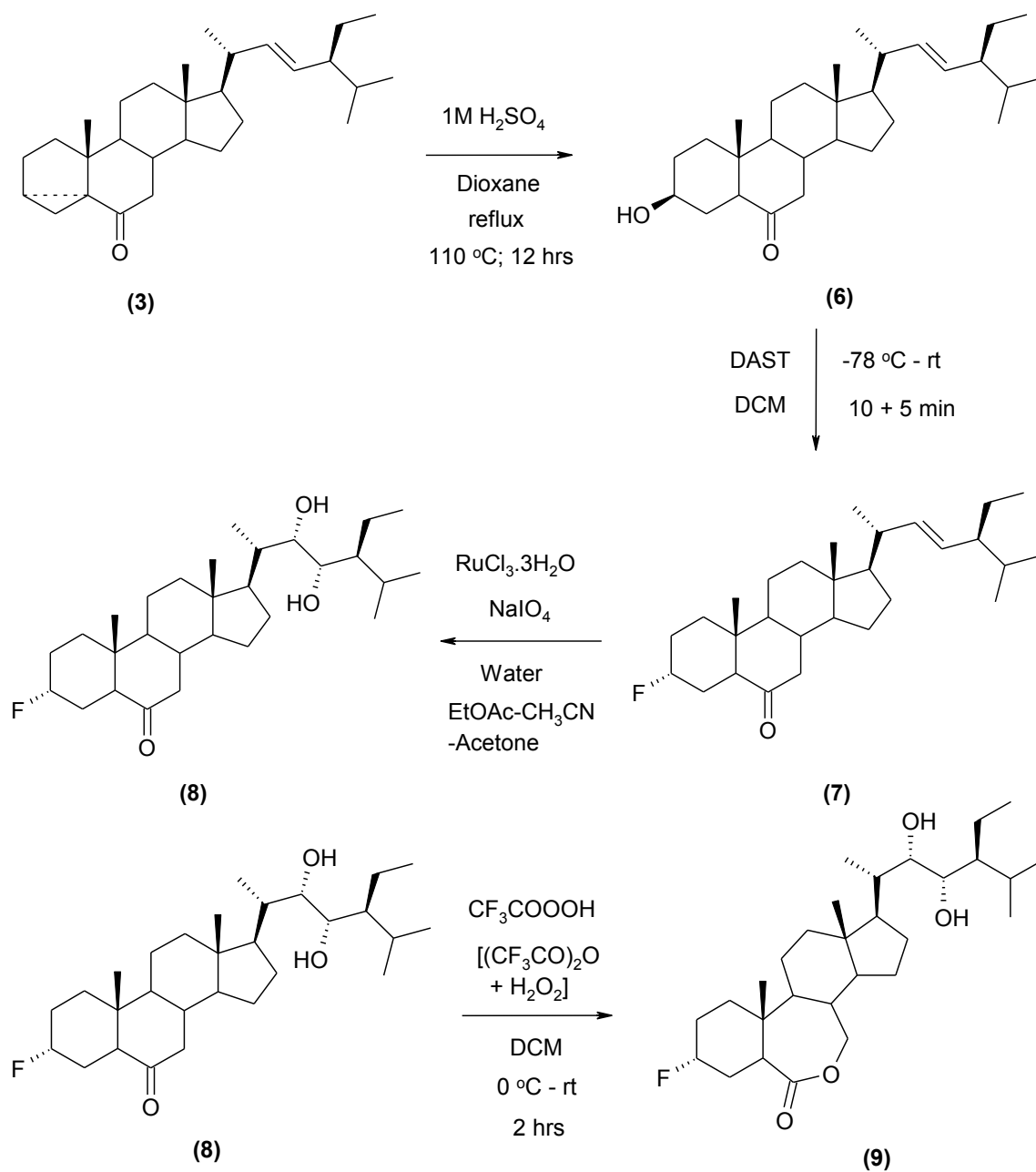


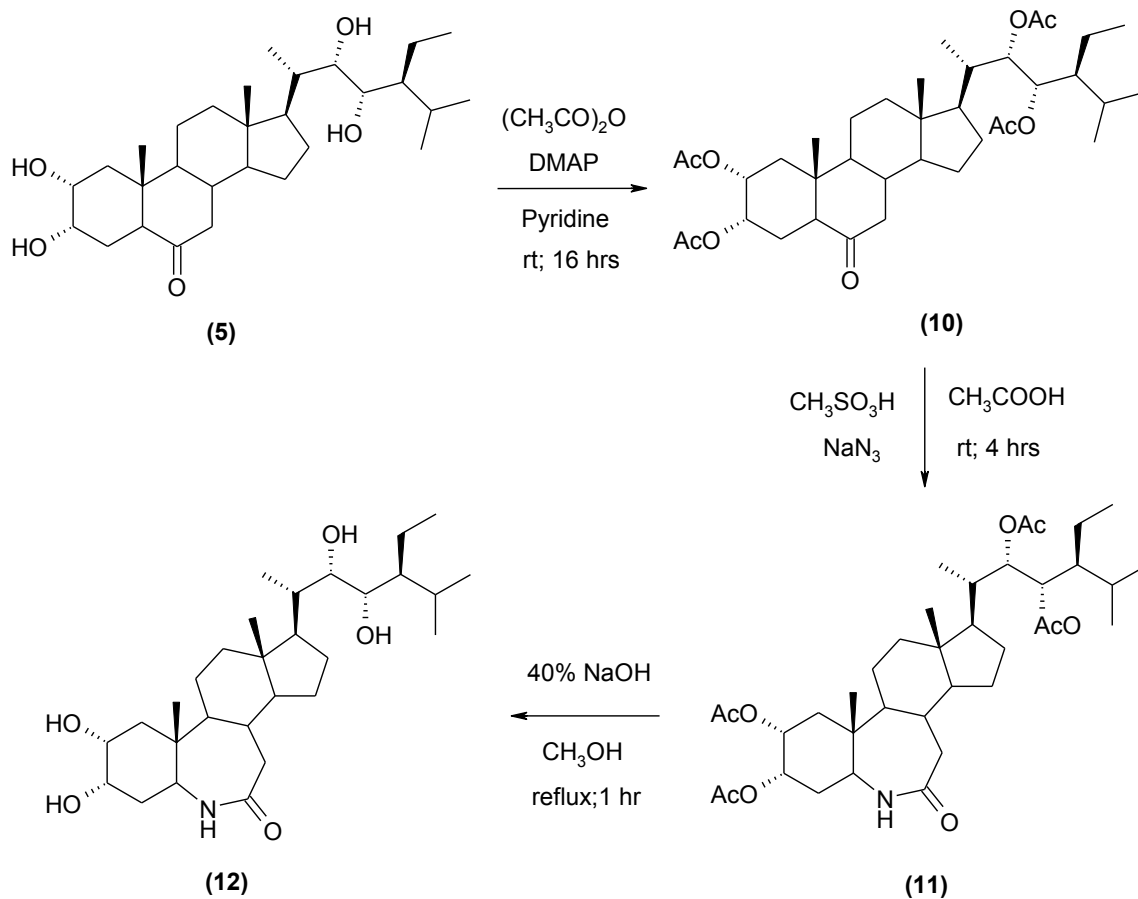
Figure 5. Pharmacogenomic effect of HB *in vivo*. (A) RNA was extracted from pooled (n=5) gastrocnemius muscle samples of control and HB-treated animals (60 mg/kg for 24 d) and analyzed using a rat insulin signaling pathway PCR array to measure relative gene expression levels for 84 genes. The central black line indicates fold changes ($2^{(-\Delta\Delta Ct)}$) of 1, while the pink lines indicate the 4 fold-change in the gene expression threshold. (B) Results for *Igf2* gene expression and (C) a set of the myogenic transcriptional factors that modulate muscle growth and differentiation were further confirmed by conventional RT-PCR on individual muscle samples (n=5) from control and HB-treated animals. Results are expressed as the mean \pm SEM of determinations performed in duplicate (* P<0.05 when compared with control by Student t test).



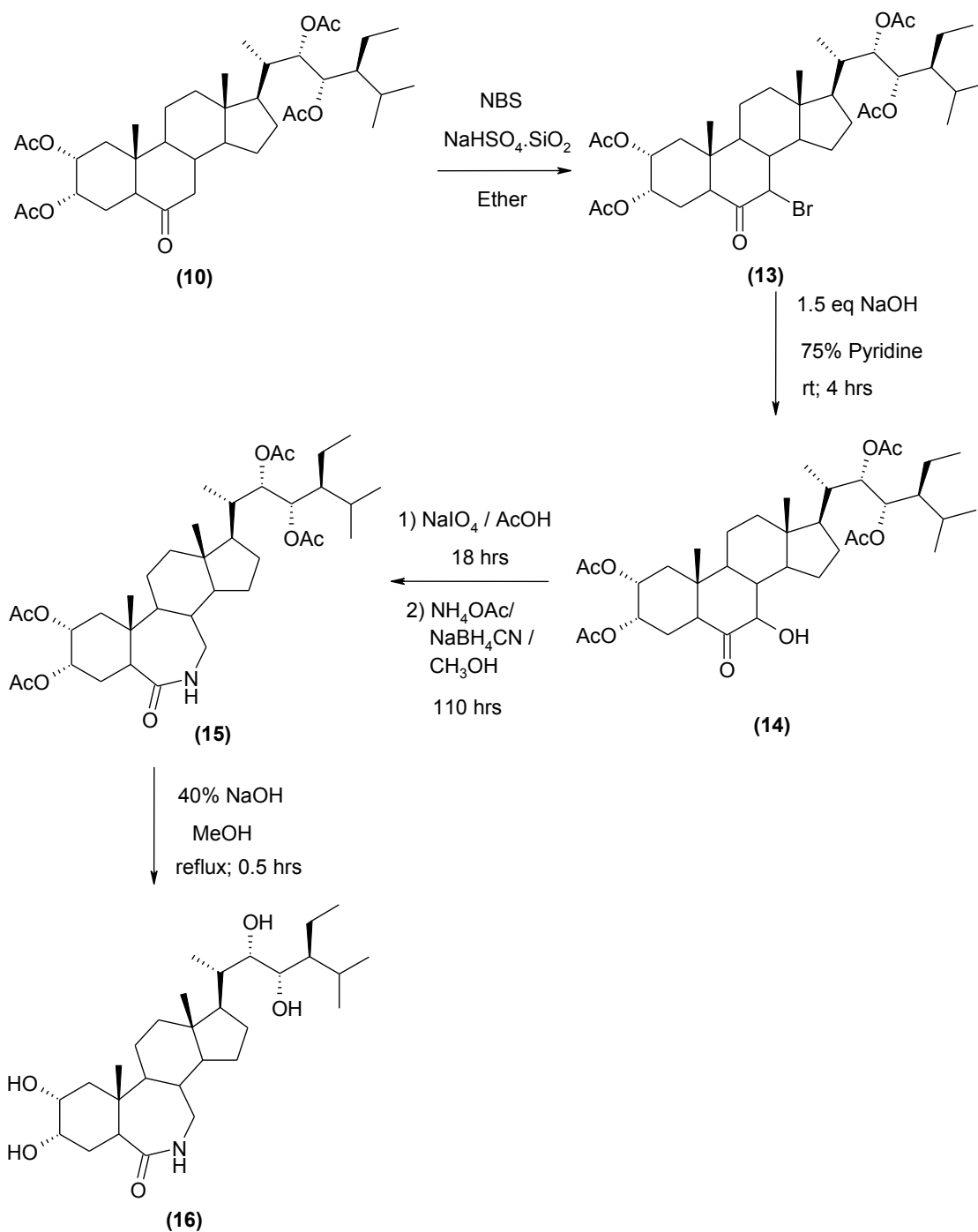
Supporting Figure 1. Synthesis of (22S, 23S, 24S)-2 α , 3 α , 22, 23-tetrahydroxy-24-ethyl-5 α -cholestan-6-one (2) from stigmasterol.



Supporting Figure 2. Synthesis of (22S, 23S, 24S)-3 α -fluoro- 22, 23-dihydroxy-24-ethyl-5 α -cholestan-6-one and (22S, 23S, 24S)-3 α -fluoro- 22, 23-dihydroxy-7-oxo-24-ethyl-5 α -cholestan-6-one.



Supporting Figure 3. Synthesis of (22S, 23S, 24S)-2 α ,3 α ,22, 23-tetraacetoxy-24-ethyl-B-homo-6-aza-5 α -cholestan-6-one.



Supporting Figure 4. Synthesis of (22S, 23S, 24S)-2 α ,3 α ,22,23-tetrahydroxy-24-ethyl-B-homo-7-aza-5 α -cholestan-6-one.

CHAPTER IV

**BRASSINOSTEROID TREATMENT IMPROVES GLUCOSE HOMEOSTASIS
IN OBESE MICE**

Submitted to: Mol Nutr Food Res (2011)

4.1 Abstract

The prevalence of obesity is increasing globally, and obesity is a major risk factor for metabolic diseases such as type 2 diabetes. Previously we reported that oral administration of homobrassinolide (HB) to healthy rats triggered a selective anabolic response, that was associated with lower blood glucose. Therefore the aim of this study was to evaluate the effects of HB administration on glucose metabolism, insulin sensitivity, body composition, and gluconeogenic gene expression profiles in the liver of C57BL/6J high fat diet-induced obese mice. Methods and results. Acute oral administration of 50-300 mg/kg HB to obese mice resulted in a dose-dependent decrease in fasting blood glucose within 3 h of treatment. Daily chronic administration of HB (50 mg/kg for eight weeks) ameliorated hyperglycemia and improved oral glucose tolerance associated with obesity without significantly affecting body weight or body composition. These changes were accompanied by a lower expression of two key gluconeogenic enzymes, phosphoenolpyruvate carboxykinase (PEPCK) and glucose-6-phosphatase (G6Pase), and increased phosphorylation of AMP-activated protein kinase in the liver tissue. *In vitro*, HB treatment (1-15 μ M) inhibited cyclic AMP-stimulated but not dexamethasone-stimulated upregulation of PEPCK and G6Pase mRNA levels in H4IIE rat hepatoma cells. Among a series of brassinosteroid analogues related to HB, only homocastasterone significantly decreased glucose production in cell culture. These results indicate the anti-diabetic effects of brassinosteroids and begin to elucidate their putative cellular targets both *in vitro* and *in vivo*.

4.2 Introduction

Brassinosteroids are plant-specific polyhydroxylated derivatives of 5 α -cholestane, structurally similar to cholesterol-derived animal steroid hormones and ecdysteroids from insects. They are found at low levels in pollen, seeds, leaves, and young vegetative tissues throughout the plant kingdom (2). The first biologically active plant brassinosteroid was isolated from the pollen of rapeseed *Brassica napus* in 1979 (3). The natural occurrence of more than 50 compounds of this group has been reported following the initial discovery (4). Similar to animal steroid hormones (24), brassinosteroids regulate the expression of specific plant genes and complex physiological responses involved in growth (25), partly via interactions with other hormones setting the frame for brassinosteroid responses (26). Brassinosteroid signaling in plants resembles the Wnt pathway and is mediated by GSK3-like kinase (6). Moreover, application of brassinosteroids increased sugar and starch content (93), while a brassinosteroid-deficient *Arabidopsis* mutant had an impaired carbohydrate metabolism (94).

Very little is known about the effects of brassinosteroids in animals. Natural brassinosteroids inhibited growth of several human cancer cell lines without affecting the growth of normal cells (11). A synthetic brassinosteroid analogue prevented HSV-1 multiplication and viral spreading in a human conjunctival cell line with no cytotoxicity and reduced the incidence of herpetic stromal keratitis in mice when administered topically (37), possibly by the modulation of the response of epithelial and immune cells to HSV-1 infection (38). 24-Epibrassinolide, the most widely used brassinosteroid in agriculture, has a favorable safety profile. The median lethal dose (LD₅₀) of this

compound is higher than 1000 mg/kg in mice and higher than 2000 mg/kg in rats when applied orally or subcutaneously (12).

In our previous study, we observed that oral administration of homobrassinolide (HB, Fig. 1A) to healthy rats triggered selective anabolic response that was associated with lower blood glucose (95). Since another plant ecdysteroid 20-hydroxyecdysone (20HE) was shown to decrease weight and hypoglycemia in obese mice (60), we sought to explore the effects of HB on glucose metabolism and insulin resistance in high fat diet-induced obese C57BL/6J mouse model. These mice were selectively bred for divergent body fat mass and thus a model of complex polygenic human obesity (96).

4.3 Materials and methods

4.3.1 Reagents

HB [(22S, 23S, 24S)-2 α , 3 α , 22,23-tetrahydroxy-24 ethyl- β -homo-7-oxo-5 α -cholestane-6-one] (Fig. 1A) was purchased from Waterstone Technology (Carmel, IN) and its structure was confirmed by ESI-LCMS and NMR. Brassinosteroid analogues 2-9 (Fig. 1B), including homocastasterone (22S, 23S, 24S)- 2 α , 3 α , 22, 23-tetrahydroxy-24-ethyl-5 α -cholestan-6-one (2), (22S,23S,24R)-3a-fluoro-22,23-dihydroxy-24-ethyl- β -homo-7-oxa-5 α -cholestan-6-one (3), (22S,23S,24S)-3a-fluoro-22,23-dihydroxy-24-ethyl-5 α -cholestan-6-one (4), (22S,23S,24S)-2 α ,3 α ,22,23-tetrahydroxy-24-ethyl- β -homo-7-aza-5 α -cholestan-6-one (5), (22S,23S,24S)-2 α ,3 α ,22,23-tetrahydroxy-24-ethyl- β -homo-6-aza-5 α -cholestan-7-one (6), (22R,23R,24S)-2 α ,3 α ,22,23-tetrahydroxy- β -homo-7-oxa-5 α -cholestan-6-one (7), (22S,23S,24R)-2 α ,3 α ,22,23-tetrahydroxy-24-methyl- β -homo-7-oxa-

5 α -cholestan-6-one (8), and (22R,23R,24R)-2 α ,3 α ,22,23-tetrahydroxy-24-methyl- β -homo-7-oxa-5 α -cholestan-6-one (9) were synthesized or purchased previously (97), and are shown in Fig. 1B. All other chemicals and cell culture media were obtained from Sigma (Saint Louis, MO) or Invitrogen (Carlsbad, CA) unless otherwise specified.

4.3.2 Cell culture and qPCR

The H4IIE hepatoma cells were cultured in 24-well tissue culture plates (Greiner Bio One, Monroe, NC) and grown to near confluence in Dulbecco's modified Eagle's medium containing 2.5% (v/v) newborn calf serum and 2.5% (v/v) fetal calf serum. When appropriate, cells were treated for 8 h with 500 nM dexamethasone and/or 0.1 mM 8-CTP-cAMP (Dex-cAMP) to induce PEPCK and G6Pase gene expression together with different concentrations of brassinosteroid, or 10 nM insulin. Three wells were allocated for each treatment, including the negative control (vehicle). Total RNA extraction, cDNA synthesis, and quantitative PCR were performed essentially as described earlier (98).

4.3.3 Glucose production assay

H4IIE rat hepatoma cells were serum starved overnight in the glucose production buffer (glucose-free Dulbecco's modified essential medium pH 7.4, containing 20 mM sodium lactate and 2 mM sodium pyruvate without phenol red) and treated for 8 h with Dex-cAMP in the presence or absence of 10 nM insulin or different concentrations of brassinosteroid for 8 h. At the end of the incubation, 0.5 ml of medium was taken to measure the glucose concentration in the culture medium using the Amplex Red glucose assay kit (Invitrogen). Corrections for cell number were made on the basis of the protein

concentration measured using the BCA Protein assay kit (Pierce Biotechnology, Rockford, IL).

4.3.4 Western blot analysis

H4IIE cells were cultured as described above, and whole cell extracts were prepared in ice-cold RIPA buffer supplemented with 10 mM sodium fluoride, 2 mM sodium orthovanadate, 1 mM PMSF, and protease inhibitor cocktail (Sigma) and centrifuged at 12,000 g for 20 min at 4°C. Equal amounts of protein (50 µg) from the supernatants were separated on 10% SDS polyacrylamide gels and blotted onto a nitrocellulose membrane. Western blot detection was performed with monoclonal phospho-AMPK antibodies according to the manufacturer's instructions (Cell Signaling Technology, Danvers, MA). After being washed, the blots were incubated with an anti-rabbit peroxidase-labeled secondary antibody and visualized using the ECL Western Blotting Detection Reagent (GE Healthcare, Piscataway, NJ). After being stripped, the same blots were probed with total AMPK antibodies to serve as loading controls.

4.3.5 Animal studies

All animal experiments were performed according to procedures approved by the Rutgers Institutional Animal Care and Use Committee in AAALAC accredited animal care facility. Six-week-old male C57BL/6J mice were obtained from the Jackson Laboratory (Bar Harbor, ME) and maintained on a high fat diet containing 60% fat-derived calories (D12492, Research Diets) with 12-h light and dark cycles for an additional four weeks. Then animals were further randomized into two groups. The

control group (n=8) was gavaged daily with a vehicle solution alone (10% DMSO in corn oil), while a treatment group (n=8) received 50 mg/kg of body weight of HB for 8 weeks. The body weight of each animal and the total amount of food consumed (accounting for spillage) were recorded every week for the duration of the experiment.

Plasma glucose concentrations were measured immediately prior to gavage and 3 h postgavage at week 1 and week 8 of treatment in submandibular vein blood samples using a glucometer (Lifescan, Johnson and Johnson, NJ). Blood samples were collected in EDTA-coated tubes, centrifuged 1,500 g for 20 min, and the separated plasma was stored at -80°C until analysis. Plasma concentrations of insulin were determined by a rat/mouse insulin ELISA kit (Millipore, Billerica, MA). Plasma triglycerides and total cholesterol were measured by enzymatic colorimetric assays (Wako Diagnostics, Richmond, VA).

To perform the glucose tolerance test at week 8 of the experiment, mice were fasted overnight (16 h) and gavaged orally with 2 g/kg of glucose solution. Plasma glucose levels were measured immediately before and 30, 60, and 120 min after the glucose challenge.

At the end of the experiment, blood was collected by heart puncture after CO₂ inhalation and animal body composition was assessed prior to necropsy using dual-energy X-ray absorptiometry (DEXA) analysis on PIXImus equipment (Lunar, Madison, WI). At necropsy, tissue weights were recorded, and then tissue samples were collected by snap-freezing in liquid nitrogen and stored at -80°C for further studies.

4.3.6 Statistics

Statistical analyses were performed using Prism 4.0 (GraphPad Software, San Diego, CA) and expressed as mean \pm SEM. Unless otherwise noted, the two tailed t-test or one-way ANOVA (as appropriate) were applied and $p < 0.05$ was considered significant. Post hoc analyses of differences between individual experimental groups were made using the Dunnett's multiple comparison test. Body weight gain and glucose tolerance were analyzed by two-factor repeated-measures ANOVA, with time and treatment as independent variables.

4.4 Results

4.4.1 HB decreases fasting blood glucose

Obesity was induced by feeding C57BL/6J mice for six weeks before randomizing the animals into control and treatment groups. At the beginning of the treatment, all animals had similar weight (33.2 ± 0.9 g) and developed hyperglycemia (204 ± 11 mg/dl fasting blood glucose). HB showed moderate efficacy at lowering blood glucose levels in C57BL/6J mice following the acute, single dose treatment (Fig. 2). The effect was dose-dependent in the range of 50 to 300 mg/kg body weight and reached half of that observed for metformin (a standard reference drug used at the highest 300 mg/kg dose) 3 h after oral administration.

4.4.2 HB improves insulin sensitivity without affecting body weight

To test the chronic effect of HB in the *in vivo* diabetes model, C57BL/6J mice were kept on the high fat diet for an additional eight weeks. During this time, the

treatment group received an oral gavage of 50 mg/kg HB daily, while control animals were gavaged with vehicle alone. The final body weights did not differ between the two groups (Table 1); no changes in food intake (not shown) or body weight gain were also seen (Fig. 3A). DEXA analysis confirmed these findings by showing no significant changes in either body composition (lean or fat mass) or bone mineral content. The baseline blood glucose levels continued to rise for the duration of the treatment, and were not significantly different between both groups at the end of the treatment (229 ± 17 mg/dl). However, animals administered with 50 mg/kg HB exhibited lower blood glucose levels following an acute treatment with HB several days before the end of the study (Fig. 3B). Moreover, an oral glucose tolerance test performed at the end of the study revealed significantly increased insulin sensitivity in HB-treated animals. While blood glucose levels peaked similarly in both groups 30 min following an oral glucose challenge, they were significantly lower at 60 and 120 min after administration of HB to treated animals relative to the control group (Fig. 3C). The total area under the curve (AUC) decreased by an average of 18% by treating mice with HB.

4.4.3 HB inhibits liver gluconeogenesis in obese mice

Glucose homeostasis requires a precise balance between glucose production and utilization. Both acute and chronic effects of HB administration on blood glucose levels could be partially explained by reduced gluconeogenesis in liver tissue of these animals. In order to test this hypothesis, we evaluated mRNA expression levels for two key gluconeogenic enzymes, phosphoenolpyruvate carboxykinase (PEPCK) and glucose-6-phosphatase (G6Pase), which are regulated on the transcriptional level. PEPCK is highly

expressed in the liver, where it is adaptively regulated by a variety of different hormones and other agents in a manner that parallels gluconeogenic flux (99). G6Pase is expressed mainly in the liver and in the kidney cortex, most particularly in the starved and diabetic states (100). In animals treated with HB, the mRNA levels were significantly reduced for PEPCK and G6Pase by two and three fold, respectively (Fig. 4A). Additionally, western blot analysis of liver tissue of these animals revealed an increased phosphorylation of the AMP-activated protein kinase (Fig. 4B), a key regulator of cellular energy homeostasis and suppressor of gluconeogenesis (101).

4.4.4 HB inhibits cAMP- but not dexamethasone-induced upregulation of PEPCK and G6P

Starvation and diabetes cause a two to three fold increase in the activity of gluconeogenic enzymes in the liver that is associated with a two to four fold increase in PEPCK and G6Pase mRNA (102). Glucocorticoids and specifically dexamethasone cause a larger (up to 10-fold) increase in G6Pase activity and in the level of its mRNA in cultured hepatoma cells (103). Changes in cAMP concentration are also directly involved in transcriptional regulation of these genes through several cis-acting sequences present in their promoters (104). In order to confirm our observation that HB treatment decreased PEPCK and G6Pase mRNA levels in liver tissue of obese animals, a quantitative analysis of the mRNA expression patterns of PEPCK and G6Pase in cAMP-stimulated and dexamethasone/cAMP-induced H4IIE cells was performed to determine whether or not the effect of HB on glucose production is related to its effect on expression of these genes. Untreated cells were used to measure the basal level of PEPCK and G6Pase

expression, while the β -actin gene was chosen as an internal standard because the level of β -actin mRNA remained unaffected by the treatments. HB treatment (1 or 10 μ M for 8 h) achieved weak suppression of glucose production (20%) from dexamethasone/cAMP-induced H4IIE cells *in vitro* (Fig. 5A). A similar weak decrease in PEPCK and G6Pase mRNA levels (0-10%) was observed following an induction with a dexamethasone/cAMP mixture (Fig. 5B), however a very strong, dose-dependent decrease in target gene expression (up to 70% for PEPCK and 85% for G6Pase) was observed in cells induced by cAMP alone (Fig. 5C). Under the same conditions, insulin at 10 nM decreased glucose production by 50%, PEPCK mRNA expression by 80%, and G6Pase mRNA was totally suppressed.

4.4.5 Effect of brassinosteroid analogues on glucose production in vitro

Next we compared the bioactivity of HB to that of its natural and synthetic analogues (97). Among eight compounds tested, only homocastasterone (2) was able to suppress glucose production from dexamethasone/cAMP-induced cells similar to HB (Fig 6). Removal of 2 α -hydroxyl group and fluorination at C-3 in the A ring (compounds 3-4) led to a 80% decrease in bioactivity. Replacement of 7-oxalactone group with amine in the B ring of compound 5 reduced biological activity by 90%, while a similar replacement of the 6-carbonyl group with amine in 6 resulted in a complete loss of suppression of glucose production. Modifications in the side chain (compounds 7-9) also abolished the activity.

4.5 Discussion

Brassinosteroids are present in small quantities in foods and plants (2). They are similar in many respects to animal steroids (Fig. 1), but appear to function very differently at the cellular level. While animal steroid hormones act through the nuclear receptor family of transcription factors, plant brassinosteroids signal through a cell surface receptor kinase-mediated signal transduction pathway (27, 28). At the same time, brassinosteroids share some similarities with ecdysteroids that have a wide array of physiological and pharmacological effects in animals and insects (58), including modulation of protein synthesis (59) and carbohydrate metabolism (60).

Oral administration of HB to obese mice with hyperglycemia lowered blood glucose levels after the acute, single dose treatment (Fig. 2). This hypoglycemic activity was approximately half of that of the known anti-diabetic drug metformin. The principal function of metformin is to reduce hepatic glucose production and to improve peripheral insulin sensitivity, thus ameliorating hyperglycemia (105). Metformin has been shown to activate AMP-activated protein kinase (AMPK), and to inhibit the expression of the hepatic gluconeogenic genes PEPCK and G6Pase similar to insulin (106). The activation of AMPK improves insulin sensitivity by stimulating glucose uptake and lowering blood glucose, whereas the activity of AMPK is suppressed in disorders associated with insulin resistance (107). At molecular levels, a complex relationship exists between the AMPK and insulin signaling pathways. It has been reported that AMPK regulates IRS1 and Akt/PKB (108), while insulin and Akt have negative impacts on AMPK activation in adipocytes (109).

To test the effect of HB in the *in vivo* diabetes model, male C57BL/6J mice were fed a high fat diet and treated daily by oral administration of 50 mg/kg HB for eight

weeks (Fig. 3). At the end of the treatment, the body weight of the HB group was not significantly different from that of the controls. No differences in animal feeding behavior or lean/fat body mass composition were noted by DEXA as well (Table 1). However, at the end of the treatment HB animals had lower blood glucose and improved glucose tolerance, suggesting that liver or muscle tissue is the primary target for brassinosteroid bioactivity. Previously, we have observed that 20-hydroxyecdysone (20HE), a plant ecdysteroid structurally similar to brassinosteroids, lowered blood glucose in obese mice while causing a significant decrease in body weight gain and adipose mass. Similar to HB, 20HE had no effect on food consumption in this model (60). Taken together, these data suggest that plant brassinosteroids and ecdysteroids have similar effects on glucose metabolism and insulin sensitivity in animals, however the underlying molecular mechanisms and targets may be different. For example, similar to 20HE, HB decreased PEPCK and G6Pase mRNA levels and induced AMPK phosphorylation in liver tissue of the treated animals (Fig. 4). Normally, PEPCK and G6Pase gene expression is induced by glucagon (through cAMP), glucocorticoids and catecholamines during periods of fasting and in response to stress, but is dominantly inhibited by glucose-induced increases in insulin secretion upon feeding. The impaired insulin response in the liver caused by insulin resistance secondary to type 2 diabetes results in a continuous elevated expression of PEPCK and G6Pase due to the unopposed action of glucagon. This permits continuous hepatic glucose output, thereby contributing significantly to basal and fasting hyperglycemia and the complications associated with diabetes. Both 20HE (60) and HB decreased glucose production in H4IIE rat hepatoma cell culture, however HB treatment suppressed only gluconeogenic gene expression

induced by cAMP, but not the dexamethasone/cAMP combination (Fig. 5). In this instance, HB acted similar to metformin in regards to its inability to repress hormone-induced PEPCK expression (110).

Previously we have also described the anabolic effect of HB in muscle tissue of healthy rats that was mediated by Akt activation (95) and synthesis of several brassinosteroid analogues with various abilities to induce Akt signaling in L6 rat skeletal muscle cells (97). Therefore a possibility that HB modulates glucose metabolism in liver by a combined effect on both the Akt and AMPK signaling pathways in liver and muscle tissues; however this hypothesis has not been tested in the present study and needs further clarification. It is clear though that several structural similarities are required for plant sterols to modulate carbohydrate metabolism in mammals. These include 2α - and 3α -hydroxyl groups at the C-3 position in the A ring, 6-keto group in B ring, and $22\alpha,23\alpha$ -hydroxyls in the side chain of the molecule (Fig. 6). These requirements are very similar to those reported from plants, where (2,3)- and (22,23)-vicinal diol moieties are required for optimum bioactivity (75). Another interesting observation is that 6-keto group shared by 20HE, HB, and homocastasterone is preferable for retaining glucose metabolism-modulating activity rather than a 6-keto-7-lactone group present in classical brassinosteroids.

In conclusion, we hypothesize that HB may exert its glucose lowering effect by repressing glucose production and activating AMPK in liver tissue. Stimulatory effects of HB on glucose metabolism subsequently translates into a whole body insulin sensitizing effect, such as improved oral glucose tolerance.

4.6 Acknowledgments

The authors thank Reneta Pouleva and Ruth Dorn for excellent technical assistance, and Dr. Sue Shapses for reviewing and commenting on the manuscript. This work was supported, in part, by Rutgers University, by the 5P50AT002776-05 grant from the National Center for Complementary and Alternative Medicine (NCCAM).

Table 1. Body composition and blood biochemistry of mice treated with HB.

	Control	HB
Body weight, g	39.4 ± 1.5	38.4 ± 3.4
Lean mass, g	20.6 ± 0.4	20.1 ± 0.7
Fat mass, g	18.8 ± 1.3	19.3 ± 3.5
Bone mineral content, g	0.439 ± 0.02	0.430 ± 0.02

Mice were fed a high fat diet and gavaged daily with 50 mg/kg body weight HB for eight weeks. Body composition was measured by DEXA. Results are expressed as the mean ± SEM.

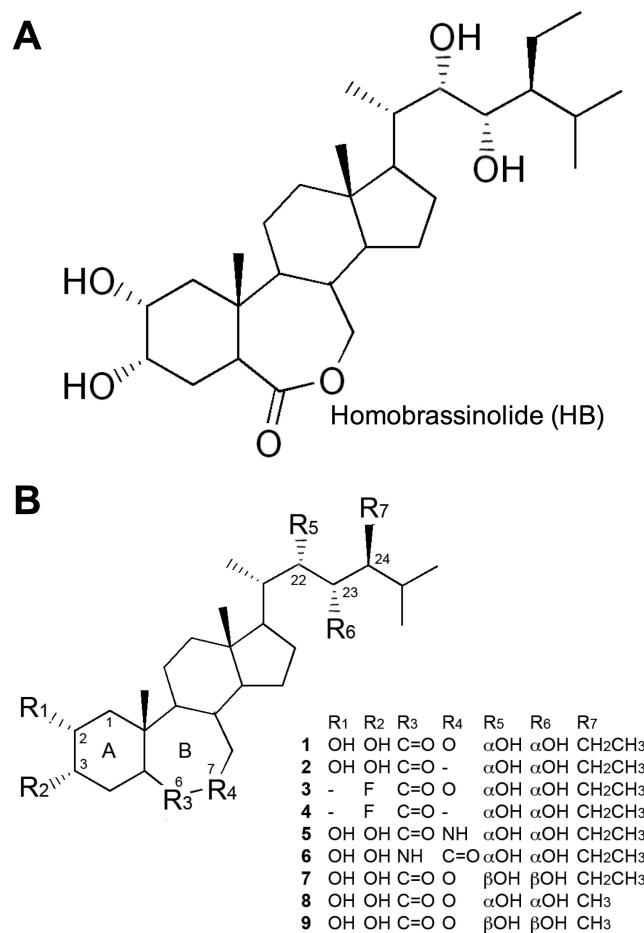


Figure 1. Chemical structure of (A) 28-homobrassinolide, HB in comparison with (B) other synthetic and natural brassinosteroid analogues.

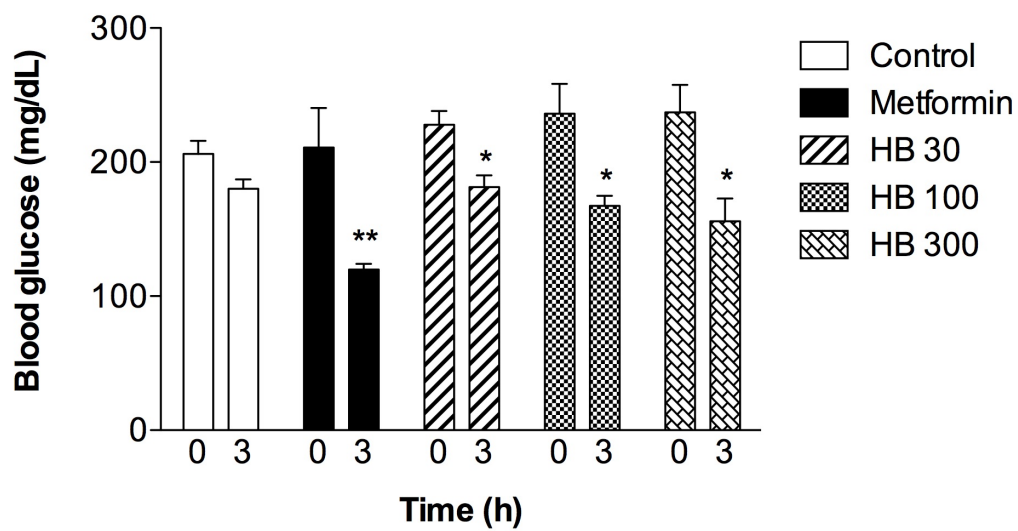


Figure 2. Acute lowering effect of HB on plasma glucose in C57BL/6J mice 3 h after administration of 50, 100, or 300 mg/kg HB (n = 8). Metformin at 300 mg/kg was used as a positive control. Values are means \pm SEM. *P < 0.05, **P < 0.01 when compared with control by one-way ANOVA followed by Dunnett's post hoc test.

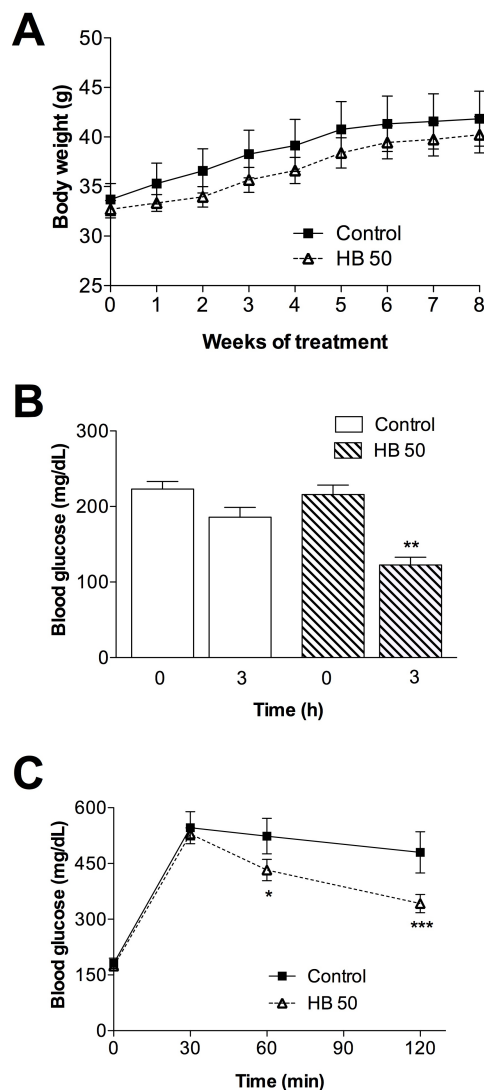


Figure 3. Chronic insulin sensitizing effect of HB on (A) body weight gain, (B) fasting blood glucose, and (C) oral glucose tolerance test (OGTT) in the C57BL/6J mice. Six-week-old male mice were fed a high-fat diet for six weeks, and kept on the same diet for additional eight weeks combined with a daily gavage with vehicle or 50 mg/kg HB. (B) Fasting blood glucose levels in animals fed with HFD (n = 8), or HFD treated with 50 mg/kg HB (n = 8) at six weeks. (C) IGTT curves of groups fed either HFD, or HFD animals receiving the HB treatment. Values are means \pm SEM. *P < 0.05, ***P < 0.001 when compared with control by one-way ANOVA followed by Dunnett's post hoc test.

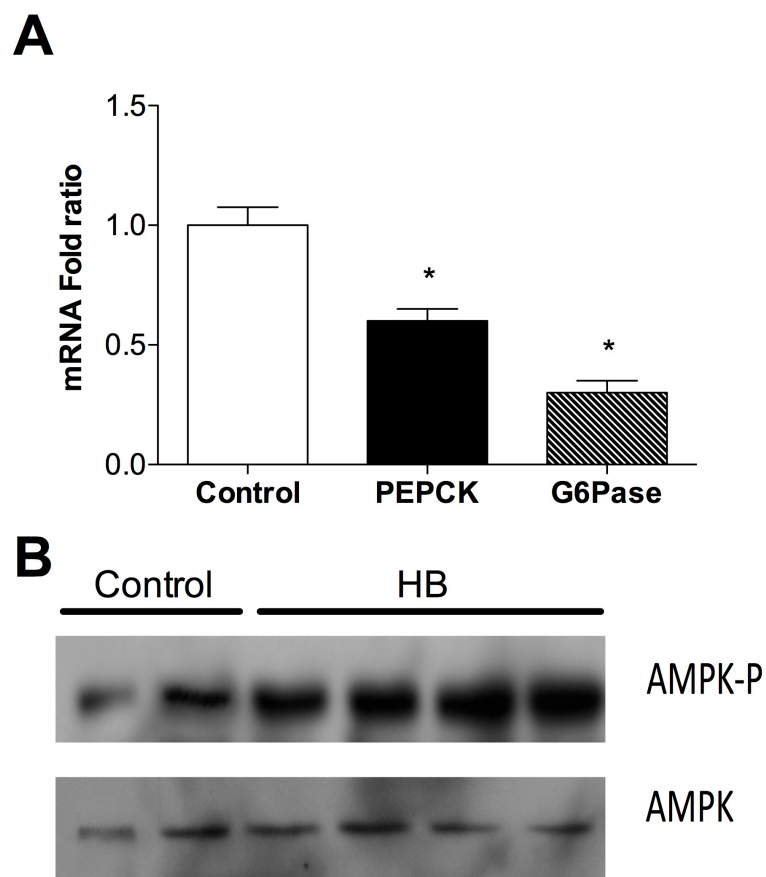


Figure 4. Hepatic expression of gluconeogenic enzymes PEPCK and G6Pase (A) and activation of liver AMPK phosphorylation (B) in C57BL/6J mice treated with 50 mg/kg HB. PEPCK and G6Pase mRNAs were normalized to β -actin mRNA. Liver tissue lysates were analyzed by immunoblotting with phospho- and nonphospho-specific AMPK antibodies. Values are means \pm SEM. * $P < 0.05$, two tailed t-test versus control.

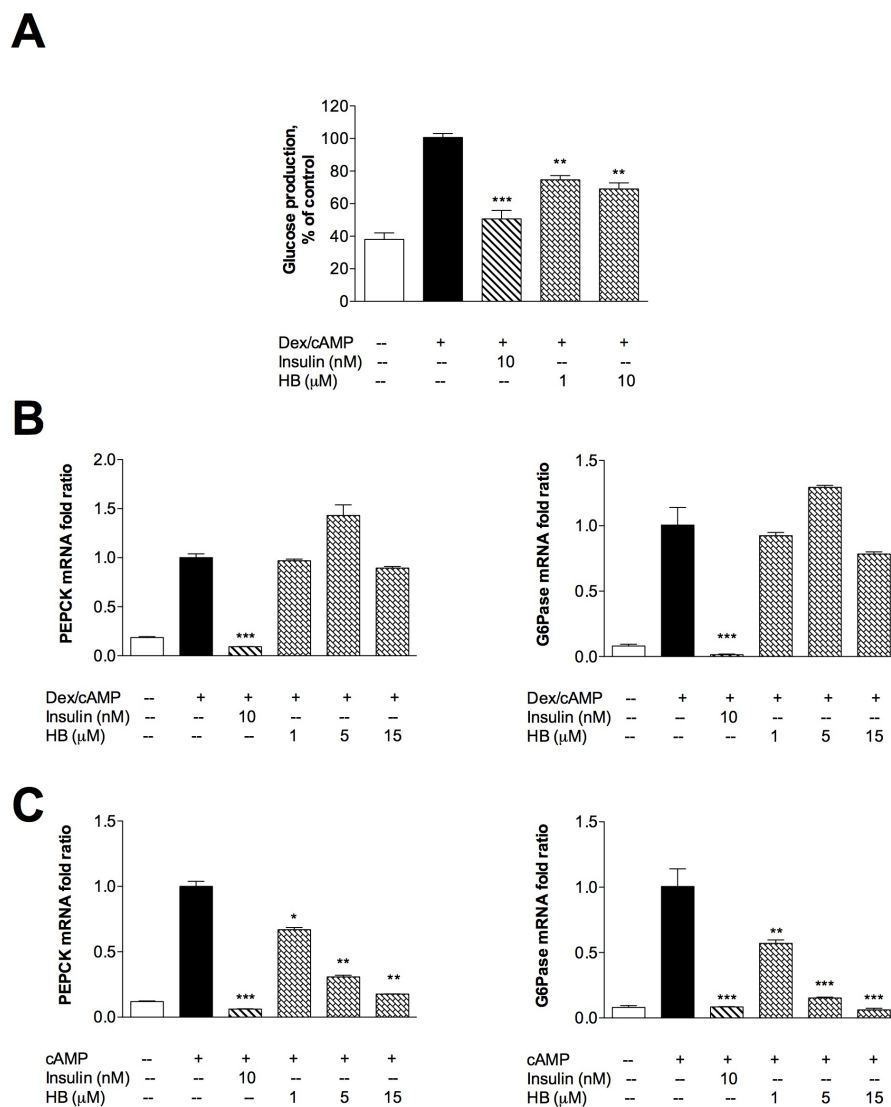


Figure 5. Production of glucose in the H4IIE rat hepatoma cell culture in response to HB treatment following induction with the dexamethasone/cAMP mixture (A). Hepatic expression of gluconeogenic enzymes PEPCK and G6Pase in cell culture induced with the dexamethasone/cAMP mixture (B) or cAMP alone (C). PEPCK and G6Pase mRNAs were normalized to β -actin mRNA. Values are means \pm SEM. * $P < 0.05$, ** $P < 0.01$, *** $P < 0.001$ when compared with control by one-way ANOVA followed by Dunnett's post hoc test.

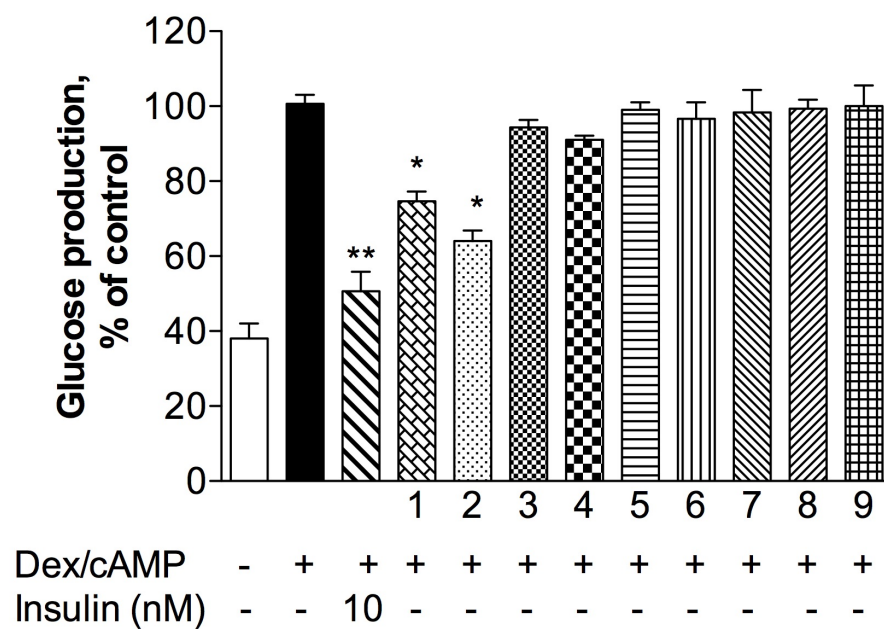


Figure 6. Production of glucose in H4IIE rat hepatoma cell culture in response to treatment of HB (1), homocastasterone (2), and other synthetic and natural brassinosteroid analogues (3-9). Cells were incubated with 10 μ M of brassinosteroids for 8 h at 37 C. Values are means \pm SEM. *P < 0.05, **P < 0.01 when compared with control by one-way ANOVA followed by Dunnett's post hoc test.

CHAPTER V

**CUTANEOUS WOUND HEALING IS ACCELERATED BY TOPICAL
BRASSINOSTEROIDS**

Submitted to: Exp Dermatol (2011)

5.1 Abstract

Akt is a key signaling integrator suppressed in slow healing wounds. As previous studies showed that anabolic effects of plant brassinosteroids is mediated in part by stimulation of the PI3K/Akt signaling pathway, we examined the effects of a topical homobrassinolide on the progression of wound healing and inflammation. C57BL/6J mice were given a full thickness dermal wound, and the rate of the wound closure was assessed daily for 10 days along side the adenosine receptor agonist CGS-21680 as a positive control. Wound tissue was analyzed for TGF- β , TNF- α and iCAM markers of inflammation, and the biological activity of the homobrassinolide and its synthetic analogues was determined using *in vitro* proliferation, fibroblast migration, and inflammation cell culture assays. Topical application of brassinosteroids significantly reduced wound size in treated animals. mRNA levels of TGF- β and iCAM were significantly lower, while TNF- α was suppressed in wounds from treated mice compared with the control. Several bioactive homobrassinolide analogues induced fibroblast migration *in vitro* and showed no direct anti-inflammatory effect in the LPS-stimulated macrophage assay. Our data suggest that topical brassinosteroids accelerate the wound-healing process in part by shortening the early inflammatory phase and stimulating migration and wound repair by stimulating Akt. Targeting this specific signaling pathway may represent a promising approach to the therapy of delayed wound healing.

5.2 Introduction

Beyond just the economic and cosmetic impacts, impaired wound healing causes increased pain, suffering, and decreased mobility of the trauma and chronic metabolic disease (i.e. diabetes) for patients, which can further exacerbate the inactivity and related disorders. There are many applications that promote wound healing, including topical hormones (111), growth factors (112), silver-containing antimicrobial agents (113), and natural complex remedies like pollen (114) and honey (115). However, the emergence of antibiotic resistant strains of bacteria and adverse reactions associated with the silver sulfadiazine treatment underline the importance of finding more effective agents with a shorter time of application and novel mechanisms of action.

Cutaneous wound healing is characterized by an initial inflammatory response, followed by tissue repair and remodeling. Recruitment of polymorphonuclear neutrophils and macrophages by release of the inflammatory cytokines and chemokines with a peak concentration occurring slightly before maximum macrophage infiltration is a critical first step in wound healing (116). When this stage is compromised or excessive, the exaggerated inflammatory phase of wound healing may be causally related to slower wound healing and scarring. Indeed, wounds created in fetal mice that exhibit lower levels of inflammation heal faster and without scarring (117). PU1 null mice, lacking polymorphonuclear neutrophils and macrophages, have greatly reduced levels of inflammation in their wounds that are associated with enhanced healing (118). Exercise also improves cutaneous wound healing in aged mice in association with decreased levels of TNF- α and proinflammatory chemokines in the wound tissue (119).

Akt is a central element in the PI3K/Akt network, and there is increasing evidence that this pathway plays a role in wound healing. The importance of PI3K in collagen gene regulation was previously demonstrated in human dermal fibroblasts (120), and analysis of the Akt1 null mice is skin revealed an impaired matrix organization with a reduced amount of collagen (121). Inhibition of Akt upregulated basal matrix metalloproteinase 1 production and reversed the inhibitory effect of transforming the growth factor- β (TGF- β) (122), thus establishing the link between Akt activation, inflammatory response, and wound healing. Recently we have shown that oral administration of homobrassinolide (HB, Fig. 1A) to healthy rats triggered a selective anabolic response that was associated with activation of Akt (95). HB belongs to the group of plant-derived polyhydroxylated derivatives of 5 α -cholestane, structurally similar to cholesterol-derived animal steroid hormones and insect ecdysteroids. Brassinosteroids were isolated from all plant organs, however seeds and pollen contain highest levels of naturally available brassinosteroids (2). In plants, the growth promoting effect of brassinosteroids is associated with the increased synthesis of nucleic acids and proteins (7, 43). Although the structural requirements for the biological activity of brassinosteroids have been clearly recognized, a number of compounds bearing slight to drastic structural modifications are potent plant growth promoters (76). Structure-activity studies of brassinosteroids have revealed that the 5 α -configuration is required for optimum activity, but the B-ring tolerates considerable variation, providing that the presence of a polar functional group, which does not have to be a lactone, is maintained (74). Following this principle, we previously synthesized a group of HB analogues (Fig. 1B) and compared them to several natural brassinosteroids in their ability to stimulate Akt (97).

The aim of this study was to examine the effects of topical brassinosteroid application in the mouse model of wound healing and to analyze the possible underlying mechanisms in fibroblast and macrophage cell cultures.

5.3 Materials and methods

5.3.1 Reagents

HB [(22S, 23S, 24S)-2 α , 3 α , 22,23-tetrahydroxy-24 ethyl- β -homo-7-oxo-5 α -cholestane-6-one] (Fig. 1A) was purchased from Waterstone Technology (Carmel, IN) and its structure was confirmed by ESI-LCMS and NMR. Brassinosteroid analogues 2-9 (Fig. 1B), including homocastasterone (22S, 23S, 24S)- 2 α , 3 α , 22, 23-tetrahydroxy-24-ethyl-5 α -cholestan-6-one (2), (22S,23S,24R)-3 α -fluoro-22,23-dihydroxy-24-ethyl- β -homo-7-oxa-5 α -cholestan-6-one (3), (22S,23S,24S)-3 α -fluoro-22,23-dihydroxy-24-ethyl-5 α -cholestan-6-one (4), (22S,23S,24S)-2 α ,3 α ,22,23-tetrahydroxy-24-ethyl- β -homo-7-aza-5 α -cholestan-6-one (5), (22S,23S,24S)-2 α ,3 α ,22,23-tetrahydroxy-24-ethyl- β -homo-6-aza-5 α -cholestan-7-one (6), (22R,23R,24S)-2 α ,3 α ,22,23-tetrahydroxy- β -homo-7-oxa-5 α -cholestan-6-one (7), (22S,23S,24R)-2 α ,3 α ,22,23-tetrahydroxy-24-methyl- β -homo-7-oxa-5 α -cholestan-6-one (8), and (22R,23R,24R)-2 α ,3 α ,22,23-tetrahydroxy-24-methyl- β -homo-7-oxa-5 α -cholestan-6-one (9) were synthesized or purchased previously (97), and are shown on Fig. 1B. All other chemicals and cell culture media were obtained from Sigma (Saint Louis, MO) or Invitrogen (Carlsbad, CA) unless specified otherwise.

5.3.2 Animal model of wound healing

All animal experiments were performed according to procedures approved by the Rutgers Institutional Animal Care and Use Committee in AAALAC accredited animal care facility. Twenty seven six-week-old male C57BL/6J mice obtained from Jackson Laboratory (Bar Harbor, ME) were housed in individual chambers, in a room maintained at a constant temperature with a 12 h light-dark cycle and had free access to food and water. Animals were allowed to adapt to their new conditions for seven days and handling the animals was performed daily during this time to reduce the stress of physical manipulation. Animals were randomized into groups (n=9) according to body weight one day prior to dosing. Under volatile anesthesia (5% isoflurane to effect), the shoulder and back region of each animal was shaved. A sharp punch (ID 6 mm) over the lumbar spine was applied to remove the skin including panniculus carnosus and adherent tissues. The test substance (control vehicle 1.5% carboxymethyl cellulose, or 10 µg/mouse of either HB or positive control CGS-21680) was administered topically, immediately following cutaneous injury, and then daily for 10 d. To investigate the kinetics of the wound healing, wound sizes were photographed and measured every two days with ImageJ software (rsbweb.nih.gov/ij/). The time to wound closure was estimated by comparing the area of treatment wounds to the area of control wounds. The percent closure of the wound (%) was calculated, and wound half-closure time (CT₅₀) was analyzed by linear regression. At the end of experiment, animals were euthanized by CO₂ gas inhalation, wounded tissue samples were collected by snap-freezing in liquid nitrogen and stored at -80°C for wound healing factor assays or fixed in 4% paraformaldehyde for routine histological sectioning and staining using Mayers haematoxylin and eosin.

5.3.3 Cell culture

The NIH 3T3 murine embryonic fibroblast cell line CCL-92 was obtained from ATCC (Manassas, VA). Cells were routinely maintained in Dulbecco's modified Eagle's medium (DMEM) containing 10% FBS and 0.1% penicillin-streptomycin at 37°C and 5% CO₂ and passaged every 3-4 days. Cells were subcultured into 96 well plates for proliferation and cell viability assays, and into 24 well plates for scratch wound closure studies (Greiner Bio One, Monroe, NC).

5.3.4 Cell viability and proliferation assays

3T3 fibroblasts were seeded in a 96-well flat bottom plate at a density of 1×10^4 cells/well. Cell viability was measured by the MTT (3-(4,5-Dimethylthiazol-2-yl)-2,5-diphenyltetrazolium bromide) assay in triplicate essentially as described (0.3-30 mM of test substance for 4 h) (45) and quantified spectrophotometrically at 550 nm using a microplate reader (Molecular Devices, Sunnyvale, CA). The concentrations of test reagents that showed no changes in cell viability compared with that of the vehicle (0.1% ethanol) were selected for further studies. For cell proliferation studies, cells were treated in triplicate with 0.1-10 mM of test substance for 24 h and assayed using BrdU (5-bromo-2'-deoxyuridine) kit from Amersham (Uppsala, Sweden).

5.3.5 Scratch wound closure

The 3T3 Swiss fibroblast were seeded into 24-well tissue culture plates at a concentration of 3×10^5 cells/ml and cultured to nearly confluent cell monolayers. Then, a linear wound was generated in the monolayer with a sterile 100 μ l plastic pipette tip. Any

cellular debris was removed by washing with phosphate buffer saline. DMEM medium with vehicle (0.1% ethanol), FBS (1%, positive control), or various concentrations of the pure compounds was added to a set of 3 wells per dose and incubated for 12 h at 37°C with 5% CO₂. The cells were visualized in 10% methylene blue for 5 minutes. Three representative images from each well of the scratched areas under each condition were photographed to estimate the relative migration of cells at 0 and 12 h past treatment. The data were analyzed using ImageJ software (rsbweb.nih.gov/ij/) by calculating the percentage of scratch closure at each dose point relative to control.

5.3.6 Real time PCR

Total RNA was extracted from fibroblasts using Trizol (Invitrogen). RNA was quantified spectrophotometrically by absorbance measurements at 260 and 280 nm using the NanoDrop reader (NanoDrop Technologies, Wilmington, DE). The quality of RNA was assessed by gel electrophoresis. RNA was then treated with DnaseI (Invitrogen) to remove traces of DNA contamination and the cDNAs were synthesized with 2.5 µg of RNA using Stratascript reverse transcriptase (Stratagene) according to the manufacturers' protocols. Quantitative PCR was performed in duplicate essentially as described (123) using the following gene-specific primers (IDT, Coralville, IA) selected using the Primer Express 2.0 software (Applied Biosystems, Foster City, CA): β-actin, forward primer 5'-GGG AAA TCG TGC GTG ACA TT-3', reverse primer 5'-GCG GCA GTG GCC ATC TC-3'. Samples were subjected to a melting curve analysis to confirm the amplification specificity. The relative change in the target gene with respect to the endogenous control gene was determined using the 2^{ΔΔCT} method (124).

5.3.7 Statistical analysis

Data are represented as mean \pm SEM. Statistical analyses were performed with GraphPad Prism 4.0 (San Diego, CA) using one-way ANOVA completed by a multicomparison Dunnett's test. Wound closure associated with body weight change was analyzed by two-factor repeated-measures ANOVA, with time and treatment as independent variables. P- values of less than 0.05 were considered significant.

5.4 Results

5.4.1 Body weight and food intake

While there were no overall effects for body weight in the 10-day period following wounding, we noticed that all mice lost weight on day 2 post-wounding, with weight regain starting on day 4. Mice lost 1.5 g of body weight by day 2, and there was no significant difference between the treatments, although there was a tendency for HB to reduce weight loss associated with injury (Fig. 2). There was also a transient reduction in food intake that lasted for 48 h post-wounding with no significant differences noted between the treatments (data not shown).

5.4.2 HB treatment improves wound healing

We found that cutaneous wound healing was significantly improved in animals receiving 10 μ g topical HB per mouse per day for 10 d compared with the control group treated with vehicle alone (Fig. 3A). The brassinosteroid effect appeared to occur in the

early phases (up to d 6 post-wounding) of wound healing (Fig. 3B). The CT_{50} time at which 50% of the cutaneous wound was closed was significantly reduced by both HB (5.4 ± 0.3 days) and the positive control CGS-21680 (6.2 ± 0.4 days) compared with the vehicle controls (7.2 ± 0.2 days). The strongest effect associated with HB treatment was observed on d 4. When wound data were expressed in terms of percent of original wound size, there was a two fold increase in the speed of wound closure relative to the control mice. Another interesting morphological observation associated with HB treatment was increased volume of the wound edges that reached prominence on d 4 and slowly subsided on d 6-8 to completely disappear on d 10 post-wounding. This feature was absent in both the negative and positive controls, and may represent enhanced epidermis re-grows from germinative cells left in the skin at the edges of the wound.

5.4.3 HB reduces proinflammatory markers in healing wounds

We examined mRNA levels of the proinflammatory cytokines TNF- α and TGF- β along with an adhesion chemokine iCAM in the wound tissue of control and treated mice on d 10 post-wounding. We chose to examine the cytokine TNF- α since it has been shown to play an important function in the development of inflammation (125). TGF- β , on the other hand, acts as an antiproliferative factor in normal epithelial cells with potent regulatory and inflammatory activity that is context-specific (126). Finally, iCAM regulates inflammation and vascular permeability that permits the excessive transfer of solutes to peripheral tissues (127). Transcriptional regulation plays an important role in the physiological relevance of these factors in the context of wound healing (128). Wound tissue from animals treated with the adenosine receptor agonist CGS-21680 as a

reference control (129) showed a remarkable suppression of TNF- α mRNA, but no effect on either TGF- β or iCAM mRNA levels. Contrary to this, HB treatment was associated with a weak effect on TGF- β , significant suppression of iCAM, as well as nearly complete downregulation of TNF- α (Fig. 4).

5.4.4 Effect of brassinosteroids on cell viability and proliferation

To further elucidate effects of brassinosteroid treatment on cell proliferation and to determine the structure-activity requirements for their biological activity, we analyzed cytotoxic and cell proliferation effects of HB and its natural or synthetic analogues (97) (Fig. 1B) in 3T3 mouse fibroblast cell culture. Compound 5 synthesized to carry a 7-aza substitution in the B ring of the molecule showed the highest cytotoxicity with IC₅₀ of 12.5 mM. Two other synthetic brassinosteroids with fluorinated substitutes in the A ring of the molecule showed weak toxicity at 30 mM, the highest concentration tested. There was no correlation between compound's ability to induce cell proliferation and stimulation of cell migration (Table 1).

5.4.5 Effect of brassinosteroids on scratch wound closure

Microscopic observation of 3T3 fibroblasts demonstrated that HB promotes cell migration into a scratch wound zone with maximum efficacy of $30 \pm 4.2\%$ at 5 mM after 12 h of incubation. This compares favorably with 1% fetal bovine serum used as a positive control in this assay ($41.5 \pm 6.5\%$), as well as reference activity of the platelet-derived growth factor reported earlier (130). Several HB analogues showed similar or decreased scratch wound closure activity in this assay, with no specific reference to

structural modifications (Table 1). The cytotoxic compound 5 showed no effect on fibroblast migration, as expected. A dose dependent migration activity was evaluated for all active compounds that significantly accelerated wound closure at concentrations of 0.1-10 μ M. Compound 4 turned out to possess high activity similar to HB, while compound 6 showed the highest activity at 3 mM, possibly due to weak cytotoxicity associated with the higher doses of this treatment (Fig. 5A-C).

5.5 Discussion

Previously we reported that orally applied brassinosteroids produced significant anabolic effects and improved physical fitness in healthy animals with minimal androgenic effects (77). Brassinosteroids are a class of plant hormones with a polyoxygenated steroid structure showing pronounced plant growth regulatory activity (79). They also exhibit striking structural similarities (Fig. 1) with animal sex hormones and arthropod hormones of the ecdysteroid type such as 20-hydroxyecdysone (80) that have been reported to produce anabolic effects in mammals (58).

Animal sex hormones play a gender- and age-modified role in wound healing. For example, aged males were shown to have delayed healing of acute wounds when compared to aged females. A partial explanation for this is that the male androgens (testosterone and 5α -dihydrotestosterone), female estrogens (estrone and 17β -estradiol), and their steroid precursor dehydroepiandrosterone have significant effects on the wound-healing process (131). Estrogen affects wound healing by regulating a variety of genes associated with regeneration, matrix production, protease inhibition, epidermal function, and the genes primarily associated with inflammation (132). Conversely, oral mucosal

wounds heal faster in males (133). The skin also acts as a steroidogenic tissue containing the full cytochrome P450 system required for the de novo production of sex steroids from cholesterol (134). This raises the possibility that bioactive hormones locally synthesized within the wound microenvironment may also be important in healing.

In this study, we hypothesized that since brassinosteroids activate the PI3K/Akt signaling pathway with minimal androgenic effects (77), they may have potential applications to wound healing. Indeed, topical application of brassinosteroids significantly reduced wound size in treated C57BL/6J mice (Fig. 2 and 3). These findings are in agreement with previous studies that found androgens to delay wound healing. Testosterone appears to modulate healing by directly altering wound cell populations and cytokine profiles, thereby enhancing the inflammatory response and reducing matrix deposition. This is supported by androgen receptor expression in keratinocytes, fibroblasts, and inflammatory cells within the wound (135). Moreover, in our study HB exerted its effect on wound healing early in the healing process (Fig. 3). Proinflammatory cytokines and chemokines initiate and coordinate the early inflammatory phase of wound healing (136). However, it is now well established that uncontrolled or elevated inflammation might be responsible for the delay in wound healing rates. We next examined whether or not the HB-induced alteration in wound healing in mice was related to a reduction in inflammatory cytokines and chemokines within wound tissue (Fig. 4). HB treatment was associated with a weak effect on TGF- β , significant suppression of iCAM, as well as nearly complete downregulation of TNF- α . This result has two possible explanations. On one hand, it may suggest that brassinosteroids (and more specifically, HB) have anti-inflammatory activity, however this conclusion was not supported by our

preliminary data as no anti-inflammatory effect of HB on LPS-stimulated inflammation in macrophage cell culture was observed (data not shown). Significantly lower levels of TNF- α and iCAM in wound tissues could be also explained by the time of sampling and analysis. Since the strongest effect of HB was observed at the end of the early phase of skin wound healing when inflammatory and tissue repair stages overlap (day 4), it is possible that HB promotes wound healing by stimulation of cell proliferation or migration into the wound area. In this case, HB-treated wound tissues analyzed 10 days post-wounding will appear more advanced in the wound healing process than the respective control samples that remain inflamed.

This hypothesis was tested in the 3T3 mouse fibroblast cytotoxicity, proliferation, and scratch wound assays (130). While HB showed no cytotoxicity *in vitro* when tested up to 30 mM concentration, several brassinosteroid analogues containing either 6-aza group in the B ring of the molecule, or fluorinated substitutes in the A ring, showed weak toxicity at the highest concentrations tested (Table 1). This is in agreement with a previous study that analyzed cytotoxicity of various brassinosteroids against several human cancer cell lines despite having minimal effects on BJ human foreskin fibroblasts (11). For example, (22R,23R)-homocastasterone showed highest cytotoxicity ($IC_{50} = 13$ mM) against the the T-lymphoblastic leukaemia CEM cells, while its synthetic counterpart (22S,23S)-homocastasterone (compound 2 in this study) showed weak to no cytotoxicity below 50 mM. (22S,23S)-homobrassinolide (HB or compound 1 in this study) had an IC_{50} of ~ 30 mM against CEM and RPMI 8226 cancer cells, but no cytotoxicity was observed towards the K562, A549, HeLa, and HOS cancer cell lines (11). Additionally, 24-epibrassinolide (compounds 8-9 in this study) increased the

proportions of viable hybridoma mouse cells at nM concentrations (137). All four brassinosteroids tested in this study for their ability to induce cell proliferation at 5 mM, showed moderate biological activity that had no correlation to structural changes in either the A or B ring of the molecule (Table 1). There was also no correlation between the compound's ability to induce cell proliferation and stimulation of cell migration, as both R,R- and S,S-24-epibrassinolides promoted cell proliferation but not migration, while HB treatment resulted in a significant increase in both parameters. However, there was a direct correlation between the compound's ability to promote cell migration (Fig. 5) and induce Akt phosphorylation (97). Akt is a key enzyme in signal transduction pathways involved in cell survival, cell-cycle progression, and migration (138). Increasing evidence suggests that Akt may play a role in repair and collagen production by activated fibroblasts (139). Thus, while stimulating the components of the PI3K/Akt network ultimately leads to increased collagen deposition by fibroblasts and enhanced tissue repair, distinct cellular mechanisms may be involved in mediating the proliferation and migration effects.

In summary, our study shows that brassinosteroid analogues positively modulate inflammatory and re-epithelialization phases of the wound-repair process *in vivo* and *in vitro*, in part by enhancing migration of fibroblasts in a wounded area. Brassinosteroids promote skin regeneration and, thus, may have applications in medicine and skin care. Further research is needed to address the precise underlying mechanisms of their action and to find the optimal therapeutic concentration for use in clinical practice. These results bring scientific support to potential applications of bioactive compounds from plant steroid analogues in regenerative medicine.

5.6 Acknowledgments

The authors thank Reneta Pouleva, Ruth Dorn, and Teresa Lucibello for excellent technical assistance. This work was supported, in part, by Rutgers University, by the 5P50AT002776-05 grant from the National Center for Complementary and Alternative Medicine (NCCAM).

Table 1. Effect of HB (1) and its analogues (2-9) on cell viability, proliferation, and scratch wound closure in 3T3 mouse fibroblasts. Results are expressed as the mean \pm SEM of determinations performed in triplicate (* $P < 0.05$ when compared with control by one-way ANOVA and Dunnett's post-test). FBS (fetal bovine serum) and PDGF (platelet-derived growth factor) are shown as reference treatments. Nt, not tested.

ID	Common name	Scratch wound closure at 5 mM, %	Cell proliferation at 5 mM, % of control	Cell cytotoxicity, IC ₅₀ (mM)
1	(22S,23S)-homobrassinolide (HB)	30 \pm 4.2*	37.7 \pm 3.4*	>30
2	(22S,23S)-homocastasterone	32.9 \pm 4.1*	Nt	>30
3	(22S,23S)-3 α -fluoro-homobrassinolide	15.3 \pm 2.6	Nt	~30
4	(22S,23S)-3 α -fluoro-homocastasterone	27.7 \pm 4.0*	Nt	~30
5	(22S,23S)-6-aza-homobrassinolide	13.0 \pm 0.7	Nt	12.5
6	(22S,23S)-7-aza-homobrassinolide	30.5 \pm 4.2*	Nt	>30
7	(22R,23R)-homobrassinolide	16.5 \pm 0.5	29.1 \pm 3.4*	>30
8	(22S,23S)-epibrassinolide	13.2 \pm 1.5	31.9 \pm 5.3*	>30
9	(22R,23R)-epibrassinolide	8.1 \pm 1.6	31.0 \pm 2.6*	>30
Ref	FBS, 1%	41.5 \pm 6.5*	39.3 \pm 5.7*	--
Ref	PDGF, 2 nM (130)	64.8 \pm 1.7*	--	--

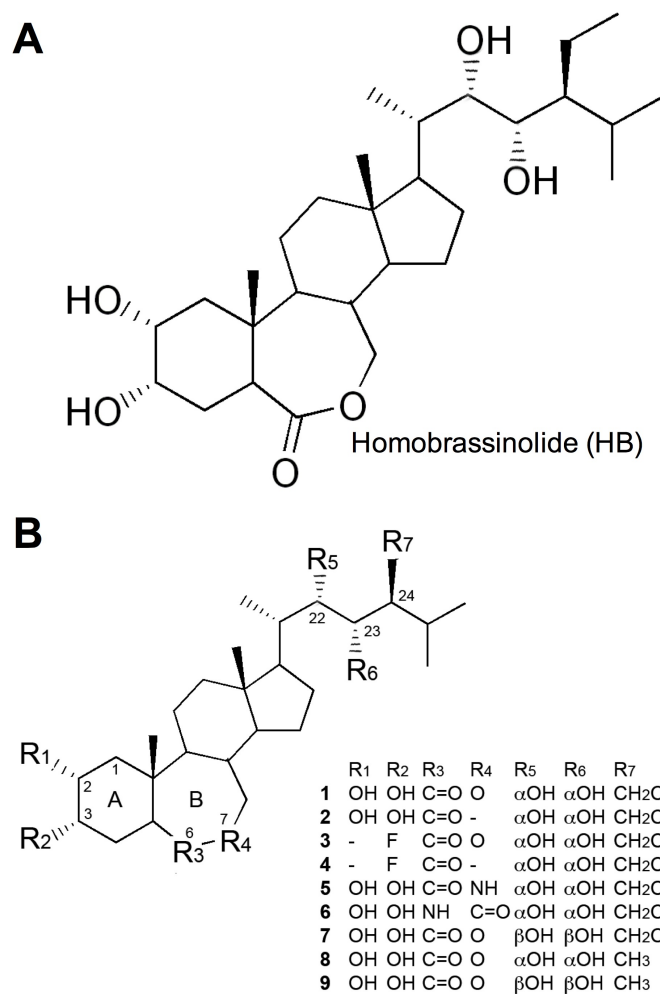


Figure 1. Chemical structure of (A) 28-homobrassinolide, HB in comparison with (B) other synthetic and natural brassinosteroid analogues.

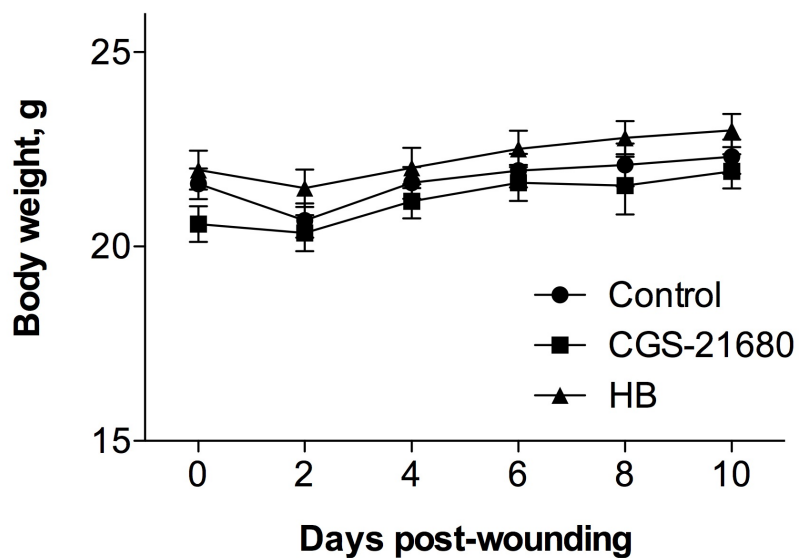


Figure 2. Effect of HB treatment on body weight change associated with wounding.

A sharp punch over the lumbar spine was applied to remove the skin and vehicle, or 10 $\mu\text{g}/\text{mouse}$ of either HB or the positive control CGS-21680 was administered topically daily for 10 d. Two-factor repeated-measures ANOVA, * $P < 0.05$ ($n=9$).

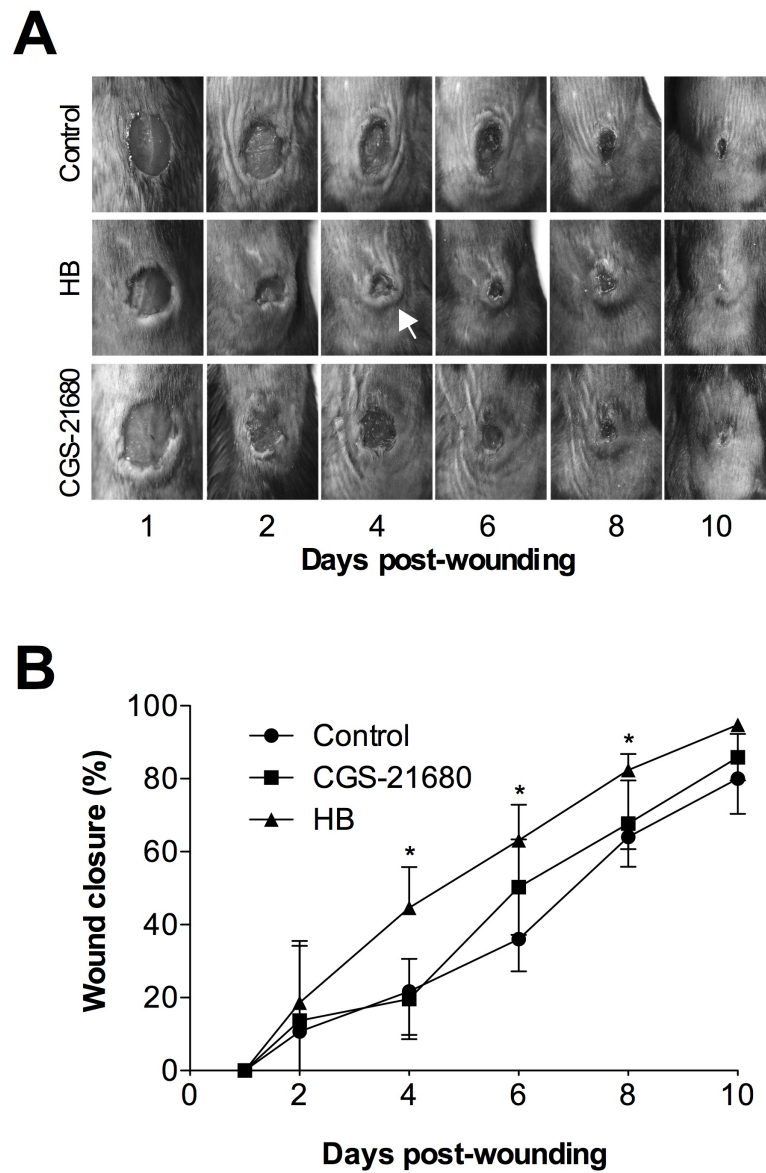


Figure 3. Time course of wound healing in mouse cutaneous injury model. (A) Wound sizes were photographed and measured every 2 d for 10 d. **(B)** The wound closure (%) relative to d 1 was determined every 2 d, and the wound half-closure time (CT_{50}) was calculated by linear regression. Two-factor repeated-measures ANOVA, * $P < 0.05$ ($n=9$).

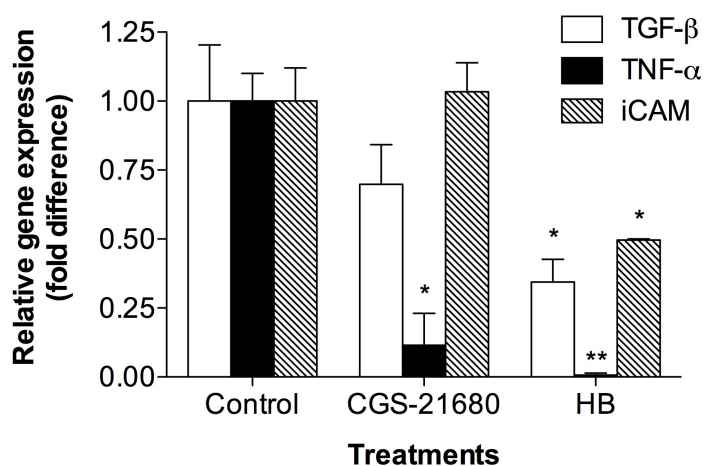


Figure 4. Effect of HB on cytokine and chemokine mRNA expression in wounds of C57Bl/6J mice. RNA was isolated from wound tissues collected 10 d post-wounding and mRNA levels for the proinflammatory cytokines TNF- α , TGF- β m and an adhesion chemokine iCAM were measured by qPCR. The target gene expression of the housekeeping gene (actin) was assigned a value of 1. *P<0.05, **P<0.01 significantly different from vehicle controls, one-way ANOVA with Dunnett's post-hoc test.

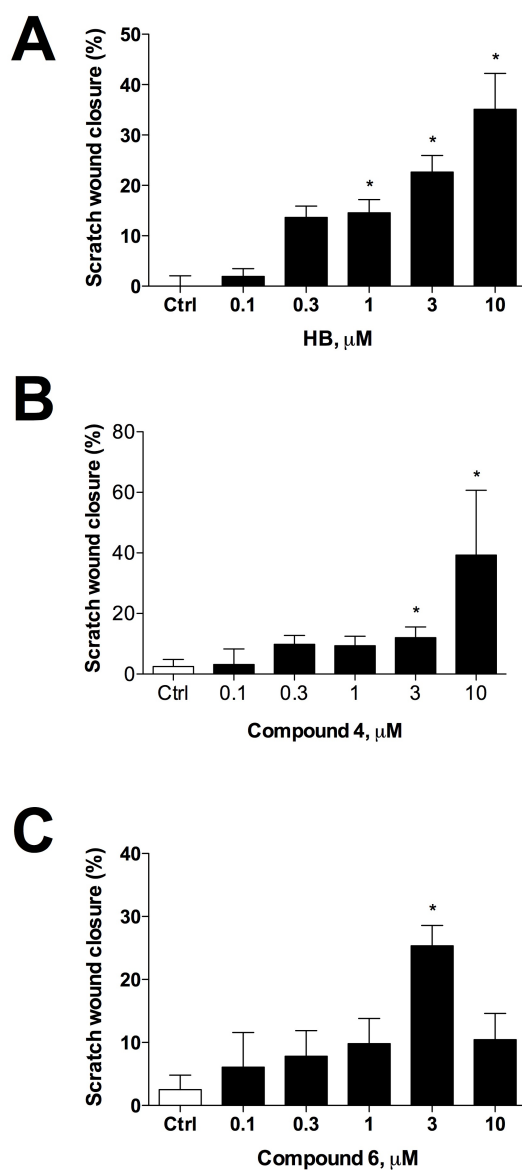


Figure 5. Dose dependent effect of brassinosteroid treatment on scratch wound closure *in vitro*. 3T3 Swiss fibroblast monolayers were scratched with a sterile pipette tip and vehicle (0.1% ethanol), FBS (1%, positive control), or various concentrations of (A) HB, (B) (22S,23S)-3 α -fluoro-homocastasterone, or (C) (22S,23S)-7-aza-homobrasinolide were added to set of 3 wells per dose and incubated for 12 h. The data represent the average of 2 experiments \pm SE. * $P < 0.05$, ** $P < 0.01$ (n=3) using one-way ANOVA and Dunnett's post-test.

CHAPTER VI

SUMMARY AND CONCLUSION

Brassinosteroids are plant-derived polyhydroxylated derivatives of 5 α -cholestane, structurally similar to cholesterol-derived animal steroid hormones and insect ecdysteroids, with no known function in mammals. This research project was designed to conduct a pharmacological characterization of brassinosteroids in cell culture and small animal models to: (1) Elucidate the putative anabolic effect of BR in mammals; (2) Establish a structure-activity relationship between brassinosteroids and their effects on protein synthesis; and (3) Measure the effects of brassinosteroids on glucose metabolism and wound healing.

Prior to this work, almost no data existed on the *in vivo* effects of brassinosteroids in animals. Given the importance of identifying novel agents that influence muscle growth, development, and/or regeneration with possible therapeutic application for age or disease-related skeletal muscle atrophy (sarcopenia), we sought to explore the effects of brassinosteroids on protein synthesis and degradation in animals, and to study the signal transduction pathways they interact with. Furthermore, we compared the activity of brassinosteroids to that of the insulin-like growth factor-1 (IGF-1) *in vitro* and showed that the PI3K/Akt pathway is upregulated in skeletal muscle cells treated with brassinosteroids. We also found that brassinosteroid treatment produced anabolic effects and improved physical fitness in healthy animals without detrimental androgenic effects. These data establish selective anabolic action of plant brassinolides in animals and provide important insight into the role of Akt signaling in mediating this activity. Moreover, our data demonstrate that this property may pharmacologically differentiate homobrassinolide from anabolic steroids.

In a separate *in vitro* study, we provided additional evidence that the 6-keto group and 22 α ,23 α -hydroxyls are critical for the anabolic activity of brassinosteroids in rat skeletal muscle cells. This may be useful for the design of novel therapeutic molecules possessing high anabolic selectivity. In addition, (22S,23S)-homobrassinolide and (22S,23S)-homocastasterone, which were confirmed to possess the greatest anabolic activity among the molecules analyzed, may be employed as pharmacological tools to investigate the biological functions of muscle growth and regeneration pathways.

Since oral administration of homobrassinolide to healthy rats triggered a selective anabolic response that was associated with lower blood glucose, we performed another study aimed at evaluating the effects of brassinosteroid administration on glucose metabolism, insulin sensitivity, body composition, and gluconeogenic gene expression profiles in liver of C57BL/6J high fat diet-induced obese mice. The stimulatory effect of the brassinosteroid on glucose metabolism via PI3K and AMPK signaling pathways subsequently translated into whole body insulin sensitizing effect, such as improved oral glucose tolerance.

Akt is also a key signaling integrator suppressed in slow healing wounds. In a separate study using a mouse cutaneous model of wound healing, we showed that brassinosteroid analogues positively modulate inflammatory and re-epithelialization phases of the wound-repair process *in vivo* and *in vitro*, in part by enhancing migration of fibroblasts in a wounded area. Brassinosteroids promote skin regeneration and, thus, may have applications in medicine and skin care. Further research is needed to address the precise underlying mechanisms of their action and to find the optimal therapeutic concentration for use in clinical practice. These results bring scientific support to

potential applications of bioactive compounds from plant steroid analogues in performance and regenerative medicine.

APPENDIX**STEROIDAL GLYCOSIDES FROM THE BULBS OF EASTER LILY PROMOTE
WOUND HEALING**

Debora Esposito, Slavko Komarnytsky, John P. Munafo Jr, Teresa Lucibello, Manuel
Baldeon, Thomas J. Gianfagna

Experiments for data presented in Table 1, Figs. 2, 5-6 were performed
by Debora Esposito

7.1 Abstract

The Easter lily (*Lilium longiflorum* Thunb.) is used as both food and medicine in many parts of Asia and is cultivated as an ornamental plant throughout the world. Among many applications, preparations made from the bulbs of *L. longiflorum* have been used traditionally for the treatment of various skin conditions. Given the increasing interest in the identification of biologically active natural products in traditionally used botanicals, the objective of this investigation was to evaluate extracts of Easter lily bulbs and identify biologically active compounds using an *in vitro* skin fibroblast migration and proliferation assay. Employing a bioassay modeling the promotion of scratch wound closure resulted in the identification of two biologically active steroidal glycoalkaloids (22R, 25R)-spirosol-5-en-3 β -yl *O*- α -L-rhamnopyranosyl-(1 \rightarrow 2)- β -D-glucopyranosyl-(1 \rightarrow 4)- β -D-glucopyranoside and (22R, 25R)-spiro-sol-5-en-3 β -yl *O*- α -L-rhamnopyranosyl-(1 \rightarrow 2)-[6-*O*-acetyl- β -D-glucopyranosyl-(1 \rightarrow 4)]- β -D-glucopyranoside, and a biologically active furostanol saponin, (25R)-26-*O*-(β -D-glucopyranosyl)-furost-5-en-3 β ,22 α ,26-triol 3-*O*- α -L-rhamnopyranosyl-(1 \rightarrow 2)- β -D-glucopyranosyl-(1 \rightarrow 4)- β -D-glucopyranoside that promote wound closure. Bulb extract fractions and two steroidal glycoalkaloids induced nitric oxide production and transforming growth factor beta (TGF- β) receptor I mRNA expression in fibroblast cell culture, suggesting multiple mechanisms of action on wound healing. These compounds isolated from *L. longiflorum* may play a role in the wound healing process and can be used for further studies to elucidate the molecular mechanisms by which the topical application of steroidal glycosides from Easter lily may improve wound healing.

7.2 Introduction

The Easter Lily (*Lilium longiflorum* Thunb., Family Liliaceae) is well known as an attractive ornamental plant. In addition to its popularity in horticulture, lily bulbs are regularly used in Asia for various culinary and medicinal purposes (140-142). In China and Japan, the most common medicinal use of lily bulbs is as a general tonic, an anti-inflammatory agent, and as a treatment for lung conditions (141, 142). In addition, preparations containing bulbs from various *Lilium* species, including the Easter lily and the Madonna lily, *Lilium candidum*, have been traditionally used to induce the healing process of skin abrasions and burns and to aid in healing from surgery (143, 144).

L. longiflorum is a rich source of natural products. Many secondary metabolites have been reported including phenolics (145), phenolic glucosides (146), flavonoids (147), carotenoids (148), sterols (148), steroidal saponins (149-151), and steroidal glycoalkaloids (151, 152). In fact, several anti-inflammatory compounds, including flavonols, flavonol glycosides, and a chalcone, have been isolated from the flowers of Easter lily and may contribute to their biological activities (147). In addition, several steroidal saponins with anti-tumor promoter activity have been identified in the bulbs (Mimaki et al., 1994). Although the traditional use of *L. longiflorum* is well documented, the compounds responsible for the reported medicinal properties remain unknown.

The cutaneous wound healing process is essential for skin homeostasis. Impaired wound healing may lead to chronic skin disorders resulting in significant decrease in quality of life and increased morbidity (153). Deregulated wound repair may also promote excessive scarring and associated loss of joint motion or cosmetic body deformations (154). When skin is injured, the immediate release of various growth

factors, cytokines, and low molecular weight components of the extracellular matrix initiate the repair process that consists of three overlapping phases: inflammation, tissue formation and remodeling (155). The first event occurring after injury is the formation of a blood clot and infiltration of the wound with neutrophils and macrophages that promote at this stage an intense phagocytic activity. The tissue formation phase involves re-epithelization by migrating keratinocytes and granulation tissue formation that depends on the activation and migration of fibroblasts, changes in extracellular matrix production, and neovascularization. The last stage of the wound healing process consists of a gradual involution of the granulation tissue and dermal regeneration (156).

Transforming growth factor beta1 (TGF- β 1) is essential for initiation of granuloma tissue formation and cell migration by transcriptional upregulation of matrix metalloproteinases (157) and cell migration-associated integrins (158, 159). Reduced TGF- β 1 expression has been observed in animal models and in humans with impaired wound healing (160, 161). Contrary to these findings, transgenic mice with disrupted TGF- β 1 signaling exhibited accelerated wound healing (162, 163). This controversial data reflects the complex nature of TGF- β 1 signaling, which in fact may be cell-type and context specific (164). In support of this finding, transgenic mice overexpressing a dominant negative TGF- β receptor exhibited accelerated wound healing (165). Ongoing experimental and clinical wound healing studies have also established the importance of nitric oxide (NO) as a critical mediator of normal tissue repair. Angiogenesis, granular tissue formation, epidermal migration, collagen deposition, and microvascular homeostasis are significant processes critical to normal wound repair that are regulated by NO production and bioactivity (166).

Aimed at identifying biologically active natural products in traditionally used botanicals, the objective of this present investigation was to evaluate fractionated Easter lily bulb extracts and five steroidal glycosides purified from the bulb fractions for the promotion of wound healing using an *in vitro* scratch wound closure assay. Easter lily bulb fractions were generated by sequential solvent extraction and gel permeation chromatography (GPC). Two steroidal glycoalkaloids, (22R, 25R)-spirosol-5-en-3 β -yl *O*- α -L-rhamnopyranosyl-(1 \rightarrow 2)- β -D-glucopyranosyl-(1 \rightarrow 4)- β -D-glucopyranoside (**1**) and (22R, 25R)-spirosol-5-en-3 β -yl *O*- α -L-rhamnopyranosyl-(1 \rightarrow 2)-[6-*O*-acetyl- β -D-glucopyranosyl-(1 \rightarrow 4)]- β -D-glucopyranoside (**2**), and three furostanol saponins, (25R)-26-*O*-(β -D-glucopyranosyl)-furost-5-en-3 β ,22 α ,26-triol 3-*O*- α -L-rhamnopyranosyl-(1 \rightarrow 2)- β -D-glucopyranosyl-(1 \rightarrow 4)- β -D-glucopyranoside (**3**), (25R)-26-*O*-(β -D-glucopyranosyl)-furost-5-en-3 β ,22 α ,26-triol 3-*O*- α -L-rhamnopyranosyl-(1 \rightarrow 2)- α -L-arabinopyranosyl-(1 \rightarrow 3)- β -D-glucopyranoside (**4**) and (25R)-26-*O*-(β -D-glucopyranosyl)-furost-5-en-3 β ,22 α ,26-triol 3-*O*- α -L-rhamnopyranosyl-(1 \rightarrow 2)- α -L-xylopyranosyl-(1 \rightarrow 3)- β -D-glucopyranoside (**5**) were isolated and purified from GPC fractions. In addition, to gain some insight into the mechanism of action of the compounds, experiments on cytotoxicity, NO production, and expression of known target genes of the TGF- β signaling pathway were performed.

7.3 Materials and methods

7.3.1 Chemicals

Sephadex LH-20 and pyridine- d_5 (0.3% v/v TMS) were obtained from Sigma-Aldrich (St. Louis, MO). All solvents (acetonitrile, ethanol, ethyl acetate, formic acid, *n*-butanol, and *n*-pentane) were chromatographic grade (Thermo Fisher Scientific, Fairlawn, NJ). Water was deionized (18 M Ω cm) using a Milli-Q-water purification system (Milli-Q, Bedford, MA). Reagents and enzymes used for qPCR were obtained from Stratagene (La Jolla, CA) and Applied Biosystems (Foster City, CA). All other chemicals and cell culture media were obtained from Sigma (Saint Louis, MO) and Invitrogen (Carlsbad, CA), respectively.

7.3.2 Plant material

L. longiflorum, cultivar 7-4, bulbs were provided by Dr. Richard Merritt (Rutgers University Easter Lily-Breeding Program) and cultivated as described previously (151). At the time of harvesting the bulbs were manually separated, immediately frozen in liquid nitrogen, lyophilized on a Virtis Advantage freeze dryer (SP Industries, Warminster, PA) and stored at -80°C until analysis.

7.3.3 Sequential solvent extraction of Lyophilized *L. longiflorum* bulbs

Lyophilized lily bulbs (100 g) were ground into a fine powder with a laboratory mill (IKA Labortechnik, Staufen, Germany) and extracted with *n*-pentane (3 x 100 ml) on a Wrist-Action autoshaker (Burrell Scientific, Pittsburg, PA) at room temperature for 30 min. After centrifugation (5000 rpm for 10 min) (Sorvall RC-3C Plus, Thermo Fisher Scientific, Fairlawn, NJ), the organic phases were pooled and evaporated under reduced pressure (30 °C; 1.0 x 10⁻³ bar) using a Laborota 4003 rotary evaporator (Heidolph

Brinkman LLC, Elk Grove Village, IL) yielding fraction I. The pellet was freed from residual solvent in a fume hood overnight and the defatted material was then extracted with a mixture of ethanol and water (7:3, v/v; 2 x 150 ml) on an autoshaker for 45 min at room temperature. After centrifugation (5000 rpm for 10 min) and vacuum filtration through a Whatman 114 filter paper (Whatman International, Maidstone, UK), the supernatant was collected and the residue (80.92 g) was discarded. The supernatant was then evaporated under reduced pressure and lyophilized twice, yielding fraction II. Fraction II was then dissolved in deionized water (100 ml), washed with ethyl acetate (5 x 100 ml) and the organic phase was pooled, evaporated under reduced pressure, and lyophilized twice, yielding fraction III. The aqueous phase was then extracted with *n*-butanol (5 x 100 ml) and the aqueous phase was evaporated under reduced pressure, and lyophilized twice, yielding fraction IV. The organic phase was pooled, evaporated under reduced pressure, dissolved in deionized water (25 ml), and lyophilized twice, yielding fraction V. The individual fractions with yields given in parentheses (in g/100 g): I (0.57), II (13.7), III (0.77), IV (8.96), and V (2.42), were stored at -80° C until used for bioassay, fractionation, and chemical analysis.

7.3.4 Gel permeation chromatography (GPC)

Fraction V (1.0 g) was dissolved in a solution of ethanol and water (7:3, v/v; 5.0 ml), filtered with a 0.45 µm PTFE syringe filter (Thermo Fisher Scientific, Fairlawn, NJ) and then applied onto a standard threaded 4.8 cm x 60 cm glass column (Kimble Chase Life Science and Research Products LLC, Vinland, NJ) packed with Sephadex LH-20 (Amersham Pharmacia Biotech, Uppsala, Sweden). The column was washed and

conditioned in the same solvent mixture for 24 h. Chromatography was performed with isocratic ethanol and water (7:3, v/v) at a flow rate of 3.5 ml min⁻¹. The first 200 ml of effluent was discarded and 30 fractions (25 ml each) were collected and subjected to LC-MS analysis. Based on the LC-MS profile, fractions 5 through 12 and 13 through 15 were individually pooled, evaporated under reduced pressure and lyophilized, yielding 2 fractions with yields given in parentheses (in mg/1 g fraction V): V-1 (180) and V-2 (50). All fractions were stored at -80° C until used for bioassay, RP-HPLC purification, and chemical analysis.

7.3.5 Semipreparative reverse-phase high performance liquid chromatography

Fractionation of GPC fraction V-1 and V-2 was achieved by semipreparative RP-HPLC performed on a Luna C18 column (250 mm x 21.2 mm i.d.; 10 µm particle size) (Phenomenex, Torrance, CA) according to the method described in the literature (151). Fractions V-1 and V-2 afforded compounds **3**, **4**, and **5** and compounds **1** and **2**, respectively. Chromatographic separations were performed on a Shimadzu LC-6AD liquid chromatograph (Shimadzu Scientific Instruments Inc, Columbia, MD) using a UV/VIS detector and a 2 ml injection loop (Rheodyne LLC, Rohnert Park, CA). Mixtures of (A) 0.1% formic acid in deionized water and (B) 0.1% formic acid in acetonitrile were used as the mobile phase. The flow rate was set to 20 ml min⁻¹. The column temperature was set to 23 ± 2 °C and UV detection was recorded at λ = 210 nm. GPC fractions were dissolved in a mixture of mobile phase A and mobile phase B (75:25, v/v) and filtered through 0.45 µm PTFE syringe filter prior to injection. Chromatography was performed using a linear gradient of 5-30% B over 45 min and then to 90% B over 10 min;

thereafter, elution with 90% B was performed for 10 min. The re-equilibration time was 10 min. The target compounds were collected, freed from solvent under reduced pressure and lyophilized. Final purification of **1** and **2** was performed with an isocratic separation using a mixture of 0.1% formic acid in deionized water and 0.1% formic acid in acetonitrile (80:20, v/v). The target compounds were collected, freed from solvent under reduced pressure and lyophilized, yielding compound **1** (10 mg) and compound **2** (5 mg) as white amorphous powders. Final purification of **3**, **4**, and **5** was performed with an isocratic separation using a mixture of 0.1% formic acid in DI water and 0.1% formic acid in acetonitrile (75:25, v/v). The target compounds were collected, freed from solvent under reduced pressure and lyophilized, yielding compound **3** (19 mg), compound **4** (5 mg), and compound **5** (5 mg) as white amorphous powders. Compounds **1** through **5** were in high purity > 98% as determined by LC-MS and NMR. Compound **1**, (22R, 25R)-spirosol-5-en-3 β -yl *O*- α -L-rhamnopyranosyl-(1 \rightarrow 2)- β -D-glucopyranosyl-(1 \rightarrow 4)- β -D-glucopyranoside. ^1H NMR and ^{13}C NMR spectra were consistent with the literature (151). Compound **2**, (22R, 25R)-spirosol-5-en-3 β -yl *O*- α -L-rhamnopyranosyl-(1 \rightarrow 2)-[6-*O*-acetyl- β -D-glucopyranosyl-(1 \rightarrow 4)]- β -D-glucopyranoside. ^1H NMR and ^{13}C NMR spectra were consistent with the literature (151). Compound **3**, (25R)-26-*O*-(β -D-glucopyranosyl)-furost-5-en-3 β ,22 α ,26-triol 3-*O*- α -L-rhamnopyranosyl-(1 \rightarrow 2)- β -D-glucopyranosyl-(1 \rightarrow 4)- β -D-glucopyranoside. ^1H NMR and ^{13}C NMR spectra were consistent with the literature (167). Compound **4**, (25R)-26-*O*-(β -D-glucopyranosyl)-furost-5-en-3 β ,22 α ,26-triol 3-*O*- α -L-rhamnopyranosyl-(1 \rightarrow 2)- α -L-arabinopyranosyl-(1 \rightarrow 3)- β -D-glucopyranoside. ^1H NMR and ^{13}C NMR spectra were consistent with the literature (151). Compound **5**, (25R)-26-*O*-(β -D-glucopyranosyl)-furost-5-en-3 β ,22 α ,26-

triol 3-*O*- α -L-rhamnopyranosyl-(1 \rightarrow 2)- α -L-xylopyranosyl-(1 \rightarrow 3)- β -D-glucopyranoside. ^1H NMR and ^{13}C NMR spectra were consistent with the literature (151).

7.3.6 Liquid chromatography-mass spectrometry (LC-MS)

LC-MS analysis was performed using an HP 1100 series HPLC (Agilent Technologies Inc., Santa Clara, CA) equipped with an auto injector, quaternary pump, column heater, diode array detector, interfaced to a Bruker 6300 series ion-trap mass spectrometer equipped with an electrospray ionization chamber. Reverse phase separations were performed using a Prodigy C18 column (250mm x 4.6mm i.d.; 5.0 μm particle size) (Phenomenex, Torrance, CA). The flow rate was set to 1.0 ml min^{-1} , the column temperature set to 25 $^{\circ}\text{C}$, and the injection volume was 1 μl . The binary mobile phase composition consisted of (A) 0.1% formic acid in deionized water and (B) 0.1% formic acid in acetonitrile. Chromatography was performed using a linear gradient of 15 - 43% B over 40 min and then to 95% B over 5 min; thereafter, elution with 95% B was performed for 10 min. The re-equilibration time was 10 min. All samples were dissolved in a mixture of mobile phase A and mobile phase B (75:25, v/v) and filtered through 0.45 μm PTFE syringe filter prior to analysis. All mass spectra were acquired in positive ion mode over a scan range of m/z 100-2000. Ionization parameters included: capillary voltage, 3.5 kV; end plate offset, -500V; nebulizer pressure, 50 PSI; drying gas flow, 10 ml min^{-1} , and drying gas temperature, 360 $^{\circ}\text{C}$. Trap parameters included: ion current control, 30000; maximum accumulation time, 200 ms; trap drive, 61.2; and averages, 12 spectra. For instrumentation control and data acquisition, HP ChemStation and BrukerData Analysis software was used.

7.3.7 Nuclear magnetic resonance spectroscopy (NMR)

1D ^1H NMR and ^{13}C NMR spectra were acquired on an AMX-400 spectrometer (Bruker, Rheinstetten, Germany). Samples for NMR analysis were dissolved in pyridine- d_5 , and chemical shifts were generated as δ values with reference to tetramethylsilane.

7.3.8 Cell culture

The 3T3 Swiss albino mouse fibroblast cells and HUVEC human umbilical vein endothelial cells were obtained from ATCC (Manassas, VA). Both cell lines were routinely passaged every 3-4 days and maintained in DMEM containing 10% fetal bovine serum (FBS) and 0.1% penicillin-streptomycin at 37 °C and 5% CO_2 . Cells were subcultured into 24-well dishes for cell proliferation/scratch wound closure assay, and 96-well dishes for cell viability and nitric oxide production studies.

7.3.9 Scratch wound closure

3T3 fibroblasts were seeded into 24-well dishes at a concentration of 3×10^5 cells/ml and cultured to nearly confluent cell monolayers. On the day of the experiment, a linear wound was generated in the monolayer with a sterile 100 μl plastic pipette tip and any cellular debris was removed by washing cells once with sterile phosphate buffered saline (PBS). Fresh DMEM medium containing vehicle (0.1% ethanol), positive control (0.5% FBS), or various concentrations of the fractions, sub-fractions or pure compounds was added to a set of 3 wells per dose and incubated for 12 h at 37 °C with 5% CO_2 . The cells were then visualized with 20 μl of 10% methylene blue in PBS for 5 min. Three

representative images of the scratched areas from each well under each condition were photographed at 0 and 12 h to estimate the scratch wound closure. Images were analyzed using ImageJ program (NIH, Bethesda, MD) and % wound closure was calculated relatively to vehicle control.

7.3.10 Nitric oxide production

Following a 24 h exposure of nearly confluent HUVEC cell monolayers to fresh DMEM medium containing vehicle (0.1% ethanol) or various concentrations of the fractions, sub-fractions or pure compounds added to a set of 3 wells per dose, an aliquot of cell culture media was removed to measure nitric oxide production. The presence of nitrite, a stable oxidized product of NO, was determined in cell culture media using Griess reagent (1% sulfanamide and 0.1% N-(1-naphthyl) ethylenediamine dihydrochloride in 2.5% H₃PO₄). Cell culture supernatant (100 µl) was combined with equal volume of Griess reagent in a 96-well plate followed by spectrophotometric measurement at 550 nm using a microplate reader (Molecular Devices, Sunnyvale, CA). Nitrite concentration in the supernatants was determined by comparison with a sodium nitrite standard curve.

7.3.11 Cytotoxicity assay

The cytotoxic activity against fibroblast cells was evaluated by using MTT (methyl thiazole tetrazolium) colorimetric assay essentially as described (45) and quantified spectrophotometrically at 550 nm using a microplate reader (Molecular Devices, Sunnyvale, CA). Percent of inhibition was calculated against the vehicle sample

and IC₅₀ values were calculated by a non-linear regression using two-fold serial dilutions of the test samples.

7.3.12 RNA extraction, cDNA synthesis, and qPCR

Total RNA was extracted from fibroblasts using Trizol (Invitrogen). RNA was quantified spectrophotometrically by absorbance measurements at 260 and 280 nm using the NanoDrop reader (NanoDrop Technologies, Wilmington, DE). Quality of RNA was assessed by gel electrophoresis. RNA was then treated with DnaseI (Invitrogen) to remove traces of DNA contamination and the cDNAs were synthesized with 2.5 µg of RNA using Stratascript reverse transcriptase (Stratagene) according to the manufacturers' protocols. Quantitative PCR was performed in duplicate essentially as described (98) using the following gene-specific primers (IDT, Coralville, IA) selected using the Primer Express 2.0 software (Applied Biosystems, Foster City, CA): β-actin, forward primer 5'-GGG AAA TCG TGC GTG ACA TT-3', reverse primer 5'-GCG GCA GTG GCC ATC TC-3'; TGFβ-I, forward primer 5'-GCT TCA GAC AGA AAC TCA CT-3', reverse primer 5'-GAA CAC TAC TAC ATG CCA TTA T-3'; TGFβRI, forward primer 5'-GAA CTG TTT TGA TTG GCA TC-3', reverse primer 5'-AAG AAG GGA CCT ACA CTA TTT-3'; and TGFβRII, forward primer 5'-TAA CAG TGA TGT CAT GGC C-3', reverse primer 5'-GGA AGT ACT GTG TGA ACC C-3'. Samples were subjected to a melting curve analysis to confirm the amplification specificity. The relative change in the target gene with respect to the endogenous control gene was determined using 2^{-ΔΔCT} method (124).

7.3.13 Statistical analysis

Data are represented as mean \pm SEM. Statistical analyses were performed using GraphPad Prism 4.0 (San Diego, CA) using one-way ANOVA completed by a multicomparison Dunnett's test. P-values of less than 0.05 were considered significant.

7.4 Results and discussion

7.4.1 *Lilium longiflorum* bulb extract promotes scratch wound closure

Preparations from *L. longiflorum* bulbs are a rich source of steroidal glycoalkaloids and steroidal saponins (151, 168); however, the physiological actions and pharmacological targets of these compounds are not well characterized. To assess the effect of *L. longiflorum* bulb extracts on wound healing *in vitro*, we utilized sequential solvent extraction to produce fractions with different polarity (Fig. 1) and tested them for stimulatory activity of scratch wound closure using the 3T3 murine fibroblast cell line. The 0.5% fetal bovine serum (FBS) was used as a positive control treatment. At this concentration FBS induced 50 to 65% scratch wound closure relative to untreated control samples after 12 hrs (Fig. 2) and complete scratch closure was observed after 24 hrs (not shown).

When bulb fractions I through V were tested at 50 $\mu\text{g/ml}$, fractions I and V accelerated scratch wound closure by $28.9 \pm 4.7\%$ and $33.1 \pm 8.5\%$, respectively ($p < 0.05$). Other fractions including the crude bulb extract (fraction II) showed only some activity, which did not reach statistical significance (Fig. 2A). Fraction I was produced by extraction of the lyophilized lily bulb powder with *n*-pentane and contained lipophilic

compounds, including sterols and fatty acids (data not shown). The wound closure activity of fraction I may be attributed to the fatty acid content of this fraction (169), or the presence of other biologically active components that are lipophilic in nature; however, further studies would be needed for confirmation. Fraction V, a steroidal glycoside rich fraction, exhibited the highest stimulatory activity. Fraction V was further fractionated by gel permeation chromatography and the effects of the two subfractions on scratch wound closure were evaluated at 3, 10, and 30 $\mu\text{g/ml}$ (Fig. 2B). Subfraction V-2 showed the highest dose-dependent scratch wound closure activity up to $19.8 \pm 6.5\%$, while wound-healing activity of subfraction V-1 was not significant at lower concentrations. Based on LCMS analysis, the GPC fraction V-2 contained predominately steroidal glycoalkaloids **1** and **2** (Fig. 3), whereas the GPC fraction V-1 contained predominately furostanol saponins **3**, **4**, and **5** (Fig. 4).

7.4.2 Cytotoxicity of bioactive compounds

The cytotoxicity of the steroidal glycoalkaloids **1** and **2** and furostanol saponins **3**, **4**, and **5** against murine 3T3 fibroblast cells is summarized in Table 1. Among the compounds examined, steroidal saponins **4** and **5** exhibited the highest inhibitory activity against 3T3 cells and induced a complete cell lysis at a concentration above 1 μM (not shown). These compounds were found predominantly in the subfraction V-1. This may explain the reduced scratch wound closure activity observed in these fractions relative to the subfraction V-2. The least cytotoxic of furostanol saponins was compound **3** with IC_{50} value of 8.7 μM . Interestingly, compounds **3**, **4**, and **5** are similar in structure except for the interglycosidic linkage and terminal sugars of the trisaccharide moiety. In compound

3, the terminal sugar is a (+)-D-glucose linked from the C-1''' carbon of the terminal sugar to the C-4' carbon of the inner glucose. In compound **4**, the terminal sugar is (-)-L-arabinose linked from the C-1''' carbon to the C-3' carbon of the inner glucose. Compound **5** has the same interglycosidic linkage as compound **4**; however, it contains a (+)-(D)-xylose as the terminal sugar. The differences in cytotoxicity of compounds **4** and **5** as compared to compound **3** may be related to the fact that compounds **4** and **5** both contain a pentose as the terminal sugar linked via the C-3' carbon of the inner glucose, compared to compound **3** which contains a hexose linked via the C-4' carbon of the inner glucose. These structural differences may be responsible for the reduced cytotoxicity of compound **3** as compared to **4** and **5**. Differential biological activity of steroidal saponins containing the same aglycone but various carbohydrate compositions have been previously reported (170).

Steroidal glycoalkaloids **1** and **2** are similar in structure and only differ by the presence of an acetyl moiety in compound **2** (Fig. 3). The acetyl moiety is linked to the C-6''' hydroxy position of the terminal glucose unit, which is absent in compound **1**. Interestingly, the acetylation of the terminal glucose unit resulted in 3-fold decrease in cell cytotoxicity associated with the compounds. The results are consistent with a role for carbohydrate moiety in the structure-cytotoxicity relationship observed for steroidal saponins against HL-60 human promyelocytic leukemia cells (170). Steroidal glycoalkaloids, **1** and **2**, sharing the same aglycone and only differing in the carbohydrate moiety, exhibited differential cytotoxicity. Compounds **1** and **2** are similar in structure to the steroidal glycoalkaloids, α -solamargine and α -solasonine, found in solanaceous

plants. These compounds have been successfully used in the treatment of human skin carcinomas (171).

While increased cytotoxicity is not favorable for *in vitro* scratch wound closure activity, it may aid in *in vivo* wound healing when Easter lily bulb extract or its components are applied topically. For example, late stages of wound healing (tissue regeneration) that cannot be reproduced in an *in vitro* scratch wound closure assay often require elimination of specific cell types from the wound prior to the progression to the next phase and the evolution of granulation tissue to scar tissue through apoptosis (172, 173). Additionally, the presence of microbial infection may disturb or delay wound healing (174). Cytotoxic saponins found in Easter lily bulbs may assist with elimination of specific cell types or microbes from the wound area; however, antimicrobial and *in vivo* wound healing studies need to be conducted to support this hypothesis.

7.4.3 Steroidal glycoalkaloids enhance scratch wound closure

To confirm scratch wound closure activity of purified compounds isolated from Easter lily bulbs, we focused on steroidal glycoalkaloids **1** and **2** and furostanol saponin **3**, which showed no measurable cytotoxicity below 5 μM concentration. Their effects on scratch wound closure was evaluated at 0.2, 1, and 5 μM (Fig. 5A). Compound **1** possessed stronger stimulatory activity on scratch wound closure (Fig. 5B-C) than the acetylated derivative, compound **2** (increase of $37.7\pm 5.1\%$ versus $25.6\pm 2.9\%$ at 5 μM), and was the only substance that showed high scratch wound closure activity at all doses tested ($28.8\pm 2.8\%$, $30.2\pm 1.8\%$, and $37.7\pm 5.1\%$). Compound **3** showed the weakest

stimulatory effect that reached statistical significance only at highest concentration tested ($23.7 \pm 5.7\%$).

7.4.4 Steroidal glycoalkaloids induce nitric oxide production

Nitric oxide (NO) is a well-known mediator of normal tissue repair. Angiogenesis, granulation tissue formation, epidermal migration, collagen deposition, and microvascular homeostasis are regulated by NO production (166). Triterpenoid saponins isolated from ginseng, *Radix rubra*, have been reported to stimulate wound healing with enhanced angiogenesis (175) and increased fibronectin synthesis by upregulation of TGF- β signaling (176). Since nitric oxide (NO) plays a critical role in both angiogenesis and wound healing (166), we tested compounds **1**, **2**, and **3** for their ability to induce NO production in HUVEC cells. Both steroidal glycoalkaloids **1** and **2** at 5 μ M increased NO production 2.5-fold, however no such effect was observed for furostanol saponin **3** (Fig. 6A).

7.4.5 Steroidal glycoalkaloids enhance TGF- β signaling

The mRNA levels of TGF- β 1 were not significantly changed in fibroblasts when treated with 5 μ M of compounds **1**, **2**, or **3** as compared to vehicle-treated controls (Fig. 6B). This is in direct contrast to Kanzaki et al. (1998), who reported up to 1.9-fold increase in TGF- β 1 in the culture medium following the treatment of saponins isolated from *R. rubra*. The saponins isolated from *R. rubra* are triterpenoid glycosides, which may explain the differences in biological activity as compared to compounds **1**, **2**, and **3**, which are steroidal glycosides. The observed lack of direct effect of the steroidal

glycoalkaloids on TGF- β 1 may be advantageous, since excessive overexpression of TGF- β 1 can result in constitutive inflammation, which may override other positive effects of TGF- β 1 on wound healing (164).

As the function of TGF- β is mediated by TGF- β receptors, quantitative PCR was performed to determine expression of TGF- β receptors type I and II in fibroblasts. The ratios of TGF- β type I receptor to actin were 2.3, 1.8, and 1.1 in cells treated with 5 μ M of compounds **1**, **2**, or **3**, respectively, compared with those observed in vehicle-treated cells (Fig. 6B). No changes in the mRNA levels of TGF- β type II receptor was observed for the compounds, suggesting that the steroidal glycoalkaloids stimulate TGF- β signaling through a specific increase of TGF- β type I receptor expression in fibroblasts. A similar observation was reported previously (176); however, both TGF- β type I and type II receptor mRNAs were upregulated by treatment with saponins isolated from *R. rubra*.

Based on these data, steroidal glycoalkaloids from Easter lily bulbs may exhibit a wound healing promoting effect by stimulating activation and migration of fibroblasts through selective upregulation of TGF- β type I receptors, while furostanol saponins found in the same extract may only play a minor role in this process. Both TGF- β type I and type II receptors were induced during wound healing (177); however, type II receptors were also associated with cell growth inhibition (178). No changes to TGF- β type I and type II receptor levels were observed following dexamethasone or retinoic acid treatment in osteoblasts (179), while upregulation of TGF- β type I receptors and suppression of TGF- β type II receptors was associated with systemic glucocorticoid treatment in animals (177). Therefore, TGF- β 1-mediated effects are cell type and context specific, and selective activation of TGF- β 1 signaling may be beneficial for optimal

wound-healing activity with less negative side effects; however, more studies need to be conducted to support this hypothesis.

7.5 Conclusions

The evaluation of fractionated *Lilium longiflorum* bulb extract and purified compounds from the bulbs led to the identification of biologically active compounds that may play a role in the reported medicinal properties of the bulbs. Two steroidal glycoalkaloids **1** and **2** and one furostanol saponin **3**, were isolated and identified from the crude biologically active glycoside extract, which stimulates scratch wound closure *in vitro* by activating the migration of fibroblasts. Although these compounds play a role in the activity of the total extract, the partial activity of other fractions suggests that other activators are present and synergism between compounds may be a factor. Steroidal glycoalkaloids may contribute to the wound healing activity of lily bulbs by inducing production of nitric oxide and increasing mRNA levels of TGF- β type I receptors, two critical mediators of early wound healing. Further research is needed to address the precise underlying mechanisms of their action and to find the optimal therapeutic concentration for use in clinical evaluations. These results bring scientific support to potential applications of bioactive compounds from lily bulbs in regenerative medicine.

7.6 Acknowledgments

We are very thankful to Dr. Richard Merritt and the Rutgers University Easter Lily Breeding Program for providing the Easter lily bulbs used for this study, to Dr, Ilya

Raskin for use of his cell culture facilities, and to Reneta Pouleva and Ruth Dorn for their technical assistance with cell culture and RNA extraction.

Table 1. Cytotoxicity of compounds 1 through 5 to 3T3 Swiss mouse fibroblast cells

ID	Chemical name	Molecular weight	Cytotoxicity IC ₅₀ , mM
1	(22R, 25R)-spirosol-5-en-3 β -yl <i>O</i> -α-L-rhamnopyranosyl-(1→2)-β -D-glucopyranosyl-(1→4)-β-D-glucopyranoside	883	8.2
2	(22R, 25R)-spirosol-5-en-3β-yl <i>O</i> -α-L-rhamnopyranosyl-(1→2)-[6- <i>O</i> -acetyl-β-D-glucopyranosyl-(1→4)]-β-D-glucopyranoside	925	25.8
3	(25R)-26- <i>O</i> -(β-D-glucopyranosyl)-furost-5-en-3β,22α,26-triol 3- <i>O</i> -α-L-rhamnopyranosyl-(1→2)-β -D-glucopyranosyl-(1→4)-β -D-glucopyranoside	1064	8.7
4	(25R)-26- <i>O</i> -(β-D-glucopyranosyl)-furost-5-en-3β,22α,26-triol 3- <i>O</i> -α-L-rhamnopyranosyl-(1→2)-α-L-arabinopyranosyl-(1→3)-β -D-glucopyranoside	1034	<1.0
5	(25R)-26- <i>O</i> -(β-D-glucopyranosyl)-furost-5-en-3β,22α,26-triol 3- <i>O</i> -α-L-rhamnopyranosyl-(1→2)-α-L-xylopyranosyl-(1→3)-β-D-glucopyranoside	1034	<1.0

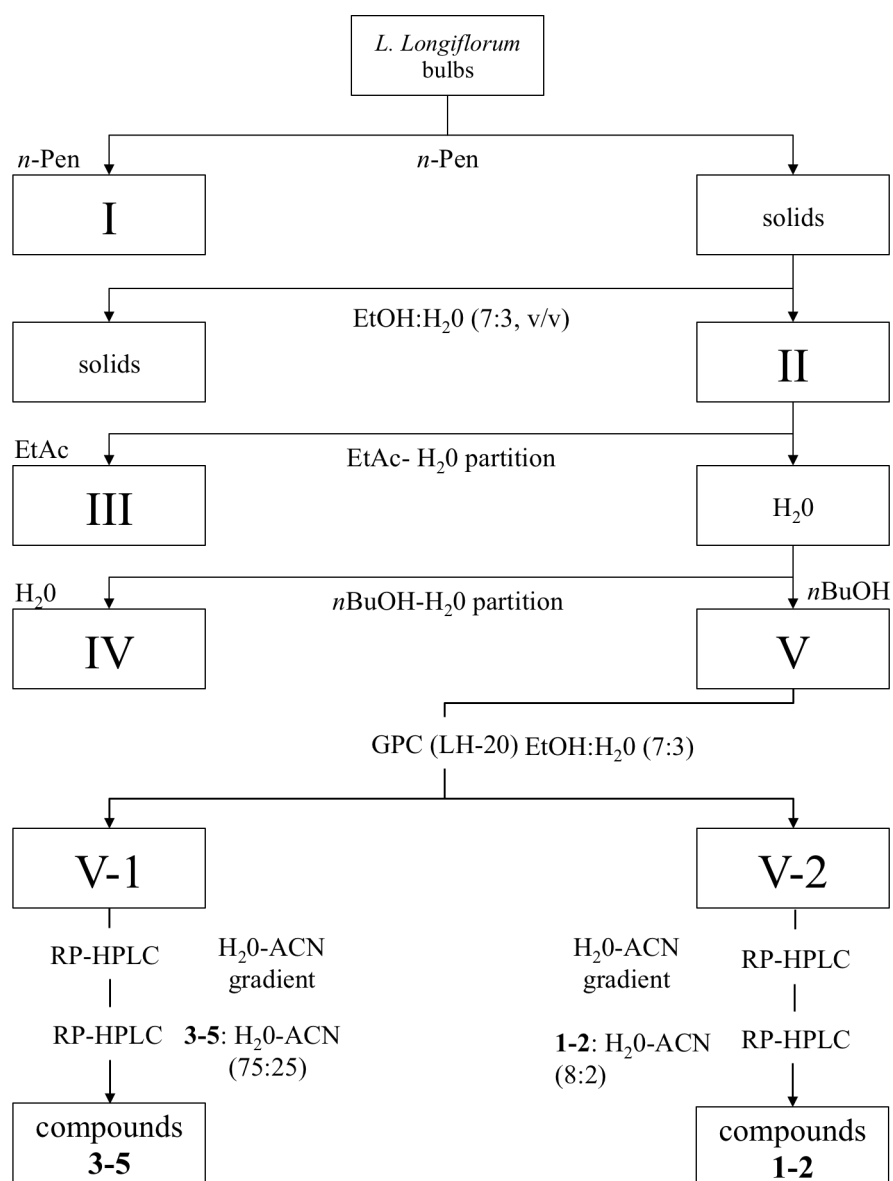


Figure 1. Schematic diagram of fractionation strategy. Lyophilized lily bulb powder was subjected to sequential solvent extraction, gel permeation chromatography, and repetitive RP-HPLC to yield compounds 1 through 5.

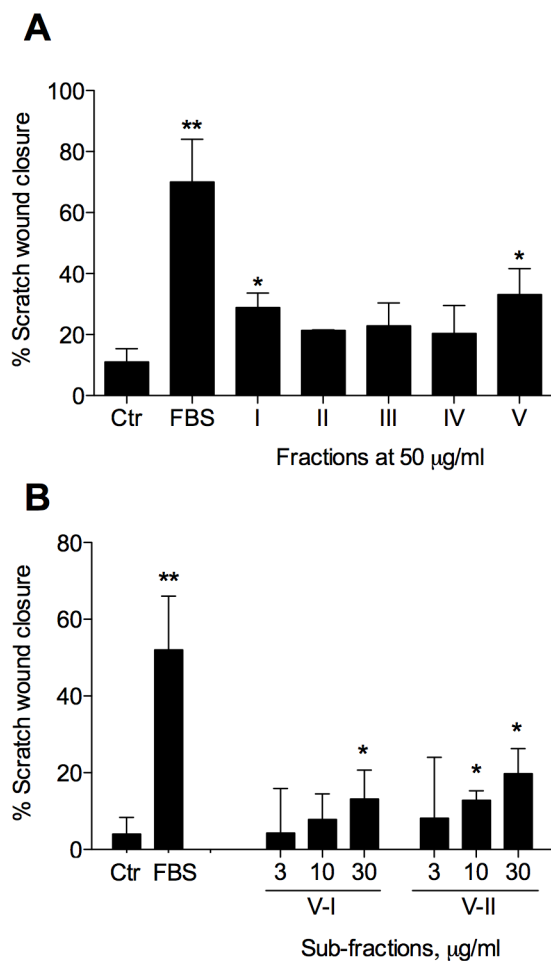


Figure 2. Bioactivity guided fractionation of the *Lilium longiflorum* bulb extract.

The effect of different fractions and subfractions of the original extract on scratch wound closure in 3T3 murine fibroblast cell line after 12 h of treatment was calculated as % of untreated controls. Fetal bovine serum (FBS, 0.5%) was used as a positive control. (A) The effect of 5 fractions of different polarity (I-V) on cell migration at 50 $\mu\text{g/ml}$. (B) Dose dependent effect of subfractions of the crude glycoside extract (V-1 and V-2) on cells migration at 3, 10, and 30 $\mu\text{g/ml}$. The data represent the average of 2 experiments \pm SEM. * $P < 0.05$; ** $P < 0.01$ ($n=3$) using one-way ANOVA and Dunnett's post-test.

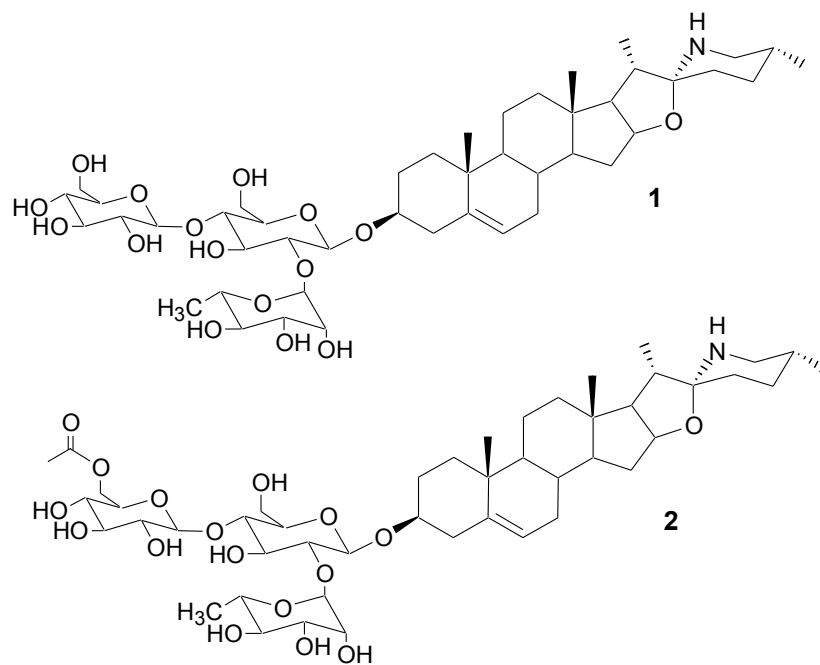


Figure 3. Structures of bioactive steroidal glycoalkaloids 1 and 2, isolated from fraction V-2. The structures were confirmed by a combination ^1H NMR, ^{13}C NMR, ESI $^+$ -MS, and comparison of retention times with authentic standards.

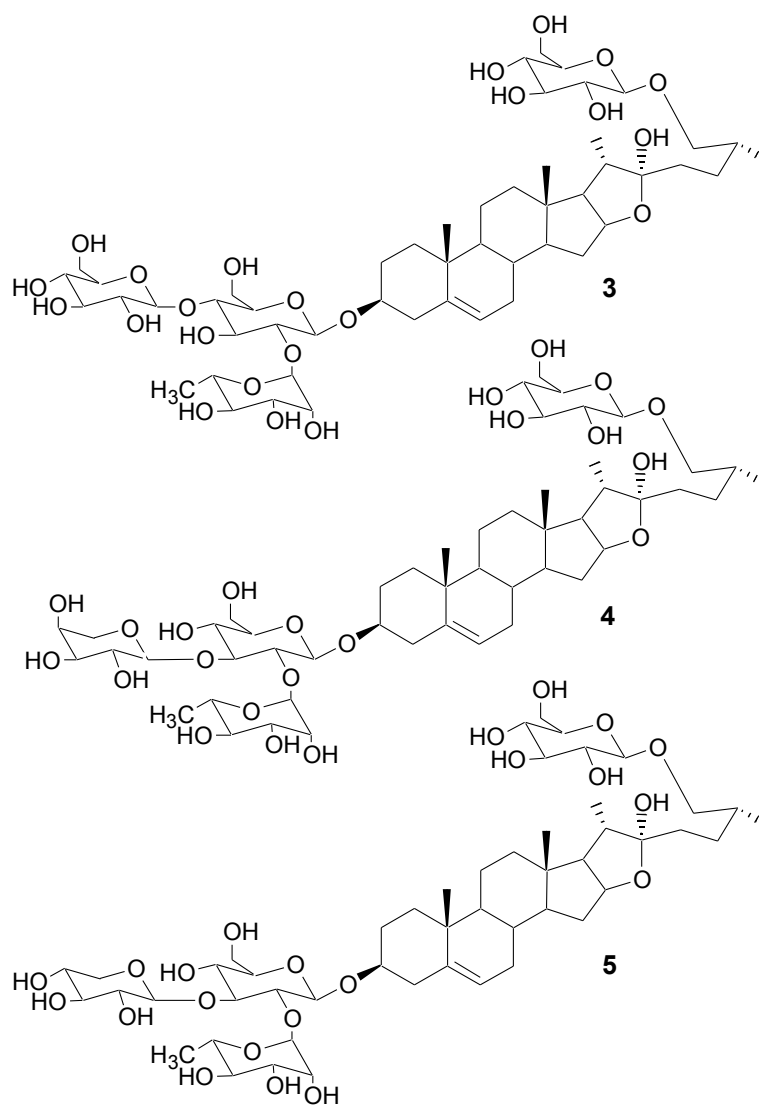


Figure 4. Structures of bioactive furostanol saponins 3, 4, and 5, isolated from fraction V-1. The structures were confirmed by a combination ^1H NMR, ^{13}C NMR, ESI⁺-MS, and comparison of retention times with authentic standards.

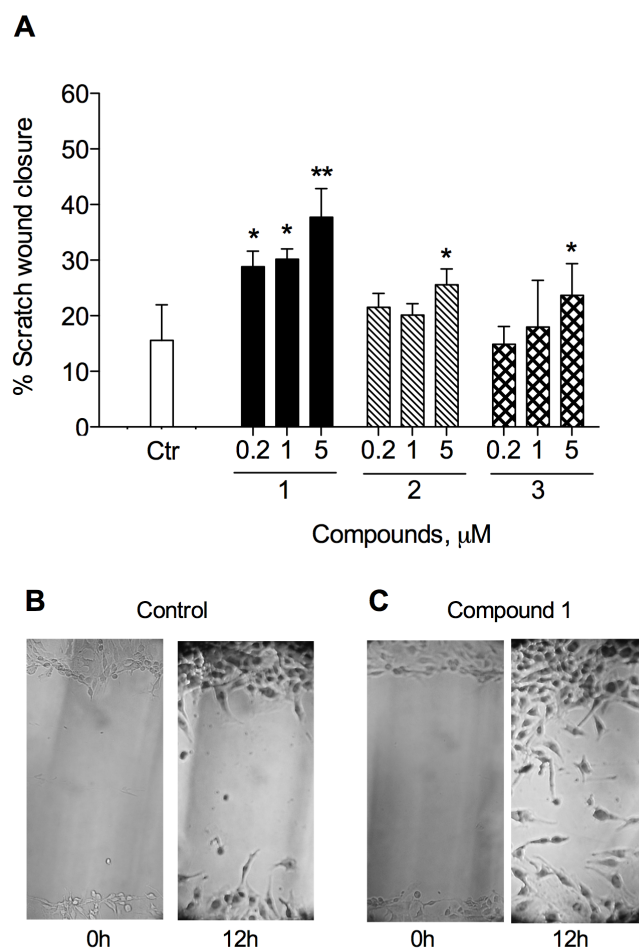


Figure 5. Effect of bioactive steroidal glycoalkaloids 1 and 2 and furastanol saponin 3 on scratch wound closure. Effect of different compounds on scratch wound closure in 3T3 murine fibroblast cell line after 12 h of treatment was calculated as % of untreated controls. Fetal bovine serum (FBS, 0.5%) was used as a positive control. **(A)** Dose dependent effect of compounds 1-3 at 0.2, 1, and 5 μM . The data represent the average of 2 experiments \pm SEM. * $P < 0.05$; ** $P < 0.01$ ($n=3$) using one-way ANOVA and Dunnett's post-test. **(B)** Representative images of vehicle-treated control cells and **(C)** cells treated with compound 1 at 5 μM , illustrating migration of the 3T3 fibroblasts into the scratch wound during 12 h exposure.

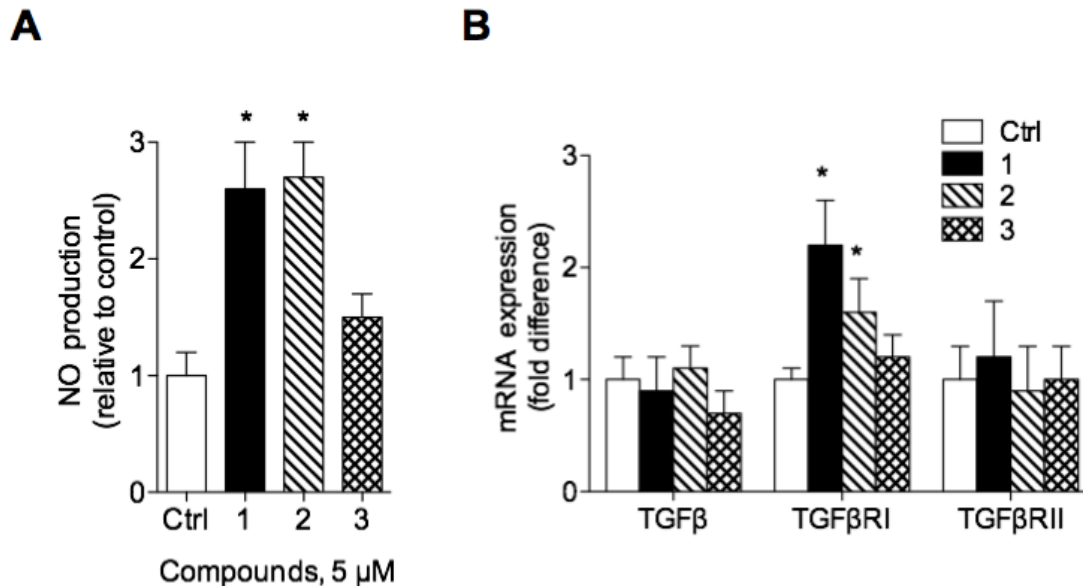


Figure 6. Bioactive steroidal glycoalkaloids 1 and 2 induce nitric oxide production and TGFβ signaling. (A) Following 12 h exposure of subconfluent HUVEC cells to the active compound at 5 μM, an aliquot of cell culture media was removed to measure nitric oxide production by Griess reagent. (B) Following 12 h exposure of scratched monolayer of the 3T3 fibroblasts to the active compound, total cell RNA was extracted with Trizol, converted to cDNA, and mRNA levels of TGFβ and its type I and type II receptors were quantified using qPCR. The data represent the average of 2 experiments ± SEM. * P<0.05 (n=3) using one-way ANOVA and Dunnett's post-test.

LITERATURE CITED

1. Rao, A. V., Vardhini, B. V. V., Sujatha, E., and Anuradha, S. (2002) Brassinosteroids - a new class of phytohormones. *Curr Sci* **82**, 1239-1245
2. Bajguz, A., and Tretyn, A. (2003) The chemical characteristic and distribution of brassinosteroids in plants. *Phytochemistry* **62**, 1027-1046
3. Grove, M. D., Spencer, G. F., Rohwedder, W. K., Mandava, N., Worley, J. F., Warthen, J. D., Steffens, G. L., Flippenanderson, J. L., and Cook, J. C. (1979) Brassinolide, a plant growth-promoting steroid isolated from Brassica-napus pollen. *Nature* **281**, 216-217
4. Fujioka, S., and Yokota, T. (2003) Biosynthesis and metabolism of brassinosteroids. *Annu Rev Plant Biol* **54**, 137-164
5. Bishop, G. J., and Koncz, C. (2002) Brassinosteroids and plant steroid hormone signaling. *Plant Cell* **14 Suppl**, S97-110
6. Kim, T. W., Guan, S., Sun, Y., Deng, Z., Tang, W., Shang, J. X., Burlingame, A. L., and Wang, Z. Y. (2009) Brassinosteroid signal transduction from cell-surface receptor kinases to nuclear transcription factors. *Nat Cell Biol* **11**, 1254-1260
7. Kartal, G., Temel, A., Arican, E., and Gozukirmizi, N. (2009) Effects of brassinosteroids on barley root growth, antioxidant system and cell division. *Plant Growth Regulation* **58**, 261-267
8. Kulaeva, O. N., Burkhanova, E. A., Fedina, A. B., Khokhlova, V. A., Bokebayeva, G. A., Vorbrodt, H. M., and Adam, G. n. (2009) Effect of Brassinosteroids on Protein Synthesis and Plant-Cell Ultrastructure under Stress Conditions. In *Brassinosteroids* pp. 141-155, American Chemical Society, Washington, DC
9. Castilla, V., Larzabal, M., Sgalippa, N. A., Wachsman, M. B., and Coto, C. E. (2005) Antiviral mode of action of a synthetic brassinosteroid against Junin virus replication. *Antiviral Res* **68**, 88-95
10. Micheli, F. M., Ramirez, J. A., Berra, A., Galagovsky, L. R., and Alche, L. E. (2008) Anti-herpetic and anti-inflammatory activities of two new synthetic 22,23-dihydroxylated stigmastane derivatives. *J Steroid Biochem Mol Biol* **111**, 111-116
11. Malikova, J., Swaczynova, J., Kolar, Z., and Strnad, M. (2008) Anticancer and antiproliferative activity of natural brassinosteroids. *Phytochemistry* **69**, 418-426
12. Kuzmitsky, B. B., and Mizulo, N. A. (1991) Study of acute toxicity of epibrassinolide and its preparative forms. *Technical report, Academy of Sciences of Belarus, Minsk*, 1-44
13. Murkunde, Y. V., and Balakrishna Murthy, P. (2010) Developmental toxicity of homobrassinolide in wistar rats. *Int J Toxicol* **29**, 517-522
14. Borst, S. E. (2004) Interventions for sarcopenia and muscle weakness in older people. *Age and Ageing* **33**, 548-555
15. Solomon, A. M., and Bouloux, P. M. (2006) Modifying muscle mass - the endocrine perspective. *J Endocrinol* **191**, 349-360
16. Blaauw, B., Canato, M., Agatea, L., Toniolo, L., Mammucari, C., Masiero, E., Abraham, R., Sandri, M., Schiaffino, S., and Reggiani, C. (2009) Inducible

- activation of Akt increases skeletal muscle mass and force without satellite cell activation. *FASEB J* **23**, 3896-3905
17. Falkenstein, E., Tillmann, H.-C., Christ, M., Feuring, M., and Wehling, M. (2000) Multiple Actions of Steroid Hormones---A Focus on Rapid, Nongenomic Effects. *Pharmacological Reviews* **52**, 513-556
 18. Basaria, S. (2010) Androgen abuse in athletes: detection and consequences. *J Clin Endocrinol Metab* **95**, 1533-1543
 19. Chuu, C. P., Kokontis, J. M., Hiipakka, R. A., Fukuchi, J., Lin, H. P., Lin, C. Y., Huo, C., and Su, L. C. (2011) Androgens as therapy for androgen receptor-positive castration-resistant prostate cancer. *J Biomed Sci* **18**, 63
 20. Allan, G., Sbriscia, T., Linton, O., Lai, M. T., Haynes-Johnson, D., Bhattacharjee, S., Ng, R., Sui, Z., and Lundeen, S. (2008) A selective androgen receptor modulator with minimal prostate hypertrophic activity restores lean body mass in aged orchidectomized male rats. *J Steroid Biochem Mol Biol* **110**, 207-213
 21. Kuhn, C. M. (2002) Anabolic steroids. *Recent Prog Horm Res* **57**, 411-434
 22. Bhasin, S., Calof, O. M., Storer, T. W., Lee, M. L., Mazer, N. A., Jasuja, R., Montori, V. M., Gao, W., and Dalton, J. T. (2006) Drug insight: Testosterone and selective androgen receptor modulators as anabolic therapies for chronic illness and aging. *Nat Clin Pract Endocrinol Metab* **2**, 146-159
 23. Clouse, S. D., and Sasse, J. M. (1998) BRASSINOSTEROIDS: Essential Regulators of Plant Growth and Development. *Annu Rev Plant Physiol Plant Mol Biol* **49**, 427-451
 24. Losel, R., and Wehling, M. (2003) Nongenomic actions of steroid hormones. *Nat Rev Mol Cell Biol* **4**, 46-56
 25. Clouse, S. D. (2002) Brassinosteroids. Plant counterparts to animal steroid hormones? *Vitam Horm* **65**, 195-223
 26. Mussig, C. (2005) Brassinosteroid-promoted growth. *Plant Biol (Stuttg)* **7**, 110-117
 27. Wang, Z. Y., Seto, H., Fujioka, S., Yoshida, S., and Chory, J. (2001) BRI1 is a critical component of a plasma-membrane receptor for plant steroids. *Nature* **410**, 380-383
 28. Nam, K. H., and Li, J. (2002) BRI1/BAK1, a receptor kinase pair mediating brassinosteroid signaling. *Cell* **110**, 203-212
 29. Tolwinski, N. S., and Wieschaus, E. (2004) Rethinking WNT signaling. *Trends Genet* **20**, 177-181
 30. Nemhauser, J. L., and Chory, J. (2004) BRing it on: new insights into the mechanism of brassinosteroid action. *J Exp Bot* **55**, 265-270
 31. Frost, R. A., and Lang, C. H. (2007) Protein kinase B/Akt: a nexus of growth factor and cytokine signaling in determining muscle mass. *J Appl Physiol* **103**, 378-387
 32. Rommel, C., Bodine, S. C., Clarke, B. A., Rossman, R., Nunez, L., Stitt, T. N., Yancopoulos, G. D., and Glass, D. J. (2001) Mediation of IGF-1-induced skeletal myotube hypertrophy by PI(3)K/Akt/mTOR and PI(3)K/Akt/GSK3 pathways. *Nat Cell Biol* **3**, 1009-1013
 33. Stitt, T. N., Drujan, D., Clarke, B. A., Panaro, F., Timofeyeva, Y., Kline, W. O., Gonzalez, M., Yancopoulos, G. D., and Glass, D. J. (2004) The IGF-1/PI3K/Akt

- pathway prevents expression of muscle atrophy-induced ubiquitin ligases by inhibiting FOXO transcription factors. *Mol Cell* **14**, 395-403
34. Wachsman, M. B., Lopez, E. M., Ramirez, J. A., Galagovsky, L. R., and Coto, C. E. (2000) Antiviral effect of brassinosteroids against herpes virus and arenaviruses. *Antivir Chem Chemother* **11**, 71-77
 35. Wachsman, M. B., Ramirez, J. A., Galagovsky, L. R., and Coto, C. E. (2002) Antiviral activity of brassinosteroids derivatives against measles virus in cell cultures. *Antivir Chem Chemother* **13**, 61-66
 36. Romanutti, C., Castilla, V., Coto, C. E., and Wachsman, M. B. (2007) Antiviral effect of a synthetic brassinosteroid on the replication of vesicular stomatitis virus in Vero cells. *Int J Antimicrob Agents* **29**, 311-316
 37. Micheline, F. M., Ramirez, J. A., Berra, A., Galagovsky, L. R., and Alche, L. E. (2004) In vitro and in vivo antiherpetic activity of three new synthetic brassinosteroid analogues. *Steroids* **69**, 713-720
 38. Micheline, F. M., Berra, A., and Alche, L. E. (2008) The in vitro immunomodulatory activity of a synthetic brassinosteroid analogue would account for the improvement of herpetic stromal keratitis in mice. *J Steroid Biochem Mol Biol* **108**, 164-170
 39. Takatsuto, S., and Ikekawa, N. (1984) Synthesis and activity of plant growth-promoting steroids, (22R,23R,24S)-28-homobrassinosteroids, with modifications in rings A and B. *J Chem Soc Perkin Trans* **1**, 439-447
 40. Ikekawa, N., Takatsuto, S., Kitsuwu, T., Saito, H., Morishita, T., and Abe, H. (1984) Analysis of natural brassinosteroids by gas chromatography and gas chromatography-mass spectrometry. *Journal of Chromatography* **290**, 289-302
 41. Watanabe, T., Yokota, T., Shibata, K., Nomura, T., Seto, H., and Takatsuto, S. (2000) Cryptolide, a new brassinolide catabolite with a 23-oxo group from Japanese cedar pollen/anther and its synthesis. *J. Chem. Res.* **2000**, 18-19
 42. Massey, A. P., Pore, V. S., and Hazra, B. G. (2003) New Route for the Synthesis of (22S,23S)-28-Homobrassinolide. *Synthesis* **2003**, 0426-0430
 43. Bajguz, A. (2000) Effect of brassinosteroids on nucleic acids and protein content in cultured cells of *Chlorella vulgaris*. *Plant Physiology and Biochemistry* **38**, 209-215
 44. Mandel, J. L., and Pearson, M. L. (1974) Insulin stimulates myogenesis in a rat myoblast line. *Nature* **251**, 618-620
 45. Mosmann, T. (1983) Rapid colorimetric assay for cellular growth and survival: application to proliferation and cytotoxicity assays. *J Immunol Methods* **65**, 55-63
 46. Montgomery, J. L., Harper, W. M., Jr., Miller, M. F., Morrow, K. J., Jr., and Blanton, J. R., Jr. (2002) Measurement of protein synthesis and degradation in C2C2 myoblasts using extracts of muscle from hormone treated bovine. *Methods Cell Sci* **24**, 123-129
 47. Fawcett, J., Hamel, F. G., and Duckworth, W. C. (2001) Characterization of the inhibition of protein degradation by insulin in L6 cells. *Arch Biochem Biophys* **385**, 357-363
 48. Chang, C. S., and Liao, S. S. (1987) Topographic recognition of cyclic hydrocarbons and related compounds by receptors for androgens, estrogens, and glucocorticoids. *J Steroid Biochem* **27**, 123-131

49. Harper, J. M., Soar, J. B., and Buttery, P. J. (1987) Changes in protein metabolism of ovine primary muscle cultures on treatment with growth hormone, insulin, insulin-like growth factor I or epidermal growth factor. *J Endocrinol* **112**, 87-96
50. Douglas, R. G., Gluckman, P. D., Ball, K., Breier, B., and Shaw, J. H. (1991) The effects of infusion of insulinlike growth factor (IGF) I, IGF-II, and insulin on glucose and protein metabolism in fasted lambs. *J Clin Invest* **88**, 614-622
51. Rooyackers, O. E., and Nair, K. S. (1997) Hormonal regulation of human muscle protein metabolism. *Annu Rev Nutr* **17**, 457-485
52. Li, B. G., Hasselgren, P. O., and Fang, C. H. (2005) Insulin-like growth factor-I inhibits dexamethasone-induced proteolysis in cultured L6 myotubes through PI3K/Akt/GSK-3beta and PI3K/Akt/mTOR-dependent mechanisms. *Int J Biochem Cell Biol* **37**, 2207-2216
53. Hajduch, E., Alessi, D. R., Hemmings, B. A., and Hundal, H. S. (1998) Constitutive activation of protein kinase B alpha by membrane targeting promotes glucose and system A amino acid transport, protein synthesis, and inactivation of glycogen synthase kinase 3 in L6 muscle cells. *Diabetes* **47**, 1006-1013
54. Jean, C., Rome, S., Mathe, V., Huneau, J. F., Aattouri, N., Fromentin, G., Achagiotis, C. L., and Tome, D. (2001) Metabolic evidence for adaptation to a high protein diet in rats. *J Nutr* **131**, 91-98
55. Feldkoren, B. I., and Andersson, S. (2005) Anabolic-androgenic steroid interaction with rat androgen receptor in vivo and in vitro: a comparative study. *J Steroid Biochem Mol Biol* **94**, 481-487
56. Hershberger, L. G., Shipley, E. G., and Meyer, R. K. (1953) Myotrophic activity of 19-nortestosterone and other steroids determined by modified levator ani muscle method. *Proc Soc Exp Biol Med* **83**, 175-180
57. Dhaubhadel, S., Browning, K. S., Gallie, D. R., and Krishna, P. (2002) Brassinosteroid functions to protect the translational machinery and heat-shock protein synthesis following thermal stress. *Plant J* **29**, 681-691
58. Bathori, M., Toth, N., Hunyadi, A., Marki, A., and Zador, E. (2008) Phytoecdysteroids and anabolic-androgenic steroids--structure and effects on humans. *Curr Med Chem* **15**, 75-91
59. Gorelick-Feldman, J., Maclean, D., Ilic, N., Poulev, A., Lila, M. A., Cheng, D., and Raskin, I. (2008) Phytoecdysteroids increase protein synthesis in skeletal muscle cells. *J Agric Food Chem* **56**, 3532-3537
60. Kizelsztejn, P., Govorko, D., Komarnytsky, S., Evans, A., Wang, Z., Cefalu, W. T., and Raskin, I. (2009) 20-Hydroxyecdysone decreases weight and hyperglycemia in a diet-induced obesity mice model. *Am J Physiol Endocrinol Metab* **296**, E433-439
61. Yang, L., Xie, S., Jamaluddin, M. S., Altuwajri, S., Ni, J., Kim, E., Chen, Y. T., Hu, Y. C., Wang, L., Chuang, K. H., Wu, C. T., and Chang, C. (2005) Induction of androgen receptor expression by phosphatidylinositol 3-kinase/Akt downstream substrate, FOXO3a, and their roles in apoptosis of LNCaP prostate cancer cells. *J Biol Chem* **280**, 33558-33565
62. Salas, T. R., Kim, J., Vakar-Lopez, F., Sabichi, A. L., Troncoso, P., Jenster, G., Kikuchi, A., Chen, S. Y., Shemshedini, L., Suraokar, M., Logothetis, C. J., DiGiovanni, J., Lippman, S. M., and Menter, D. G. (2004) Glycogen synthase

- kinase-3 beta is involved in the phosphorylation and suppression of androgen receptor activity. *J Biol Chem* **279**, 19191-19200
63. Naito, A. T., Akazawa, H., Takano, H., Minamino, T., Nagai, T., Aburatani, H., and Komuro, I. (2005) Phosphatidylinositol 3-kinase-Akt pathway plays a critical role in early cardiomyogenesis by regulating canonical Wnt signaling. *Circ Res* **97**, 144-151
 64. Oehme, I., Bossler, S., and Zornig, M. (2006) Agonists of an ecdysone-inducible mammalian expression system inhibit Fas Ligand- and TRAIL-induced apoptosis in the human colon carcinoma cell line RKO. *Cell Death Differ* **13**, 189-201
 65. Simoncini, T., Hafezi-Moghadam, A., Brazil, D. P., Ley, K., Chin, W. W., and Liao, J. K. (2000) Interaction of oestrogen receptor with the regulatory subunit of phosphatidylinositol-3-OH kinase. *Nature* **407**, 538-541
 66. Rahman, F., and Christian, H. C. (2007) Non-classical actions of testosterone: an update. *Trends Endocrinol Metab* **18**, 371-378
 67. Layman, D. K., Boileau, R. A., Erickson, D. J., Painter, J. E., Shiue, H., Sather, C., and Christou, D. D. (2003) A reduced ratio of dietary carbohydrate to protein improves body composition and blood lipid profiles during weight loss in adult women. *J Nutr* **133**, 411-417
 68. Atherton, P. J., Smith, K., Etheridge, T., Rankin, D., and Rennie, M. J. (2009) Distinct anabolic signalling responses to amino acids in C2C12 skeletal muscle cells. *Amino Acids*
 69. Mohler, M. L., Bohl, C. E., Jones, A., Coss, C. C., Narayanan, R., He, Y., Hwang, D. J., Dalton, J. T., and Miller, D. D. (2009) Nonsteroidal selective androgen receptor modulators (SARMs): dissociating the anabolic and androgenic activities of the androgen receptor for therapeutic benefit. *J Med Chem* **52**, 3597-3617
 70. Pushkala, K., and Gupta, P. D. (2001) Steroid hormones regulate programmed cell death: a review. *Cytobios* **106**, 201-217
 71. Massey, A. P., Pore, V. S., and Hazra, B. G. (2003) New route for the synthesis of (22S,23S)-28-homobrassinolide. *Synthesis Stutt* **3**, 426-430
 72. Ramirez, J. A., Brosa, C., and Galagovsky, L. R. (2005) Synthesis and bioactivity of C-29 brassinosteroid analogues with different functional groups at C-6. *Phytochemistry* **66**, 581-587
 73. Wachsman, M. B., Ramirez, J. A., L.B., T., Galagovsky, L. R., and Coto, C. E. (2004) Antiviral activity of natural and synthetic brassinosteroids. *Curr Med Chem Anti Infect Agents* **3**, 163-179
 74. Andersen, D. L., Back, T. G., Janzen, L., Michalak, K., Pharis, R. P., and Sung, G. C. (2001) Design, synthesis, and bioactivity of the first nonsteroidal mimetics of brassinolide. *J Org Chem* **66**, 7129-7141
 75. Baron, D. L., Luo, W., Janzen, L., Pharis, R. P., and Back, T. G. (1998) Structure-activity studies of brassinolide b-ring analogues. *Phytochemistry* **49**, 1849-1858
 76. Romero-Avila, M., de Dios-Bravo, G., Mendez-Stivalet, J. M., Rodriguez-Sotres, R., and Iglesias-Arteaga, M. A. (2007) Synthesis and biological activity of furostanic analogues of brassinosteroids bearing the 5alpha-hydroxy-6-oxo moiety. *Steroids* **72**, 955-959
 77. Esposito, D., Rathinasabapathy, T., Poulev, A., Komarnytsky, S., and Raskin, I. (2011) Anabolic effect of plant brassinosteroid *Nat Chem Biol* **(Submitted)**

78. Komarnytsky, S., Cook, A., and Raskin, I. (2010) Potato protease inhibitors inhibit food intake and increase circulating cholecystokinin levels by a trypsin-dependent mechanism. *Int J Obes (Lond)*
79. Zullo, M. A. T., and Adam, G. (2002) Brassinosteroid phytohormones - structure, bioactivity and applications. *Braz. J. Plant Physiol.* **14**, 143-181
80. Adler, J. H., and Grebenok, R. J. (1995) Biosynthesis and distribution of insect-molting hormones in plants--a review. *Lipids* **30**, 257-262
81. Takatsuto, S., Ikekawa, N., Morishita, T., and Abe, H. (1987) Structure-activity relationship of brassinosteroids with respect to the A/B-ring functional groups. *Chem Pharmaceutic Bulletin* **35**, 211-216
82. Anastasia, M., Allevi, P., Brasca, M. G., Ciuffreda, P., and Fiechi, A. (1984) Synthesis of (2R,3S,22S,23S)-2,3,22,23-tetrahydroxy-B-homo-6-aza-5a-stigmastan-7-one, an aza analogue of brassinolide. *Gazzeta Chimica Italiana* **114**, 159-161
83. Galagovsky, L. R., Gros, E. G., and Ramirez, J. A. (2001) Synthesis and bioactivity of natural and C-3 fluorinated biosynthetic precursors of 28-homobrassinolide. *Phytochemistry* **58**, 973-980
84. Mykhaylyk, O. M., Kotzuruba, A. V., Buchanevich, O. M., Korduban, A. M., Meged, E. F., and Gulaya, N. M. (2001) Signal transduction of erythrocytes after specific binding of ecdysterone and cholesterol immobilized on nanodispersed magnetite. *Journal of Magnetism and Magnetic Materials* **225**, 226-234
85. Strosberg, A. D. (1995) Structure, function, and regulation of the three beta-adrenergic receptors. *Obes Res* **3 Suppl 4**, 501S-505S
86. Saini, A., Al-Shanti, N., and Stewart, C. (2010) C2 skeletal myoblast survival, death, proliferation and differentiation: regulation by Adra1d. *Cell Physiol Biochem* **25**, 253-262
87. Kou, K., and Rotwein, P. (1993) Transcriptional activation of the insulin-like growth factor-II gene during myoblast differentiation. *Mol Endocrinol* **7**, 291-302
88. Alzhanov, D. T., McInerney, S. F., and Rotwein, P. (2010) Long-range interactions regulate Igf2 gene transcription during skeletal muscle differentiation. *J Biol Chem*
89. Lee, P. D., Giudice, L. C., Conover, C. A., and Powell, D. R. (1997) Insulin-like growth factor binding protein-1: recent findings and new directions. *Proc Soc Exp Biol Med* **216**, 319-357
90. Challiss, R. A., Arch, J. R., and Newsholme, E. A. (1984) The rate of substrate cycling between fructose 6-phosphate and fructose 1,6-bisphosphate in skeletal muscle. *Biochem J* **221**, 153-161
91. Lai, K. M., Gonzalez, M., Poueymirou, W. T., Kline, W. O., Na, E., Zlotchenko, E., Stitt, T. N., Economides, A. N., Yancopoulos, G. D., and Glass, D. J. (2004) Conditional activation of akt in adult skeletal muscle induces rapid hypertrophy. *Mol Cell Biol* **24**, 9295-9304
92. Izumiya, Y., Hopkins, T., Morris, C., Sato, K., Zeng, L., Viereck, J., Hamilton, J. A., Ouchi, N., LeBrasseur, N. K., and Walsh, K. (2008) Fast/Glycolytic muscle fiber growth reduces fat mass and improves metabolic parameters in obese mice. *Cell Metab* **7**, 159-172

93. Thompson, N., and Lyons, J. (2005) Recent progress in targeting the Raf/MEK/ERK pathway with inhibitors in cancer drug discovery. *Curr Opin Pharmacol* **5**, 350-356
94. Sausville, E. A. (2000) Overview. Cancer drug discovery: pathway promise or covalent certainty for drug effect--quo vadis? *Curr Opin Investig Drugs* **1**, 511-513
95. Vidya Vardhini, B., and Rao, S. S. (2002) Acceleration of ripening of tomato pericarp discs by brassinosteroids. *Phytochemistry* **61**, 843-847
96. Coimbra, R., Sanchez, L. S., Potenza, J. M., Rossoni, L. V., Amaral, S. L., and Michelini, L. C. (2008) Is gender crucial for cardiovascular adjustments induced by exercise training in female spontaneously hypertensive rats? *Hypertension* **52**, 514-521
97. Esposito, D., Rathinasabapathy, T., Poulev, A., Komarnytsky, S., and Raskin, I. (2011) Akt-dependent anabolic activity of natural and synthetic brassinosteroids in rat skeletal muscle cells. *J Med Chem* **54**, 4057-4066
98. Govorko, D., Logendra, S., Wang, Y., Esposito, D., Komarnytsky, S., Ribnicky, D., Poulev, A., Wang, Z., Cefalu, W. T., and Raskin, I. (2007) Polyphenolic compounds from *Artemisia dracunculus* L. inhibit PEPCK gene expression and gluconeogenesis in an H4IIE hepatoma cell line. *Am J Physiol Endocrinol Metab* **293**, E1503-1510
99. Michelini, E., Cevenini, L., Mezzanotte, L., Ablamsky, D., Southworth, T., Branchini, B. R., and Roda, A. (2008) Combining intracellular and secreted bioluminescent reporter proteins for multicolor cell-based assays. *Photochem Photobiol Sci* **7**, 212-217
100. Knapp, P. E., Storer, T. W., Herbst, K. L., Singh, A. B., Dzekov, C., Dzekov, J., LaValley, M., Zhang, A., Ulloor, J., and Bhasin, S. (2008) Effects of a supraphysiological dose of testosterone on physical function, muscle performance, mood, and fatigue in men with HIV-associated weight loss. *Am J Physiol Endocrinol Metab* **294**, E1135-1143
101. Lewis, M. I., Fournier, M., Storer, T. W., Bhasin, S., Porszasz, J., Ren, S. G., Da, X., and Casaburi, R. (2007) Skeletal muscle adaptations to testosterone and resistance training in men with COPD. *J Appl Physiol* **103**, 1299-1310
102. Bhasin, S., Parker, R. A., Sattler, F., Haubrich, R., Alston, B., Umbleja, T., and Shikuma, C. M. (2007) Effects of testosterone supplementation on whole body and regional fat mass and distribution in human immunodeficiency virus-infected men with abdominal obesity. *J Clin Endocrinol Metab* **92**, 1049-1057
103. Bhasin, S., and Buckwalter, J. G. (2001) Testosterone supplementation in older men: a rational idea whose time has not yet come. *J Androl* **22**, 718-731
104. Chatelain, F., Pegorier, J. P., Minassian, C., Bruni, N., Tarpin, S., Girard, J., and Mithieux, G. (1998) Development and regulation of glucose-6-phosphatase gene expression in rat liver, intestine, and kidney: in vivo and in vitro studies in cultured fetal hepatocytes. *Diabetes* **47**, 882-889
105. Kirpichnikov, D., McFarlane, S. I., and Sowers, J. R. (2002) Metformin: an update. *Ann Intern Med* **137**, 25-33
106. Kim, Y. D., Park, K. G., Lee, Y. S., Park, Y. Y., Kim, D. K., Nedumaran, B., Jang, W. G., Cho, W. J., Ha, J., Lee, I. K., Lee, C. H., and Choi, H. S. (2008)

- Metformin inhibits hepatic gluconeogenesis through AMP-activated protein kinase-dependent regulation of the orphan nuclear receptor SHP. *Diabetes* **57**, 306-314
107. Ruderman, N. B., and Saha, A. K. (2006) Metabolic syndrome: adenosine monophosphate-activated protein kinase and malonyl coenzyme A. *Obesity* **14 Suppl 1**, 25S-33S
 108. Longnus, S. L., Segalen, C., Giudicelli, J., Sajan, M. P., Farese, R. V., and Van Obberghen, E. (2005) Insulin signalling downstream of protein kinase B is potentiated by 5'AMP-activated protein kinase in rat hearts in vivo. *Diabetologia* **48**, 2591-2601
 109. Berggreen, C., Gormand, A., Omar, B., Degerman, E., and Goransson, O. (2009) Protein kinase B activity is required for the effects of insulin on lipid metabolism in adipocytes. *American journal of physiology. Endocrinology and metabolism* **296**, E635-646
 110. Yuan, L., Ziegler, R., and Hamann, A. (2002) Inhibition of phosphoenolpyruvate carboxykinase gene expression by metformin in cultured hepatocytes. *Chin Med J (Engl)* **115**, 1843-1848
 111. Ashcroft, G. S., Greenwell-Wild, T., Horan, M. A., Wahl, S. M., and Ferguson, M. W. (1999) Topical estrogen accelerates cutaneous wound healing in aged humans associated with an altered inflammatory response. *The American journal of pathology* **155**, 1137-1146
 112. Fu, X., Li, X., Cheng, B., Chen, W., and Sheng, Z. (2005) Engineered growth factors and cutaneous wound healing: success and possible questions in the past 10 years. *Wound repair and regeneration : official publication of the Wound Healing Society [and] the European Tissue Repair Society* **13**, 122-130
 113. Mooney, E. K., Lippitt, C., and Friedman, J. (2006) Silver dressings. *Plastic and reconstructive surgery* **117**, 666-669
 114. Khorasani, G., Hosseinimehr, S. J., Zamani, P., Ghasemi, M., and Ahmadi, A. (2008) The effect of saffron (*Crocus sativus*) extract for healing of second-degree burn wounds in rats. *Keio J Med* **57**, 190-195
 115. Lusby, P. E., Coombes, A., and Wilkinson, J. M. (2002) Honey: a potent agent for wound healing? *J Wound Ostomy Continence Nurs* **29**, 295-300
 116. Dipietro, L. A., Reintjes, M. G., Low, Q. E., Levi, B., and Gamelli, R. L. (2001) Modulation of macrophage recruitment into wounds by monocyte chemoattractant protein-1. *Wound repair and regeneration : official publication of the Wound Healing Society [and] the European Tissue Repair Society* **9**, 28-33
 117. Liechty, K. W., Kim, H. B., Adzick, N. S., and Crombleholme, T. M. (2000) Fetal wound repair results in scar formation in interleukin-10-deficient mice in a syngeneic murine model of scarless fetal wound repair. *J Pediatr Surg* **35**, 866-872; discussion 872-863
 118. Martin, P., and Leibovich, S. J. (2005) Inflammatory cells during wound repair: the good, the bad and the ugly. *Trends Cell Biol* **15**, 599-607
 119. Keylock, K. T., Vieira, V. J., Wallig, M. A., DiPietro, L. A., Schrementi, M., and Woods, J. A. (2008) Exercise accelerates cutaneous wound healing and decreases wound inflammation in aged mice. *American journal of physiology. Regulatory, integrative and comparative physiology* **294**, R179-184

120. Asano, Y., Ihn, H., Yamane, K., Jinnin, M., Mimura, Y., and Tamaki, K. (2004) Phosphatidylinositol 3-kinase is involved in alpha2(I) collagen gene expression in normal and scleroderma fibroblasts. *J Immunol* **172**, 7123-7135
121. Chen, J., Somanath, P. R., Razorenova, O., Chen, W. S., Hay, N., Bornstein, P., and Byzova, T. V. (2005) Akt1 regulates pathological angiogenesis, vascular maturation and permeability in vivo. *Nature medicine* **11**, 1188-1196
122. Bujor, A. M., Pannu, J., Bu, S., Smith, E. A., Muise-Helmericks, R. C., and Trojanowska, M. (2008) Akt blockade downregulates collagen and upregulates MMP1 in human dermal fibroblasts. *The Journal of investigative dermatology* **128**, 1906-1914
123. Komarnytsky, S., Cook, A., and Raskin, I. (2011) Potato protease inhibitors inhibit food intake and increase circulating cholecystokinin levels by a trypsin-dependent mechanism. *Int J Obes (Lond)* **35**, 236-243
124. Winer, J., Jung, C. K., Shackel, I., and Williams, P. M. (1999) Development and validation of real-time quantitative reverse transcriptase-polymerase chain reaction for monitoring gene expression in cardiac myocytes in vitro. *Anal Biochem* **270**, 41-49
125. Sethi, G., Sung, B., and Aggarwal, B. B. (2008) TNF: a master switch for inflammation to cancer. *Frontiers in bioscience : a journal and virtual library* **13**, 5094-5107
126. Sanjabi, S., Zenewicz, L. A., Kamanaka, M., and Flavell, R. A. (2009) Anti-inflammatory and pro-inflammatory roles of TGF-beta, IL-10, and IL-22 in immunity and autoimmunity. *Current opinion in pharmacology* **9**, 447-453
127. Sumagin, R., Lomakina, E., and Sarelius, I. H. (2008) Leukocyte-endothelial cell interactions are linked to vascular permeability via ICAM-1-mediated signaling. *American journal of physiology. Heart and circulatory physiology* **295**, H969-H977
128. Bascom, C. C., Wolfshohl, J. R., Coffey, R. J., Jr., Madisen, L., Webb, N. R., Purchio, A. R., Derynck, R., and Moses, H. L. (1989) Complex regulation of transforming growth factor beta 1, beta 2, and beta 3 mRNA expression in mouse fibroblasts and keratinocytes by transforming growth factors beta 1 and beta 2. *Molecular and cellular biology* **9**, 5508-5515
129. Valls, M. D., Cronstein, B. N., and Montesinos, M. C. (2009) Adenosine receptor agonists for promotion of dermal wound healing. *Biochem Pharmacol* **77**, 1117-1124
130. Schmidt, C., Fronza, M., Goettert, M., Geller, F., Luik, S., Flores, E. M., Bittencourt, C. F., Zanetti, G. D., Heinzmann, B. M., Laufer, S., and Merfort, I. (2009) Biological studies on Brazilian plants used in wound healing. *J Ethnopharmacol* **122**, 523-532
131. Gilliver, S. C., Ashworth, J. J., and Ashcroft, G. S. (2007) The hormonal regulation of cutaneous wound healing. *Clin Dermatol* **25**, 56-62
132. Hardman, M. J., and Ashcroft, G. S. (2008) Estrogen, not intrinsic aging, is the major regulator of delayed human wound healing in the elderly. *Genome Biol* **9**, R80
133. Engeland, C. G., Sabzehei, B., and Marucha, P. T. (2009) Sex hormones and mucosal wound healing. *Brain Behav Immun* **23**, 629-635

134. Thiboutot, D., Jabara, S., McAllister, J. M., Sivarajah, A., Gilliland, K., Cong, Z., and Clawson, G. (2003) Human skin is a steroidogenic tissue: steroidogenic enzymes and cofactors are expressed in epidermis, normal sebocytes, and an immortalized sebocyte cell line (SEB-1). *J Invest Dermatol* **120**, 905-914
135. Ashcroft, G. S., and Mills, S. J. (2002) Androgen receptor-mediated inhibition of cutaneous wound healing. *J Clin Invest* **110**, 615-624
136. Efron, P. A., and Moldawer, L. L. (2004) Cytokines and wound healing: the role of cytokine and anticytokine therapy in the repair response. *J Burn Care Rehabil* **25**, 149-160
137. Franek, R., Eckschlager, T., and Kohout, L. (2003) 24-Epibrassinolide at subnanomolar concentrations modulates growth and production characteristics of a mouse hybridoma. *Collect. Czech. Chem. Commun.* **68**, 2190-2200
138. Hennessy, B. T., Smith, D. L., Ram, P. T., Lu, Y., and Mills, G. B. (2005) Exploiting the PI3K/AKT pathway for cancer drug discovery. *Nat Rev Drug Discov* **4**, 988-1004
139. Wu, D., Peng, F., Zhang, B., Ingram, A. J., Gao, B., and Krepinsky, J. C. (2007) Collagen I induction by high glucose levels is mediated by epidermal growth factor receptor and phosphoinositide 3-kinase/Akt signalling in mesangial cells. *Diabetologia* **50**, 2008-2018
140. Mimaki, Y., Ishibashi, N., Ori, K., and Sashida, Y. (1992) Steroidal glycosides from the bulbs of *Lilium dauricum*. *Phytochemistry* **31**, 1753-1758
141. Su, J. (1979) *Encyclopedia of Chinese Medicine* Shanghai Science and Technology Publishing Company, Shanghai
142. Varrier, P. K. (2002) *Indian Medicinal Plants* Vol. 3, Orient Longman, Chennai
143. Eisenreichova, E., and Haladova, M. (1998) White lily and its healing effects. *Pharma J* **8**, 45-46
144. Kresanek, J., and Dugas, D. (1985) *Prirucny atlas liecivych rastlin (Handy atlas of medicinal plants)*, Osveta, Martin
145. Shimomura, H., Sashida, Y., and Mimaki, Y. (1986) Bitter phenylpropanoid glycosides from *Lilium speciosum* var. *rubrum*. *Phytochemistry* **25**, 2897-2899
146. Shoyama, Y., Hatano, K., and Yamagishi, T. (1987) Phenolic glycosides from *Lilium longiflorum*. *Phytochemistry* **26**, 2965-2968
147. Francis, J. A., Rumbelha, W., and Nair, M. G. (2004) Constituents in Easter lily flowers with medicinal activity. *Life Sci* **76**, 671-683
148. Tsukida, K., and Ikeuchi, K. (1965) Epoxycarotenoids. VIII. Pollen carotenoids of *Lilium longiflorum* and of its cultivated hybrid. *Bitamin* **32**, 222-226
149. Mimaki, Y., Satou, T., Kuroda, M., Sashida, Y., and Hatakeyama, Y. (1999) Steroidal saponins from the bulbs of *Lilium candidum*. *Phytochemistry* **51**, 567-573
150. Mimaki, Y., Nakamura, O., Sashida, Y., Satomi, Y., Nishino, A., and Nishino, H. (1994) Steroidal saponins from the bulbs of *Lilium longiflorum* and their antitumour-promoter activity. *Phytochemistry* **37**, 227-232
151. Munafo, J. P., Jr., Ramanathan, A., Jimenez, L. S., and Gianfagna, T. J. (2010) Isolation and structural determination of steroidal glycosides from the bulbs of easter lily (*Lilium longiflorum* Thunb.). *J Agric Food Chem* **58**, 8806-8813

152. Mimaki, Y., and Sashida, Y. (1990) Steroidal saponins and alkaloids from the bulbs of *Lilium brownii* var. *colchesteri*. *Chem Pharm Bull (Tokyo)* **38**, 3055-3059
153. Singer, A. J., and Clark, R. A. (1999) Cutaneous wound healing. *N Engl J Med* **341**, 738-746
154. Harding, K. G., Morris, H. L., and Patel, G. K. (2002) Science, medicine and the future: healing chronic wounds. *BMJ* **324**, 160-163
155. Martin, P. (1997) Wound healing--aiming for perfect skin regeneration. *Science* **276**, 75-81
156. Eckes, B., Zigrino, P., Kessler, D., Holtkotter, O., Shephard, P., Mauch, C., and Krieg, T. (2000) Fibroblast-matrix interactions in wound healing and fibrosis. *Matrix Biol* **19**, 325-332
157. Verrecchia, F., Chu, M. L., and Mauviel, A. (2001) Identification of novel TGF-beta /Smad gene targets in dermal fibroblasts using a combined cDNA microarray/promoter transactivation approach. *J Biol Chem* **276**, 17058-17062
158. Gailit, J., Welch, M. P., and Clark, R. A. (1994) TGF-beta 1 stimulates expression of keratinocyte integrins during re-epithelialization of cutaneous wounds. *J Invest Dermatol* **103**, 221-227
159. Zambruno, G., Marchisio, P. C., Marconi, A., Vaschieri, C., Melchiori, A., Giannetti, A., and De Luca, M. (1995) Transforming growth factor-beta 1 modulates beta 1 and beta 5 integrin receptors and induces the de novo expression of the alpha v beta 6 heterodimer in normal human keratinocytes: implications for wound healing. *J Cell Biol* **129**, 853-865
160. Cowin, A. J., Hatzirodos, N., Holding, C. A., Dunaiski, V., Harries, R. H., Rayner, T. E., Fitridge, R., Cooter, R. D., Schultz, G. S., and Belford, D. A. (2001) Effect of healing on the expression of transforming growth factor beta(s) and their receptors in chronic venous leg ulcers. *J Invest Dermatol* **117**, 1282-1289
161. Pierce, G. F., Mustoe, T. A., Lingelbach, J., Masakowski, V. R., Gramates, P., and Deuel, T. F. (1989) Transforming growth factor beta reverses the glucocorticoid-induced wound-healing deficit in rats: possible regulation in macrophages by platelet-derived growth factor. *Proc Natl Acad Sci U S A* **86**, 2229-2233
162. Ashcroft, G. S., Yang, X., Glick, A. B., Weinstein, M., Letterio, J. L., Mizel, D. E., Anzano, M., Greenwell-Wild, T., Wahl, S. M., Deng, C., and Roberts, A. B. (1999) Mice lacking Smad3 show accelerated wound healing and an impaired local inflammatory response. *Nat Cell Biol* **1**, 260-266
163. Koch, R. M., Roche, N. S., Parks, W. T., Ashcroft, G. S., Letterio, J. J., and Roberts, A. B. (2000) Incisional wound healing in transforming growth factor-beta1 null mice. *Wound Repair Regen* **8**, 179-191
164. Wang, X. J., Han, G., Owens, P., Siddiqui, Y., and Li, A. G. (2006) Role of TGF beta-mediated inflammation in cutaneous wound healing. *J Investig Dermatol Symp Proc* **11**, 112-117
165. Amendt, C., Mann, A., Schirmacher, P., and Blessing, M. (2002) Resistance of keratinocytes to TGFbeta-mediated growth restriction and apoptosis induction accelerates re-epithelialization in skin wounds. *J Cell Sci* **115**, 2189-2198

166. Soneja, A., Drews, M., and Malinski, T. (2005) Role of nitric oxide, nitroxidative and oxidative stress in wound healing. *Pharmacol Rep* **57 Suppl**, 108-119
167. Ori, K., Mimaki, Y., Mito, K., Sashida, Y., Nikaido, T., Ohmoto, T., and Masuko, A. (1992) Jatrophan derivatives and steroidal saponins from the bulbs of *Lilium hansonii*. *Phytochemistry* **31**, 2767-2775
168. Munafo, J. P., and Gianfagna, T. J. (2011) Quantitative Analysis of Steroidal Glycosides in Different Organs of Easter Lily (*Lilium longiflorum* Thunb.) by LC-MS/MS. *J Agric Food Chem* **59**, 995-1004
169. Manhezi, A. C., Bachion, M. M., and Pereira, A. L. (2008) The use of essential fatty acids in the treatments of wounds. *Rev Bras Enferm* **61**, 620-628
170. Mimaki, Y., Yokosuka, A., Kuroda, M., and Sashida, Y. (2001) Cytotoxic activities and structure-cytotoxic relationships of steroidal saponins. *Biol Pharm Bull* **24**, 1286-1289
171. Cham, B. E., Daunter, B., and Evans, R. A. (1991) Topical treatment of malignant and premalignant skin lesions by very low concentrations of a standard mixture (BEC) of solasodine glycosides. *Cancer Lett* **59**, 183-192
172. Chowdhury, I., Tharakan, B., and Bhat, G. K. (2006) Current concepts in apoptosis: the physiological suicide program revisited. *Cell Mol Biol Lett* **11**, 506-525
173. Greenhalgh, D. G. (1998) The role of apoptosis in wound healing. *Int J Biochem Cell Biol* **30**, 1019-1030
174. Houghton, P. J., Hylands, P. J., Mensah, A. Y., Hensel, A., and Deters, A. M. (2005) In vitro tests and ethnopharmacological investigations: wound healing as an example. *J Ethnopharmacol* **100**, 100-107
175. Morisaki, N., Watanabe, S., Tezuka, M., Zenibayashi, M., Shiina, R., Koyama, N., Kanzaki, T., and Saito, Y. (1995) Mechanism of angiogenic effects of saponin from ginseng *Radix rubra* in human umbilical vein endothelial cells. *Br J Pharmacol* **115**, 1188-1193
176. Kanzaki, T., Morisaki, N., Shiina, R., and Saito, Y. (1998) Role of transforming growth factor-beta pathway in the mechanism of wound healing by saponin from *Ginseng Radix rubra*. *Br J Pharmacol* **125**, 255-262
177. Frank, S., Madlener, M., and Werner, S. (1996) Transforming growth factors beta1, beta2, and beta3 and their receptors are differentially regulated during normal and impaired wound healing. *J Biol Chem* **271**, 10188-10193
178. Chen, R. H., Ebner, R., and Derynck, R. (1993) Inactivation of the type II receptor reveals two receptor pathways for the diverse TGF-beta activities. *Science* **260**, 1335-1338
179. Nakayama, H., Ichikawa, F., Andres, J. L., Massague, J., and Noda, M. (1994) Dexamethasone enhancement of betaglycan (TGF-beta type III receptor) gene expression in osteoblast-like cells. *Exp Cell Res* **211**, 301-306

CURRICULUM VITA

DEBORA A. ESPOSITO

EDUCATION

- 2007-2012 **Ph.D.** in Cell and Molecular Plant Biology
Rutgers University, New Brunswick, NJ
- 2010-2012 **M.B.S.** in Drug Discovery and Development
Rutgers University, New Brunswick, NJ
- 2000-2004 **B.S.** in Chemistry
Federal University of Viçosa, MG, Brazil

PUBLICATIONS

Esposito D, Komarnytsky S, Shapses S, Raskin I (2011) Anabolic effect of plant brassinosteroid. *FASEB J*, 25(10): 3708-3719

Esposito D, Rathinasabapathy T, Poulev A, Komarnytsky S, Raskin I (2011) Akt-dependent anabolic activity of natural and synthetic brassinosteroids in rat skeletal muscle cells. *J Med Chem*, 54: 4057-4066

Esposito D, Rathinasabapathy T, Komarnytsky S, Raskin I (2010) Methods of producing and using brassinosteroids to promote growth, repair, and maintenance of skeletal muscle. US patent application, MGB no 29155/45877

Alves-Júnior M, Alfenas-Zerbini P, Andrade EC, **Esposito D**, Silva FN, da Cruz ACF, Veterella MC, Otoni WC, Zerbini FM (2009) Synergism and negative interference during co-infection of tomato and *Nicotiana benthamiana* with two bipartite begomoviruses. *Virology*, 387(2): 257-266

Govorko D, Logendra S, Wang Y, **Esposito D** et al (2007) Polyphenolic compounds from *Artemisia dracunculoides* inhibit PEPCK gene expression and gluconeogenesis in an H4IIE hepatoma cell line. *Am J Physiol Endocrinol Metab*, 293(6): E1503-1510

PROFESSIONAL EXPERIENCE

- 2011- 2012 **Application Specialist**, LLTECH Inc, North Brunswick, NJ.
- 2007-2012 **Graduate Research Assistant**, Biotech Center, Rutgers University, New Brunswick, NJ.
- 2006 **Visiting Scientist**, Plant Pathology – Bioagro, Molecular Virology, Vicosa, Brazil.
- 2006 **Instructor for English classes**, Real English Center, Vicosa, Brazil.
- 2005-2006 **Visiting Scientist**, Biotech Center, Rutgers University, New Brunswick, NJ.
- 2004-2006 **Visiting Scientist**, Plant Biology & Pathology, Rutgers University, New Brunswick, NJ.
- 2004 **Laboratory Assistant**, Chemistry, Federal University of Viçosa, Brazil.
- 2003 **Instructor for Physics undergraduate classes**, Federal University of Viçosa, Brazil.
- 2002 **Teaching Assistant**, Arthur Bernardes Foundation, Vicosa, Brazil.